REPORT NO.
UCB/EERC-77/27
NOVEMBER 1977

EARTHQUAKE ENGINEERING RESEARCH CENTER

A PRACTICAL SOFT STORY EARTHQUAKE ISOLATION SYSTEM

by

JAMES M. KELLY
JOHN M. EIDINGER
and
C. J. DERHAM

A report on research conducted under
Grant ENV76-04262
from the National Science Foundation.

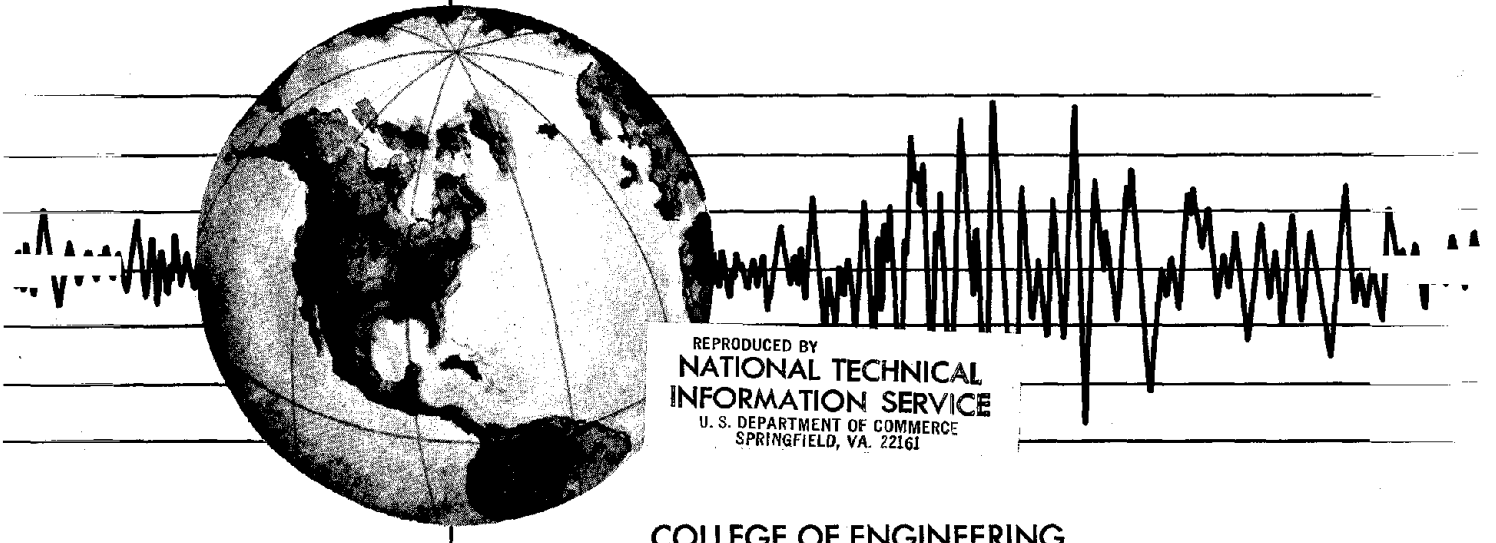

COLLEGE OF ENGINEERING

UNIVERSITY OF CALIFORNIA · Berkeley, California

BIBLIOGRAPHIC DATA SHEET	1. Report No. UCB/EERC-77/27	2.	3. Recipient's Accession No. PB270014
4. Title and Subtitle: A Practical Soft Story Earthquake Isolation System			5. Report Date: November 1977 6.
7. Author(s): J. M. Kelly, J. M. Eidinger and C. J. Derham			8. Performing Organization Rept. No. 77-27
9. Performing Organization Name and Address: Earthquake Engineering Research Center, University of California, Berkeley, 47th Street and Hoffman Blvd., Richmond, California 94804			10. Project/Task/Work Unit No. 11. Contract/Grant No. ENV76-04262
12. Sponsoring Organization Name and Address: National Science Foundation, 1800 G Street, N.W., Washington, D.C. 20550			13. Type of Report & Period Covered 14.

15. Supplementary Notes

16. Abstracts

This report describes the experimental and analytical results of a practical earthquake isolation system. The experimental work was carried out using a 20 ton three-story single-bay moment-resistant steel frame structure on the 20 by 20 foot shaking table at the Earthquake Engineering Research Center at the University of California, Berkeley.

The soft story isolation system is composed of elastic natural rubber bearings and a highly nonlinear energy-absorbing device, all placed beneath the base floor of the model structure. The bearings allow for lateral movement of the base of the model and are designed so that no adverse column P-Δ effects can occur. The energy-absorbing devices act as highly efficient dampers, and are based upon the two-way plastic torsion of steel bars.

For smaller earthquakes, the structure behaves as with a rigid foundation. For large earthquakes, the structure's first mode period increases from 0.6 to 1.0 seconds, and equivalent first mode damping is between 30% and 35%. Thus, for destructive earthquakes, the use of the isolation system typically reduces the structure's response by over 50% of that of a conventional rigid foundation structure.

An inelastic time history analysis gives good correlation with experimental test data. A simple design procedure based upon elastic response spectra is suggested.

A full scale structure located in a seismic zone and built with such an isolation system achieves two major cost benefits over a conventional structure: (1) Lower initial construction costs due to reduced lateral load requirements; (2) Lower earthquake-caused repair costs, due to decreased structural and non-structural damage.

17b. Identifiers/Open-Ended Terms

17c. COSATI Field/Group

18. Availability Statement	19. Security Class (This Report)	21. No. of Pages
Release Unlimited	UNCLASSIFIED	150
	20. Security Class (This Page) UNCLASSIFIED	22. Price A07-A01

A PRACTICAL SOFT STORY

EARTHQUAKE ISOLATION SYSTEM

by

James M. Kelly, Professor of Civil Engineering
and
John M. Eidinger, Graduate Student
University of California, Berkeley

and

C. J. Derham, Principal Physicist
Malaysian Rubber Producers' Research Association
Brickendonbury, England

Report to
National Science Foundation

Report No. UCB/EERC-77/27
Earthquake Engineering Research Center
College of Engineering
University of California
Berkeley, California

November 1977

ABSTRACT

This report describes the experimental and analytical results of a practical earthquake isolation system. The experimental work was carried out using a 20 ton three-story single-bay moment-resistant steel frame structure on the 20 by 20 foot shaking table at the Earthquake Engineering Research Center at the University of California, Berkeley.

The soft story isolation system is composed of elastic natural rubber bearings and a highly nonlinear energy-absorbing device, all placed beneath the base floor of the model structure. The bearings allow for lateral movement of the base of the model and are designed so that no adverse column P-Δ effects can occur. The energy-absorbing devices act as highly efficient dampers, and are based upon the two-way plastic torsion of steel bars.

For small earthquakes, the structure behaves as with a rigid foundation. For large earthquakes, the structure's first mode period increases from 0.6 to 1.0 seconds, and equivalent first mode damping is between 30% and 35%. Thus, for destructive earthquakes, the use of the isolation system typically reduces the structure's response by over 50% of that of a conventional rigid foundation structure.

An inelastic time history analysis gives good correlation with experimental test data. A simple design procedure based upon elastic response spectra is suggested.

A full scale structure located in a seismic zone and built with such an isolation system achieves two major cost benefits over a conventional structure: (1) Lower initial construction costs due to reduced lateral load requirements; (2) Lower earthquake-caused repair costs, due to decreased structural and non-structural damage.

ACKNOWLEDGMENTS

The authors wish to express their appreciation to the National Science Foundation, R.A.N.N. Division, for their support through Grant No. ENV76-04262, and to the Malaysian Rubber Producers' Research Association.

A number of people's contributions made this project possible. Many thanks are due to Messrs. David Steere, Ivo Van Austen, Steve Miller and John McNab for their electronic, machine shop and laboratory work. Graduate students Dan Chitty and Robert Turner helped perform the tests and reduce part of the data.

TABLE OF CONTENTS

LIST OF TABLES

LIST OF FIGURES

LIST OF FIGURES (continued)

LIST OF FIGURES (continued)

1. Introduction

The concept of limiting the earthquake-caused forces in a structure by the use of a special foundation system is not new. In the past, there have been two basic approaches to this problem.

One approach was to put the structure on a simple vibration isolation system. Various solutions have been suggested (1, 2, 3, 4, 5, 6). These include natural or synthetic rubber bearings, rollers, and self-centering rocking mechanisms. The principle of these solutions is to lower the structure's lateral stiffness so that its first mode period is well separated from most earthquake energy. The two major drawbacks to this kind of isolation system are the large base deflections possible (one foot or more) and the wind excitation problems.

The other approach was to limit the forces transmitted to the structure by the use of a 'soft' first story. First floor columns would be intentionally designed to yield at a low level, and then be able to absorb large deflections, and dissipate energy through the yielding of their connections. Thus, the structure would behave as a simple elasto-plastic system. Preliminary studies indicated that the design yield level of the soft story would be the maximum shear possible in the structure (7, 8, 9, 10). Later studies showed that higher mode effects would have significant contributions to the structure's response (11,12, 13). However, the real drawback to the soft first story approach is the column P-Δ effects under the large lateral deflections necessary for adequate performance.

This report describes in detail the experimental test results of a realistic and workable soft story earthquake isolation system which is a combination of the above two solutions. The 'soft' story is in fact a very short story only six inches tall, comprised of elastic natural rubber

bearings and highly nonlinear energy-absorbing devices, both placed beneath the base floor of a half-scale model steel frame structure. The bearings allow for lateral movement of the base of the model and are designed so that no adverse column P-Δ effects can occur. The energy-absorbing devices act as highly efficient dampers, and are based upon the two-way plastic torsion of steel bars.

Unlike the rollers, hydraulic dampers, friction plates and yielding columns that have been suggested in previous work, the rubber bearings and torsion devices do not require maintenance, do not leak oil, do not rely upon highly variable long-term friction coefficients nor require repair or replacement after every earthquake. The bearings and devices rely only on the well known material properties of natural rubber and mild steel.

A large number of earthquake simulator tests were conducted on this soft story model structure. The response of the structure depended upon earthquake intensity. For small earthquakes, the structure behaved as with a rigid foundation, and strongly amplified the ground motion. For large earthquakes, the soft story yielded, and this increased the effective first mode period of the structure. Under these circumstances, the torsion devices absorbed large amounts of energy, equivalent to 30% - 35% of critical viscous damping. Maximum base deflection due to the El Centro 1940 NS earthquake scaled to peak acceleration of 0.627g was only 2.56 inches, while peak acceleration of the model structure was only 0.625g. The Parkfield and Pacoima Dam earthquake motions produced similar results. The higher mode frequencies and responses of the soft story structure were not significantly altered due to the yielding of the energy-absorbing devices.

The model structure with a normal rigid foundation was subjected to the same earthquake motions as the soft story model structure. The soft

story isolation system reduced the structure's response typically by a factor of 2, sometimes more.

Unlike results presented in other research (9, 10), the yield level of the soft story does not directly limit the forces in the structure. Analyses show that the key parameters which directly define the structure's response are its effective first mode period after the soft story yields, its higher mode responses, and the energy absorption by the torsion device.

It is concluded that the additional foundation detailing costs of a soft story isolation system will probably be easily offset by the lower forces the structure so designed will have to be built for. With the soft story foundation design, a structure can be designed to remain totally elastic, even during a severe earthquake, and have very little damage either to it or its contents.

2. Isolation System

The isolation system on which the experimental test program was carried out has two main components; a mild steel energy-absorbing device which also serves as a mechanical fuse, and a set of natural rubber bearings which couple very low lateral stiffness with high vertical stiffness. These components are described in detail in the following sections.

2.1 Energy-Absorbing Devices

The energy-absorbing devices used in this experimental program are of the type originally designed at the Engineering and Physics Laboratory at the New Zealand D.S.I.R. by Kelly, Skinner, and Heine (14). The operating principle of the devices is the large plastic torsion of rectangular mild steel bars. Due to the interest of the New Zealand Railways in using the devices in a railway viaduct of an innovative design, considerable research and development work was carried out on the devices, the design of which is felt to be optimum in so far as they are fabricated from hot-rolled low carbon mild steel. The devices are simple, purely mechanical, and in both previous testing (15, 16) and in the present program have been demonstrated to have very favorable characteristics for the use in an isolation system.

The key energy-absorbing element in the device (Figure 2.1.1) is the rectangular torsion bar to which torque is applied through the moment arms. The devices were arranged in such a way that they applied a horizontal force to the model structure. Three different types of devices were used, being distinguished by their yield force levels, their post-yielding stiffnesses and their material compositions. In each type, the displacement at which the device yielded was on the order of 1/10 inch and

the maximum displacement during the test was on the order of 2-1/2 inches. The devices were thus subject to very large plastic strains. The ductility characteristics of mild steel, in particular resistance to low-cycle fatigue, enabled the two mild steel torsion bar devices to withstand many cycles of such deformation without deterioration. The third device, made by a high alloy TRIP steel, showed significant deterioration due to fatigue and weld cracking.

The devices play two distinct roles in the response of the soft story foundation system to earthquake loading. Since they are elastic for small displacements and their elastic stiffness is high relative to that of the rubber bearings, they act as mechanical fuses and cause the model structure to behave as a rigid foundation system for small excitation. Thus, under small excitation, the structure typically amplifies the ground acceleration. As the excitation increases in intensity, the device yields, and produces large hysteretic loops as the structure oscillates. The mild steel device's tangent stiffness when yielded is between 5% and 10% of its elastic stiffness. Thus the fundamental frequency of the structure drops, and the system acts as an isolator with a very high effective damping value. The accelerations induced in the structure are of course somewhat greater than if only a simple rubber bearing isolation system were used, but the displacements at the bearings are reduced.

The degree of damping due to the torsion bar devices depends very much on the intensity of the ground motion. It will be shown that they produce damping equivalent to 30% to 35% critical viscous damping.

2.2 Natural Rubber Bearings

The bearings used in this isolation system are a development of bearings currently used as vibration isolators in buildings constructed in areas of high traffic disturbance such as, for example, above underground railway systems (1). These vibration isolation systems have been in use since the mid-sixties and are a logical extension of bearings used in highway bridges (17). They provide isolation against groundborne vibrations in the range of 20 to 50 Hz. Earthquake isolations requirements are quite different. Most earthquake vibration is in the range of 0.3 to 5 Hz. To isolate a structure from earthquake vibrations requires that the structure's first natural frequency is lower than the excitation frequencies. The rubber bearings in an earthquake isolation system must have very low lateral stiffness, be able to accept very large lateral deflections, and to perform well under long term loadings. Natural rubber is well suited for these purposes.

Natural rubber can accept strains on the order of several hundred percent without failure. The ultimate tensile strength of natural rubber is higher than that of any artificial rubber. Another advantage is that the ratio of the bulk modulus to shear modulus can be extremely large; for example, for soft natural rubber it can be as large as 1000 (7), allowing the design of bearings that are very soft horizontally and very stiff vertically. Natural rubber has additional advantages for a seismic isolation system with regard to long-term performance because it creeps very little, is highly resistant to fire (18), and can be made to be effectively immune to oxidation attack.

The bearings used for these tests were constructed by the Malaysian Rubber Producers' Research Association. Figure 2.2.1 shows the

actual bearings, and Figure 2.2.2a, b, the details. To provide sufficient cross-sectional area of rubber for stability under the light experimental dead load, it was necessary to develop specially low modulus compounds. By multilayer construction, it was possible to increase the rocking stiffness of the isolated model structure enough to prevent bending of the bearings. At the same time, the multilayer construction provided bearings that were four hundred times stiffer in the vertical than in the horizontal direction. Each laminate of rubber is 0.079 inches (2 mm) thick. Total rubber thickness in each bearing is 2.83 inches (7.2 cm).

The first natural frequency of the light model structure using a simple rubber bearing isolation system was 0.6 Hz. Thus, the model structure was isolated from earthquake vibrations over 0.9 Hz. The increased mass of a full-scale structure would allow the rubber bearings to be designed to achieve a natural frequency of 0.3 Hz or less.

It was not possible for these experimental bearings to be made by the usual commercial process of direct chemical rubber-to-steel bonding vulcanization. They were hand-fabricated from sheets of rubber vulcanization bonded to aluminum foil. The aluminum was in turn bonded to the mild steel interleaves using industrial quality double-sided adhesive tape over two-thirds of the surface area, and epoxy resin for greater shear strength over the remaining one-third area. The bearings made in this way were adequately strong for these tests, being capable of sustaining repeated shear deformations in excess of 100%, but were clearly not as strong nor as durable as equivalent commercially produced bearings would be. The theoretical vertical stiffness of these bearings is about 500,000 lbs-per-inch. Due to the method of construction the measured effective vertical stiffness at the working load was in the area of 150,000 lbs-per-inch.

The vertical stiffness characteristics of the bearings are shown in Figure 2.2.3. The pronounced soft lead-in is primarily the result of the method of construction and would not normally be present to this extent. The bearings were cycled from 5 to 20 kip vertical loads. The bearings showed little hysteresis after the first soft lead-in cycle. Each bearing's ultimate vertical strength was 30 kips, which was three times the static dead load on them due to the model structure's weight.

The horizontal stiffness characteristics of the rubber bearings are shown in Figure 2.2.4. The hysteresis loops represent approximately 10% critical damping. The tangent stiffness at zero deflection is 320 lbs/in and the tangent stiffness at 2-1/2 inch deflection is 250 lbs/in. Thus, the rubber bearings are essentially linear to shear strains in excess of 100%.

3. Experimental Set-Up

3.1 Experimental Model and Test Facility

The experimental work was carried out using the Earthquake Simulator Laboratory at the Earthquake Engineering Research Center at the University of California, Berkeley. The work was performed in two phases, in September 1976, phase I, and May 1977, phase II.

The model steel frame structure used in both phases of the experimental work is shown in Figures 3.1.1 and 3.1.2. Except for the base floor and associated isolation systems, this model sturcture was the same as that used by Clough and Tang (19). The model weighed 39.5 kips, was twenty feet high, and was twelve feet by six feet in plan dimension. Each of the three floors and the base floor was loaded with 8-kip concrete blocks, so as to simulate the dead weight of a real structure and to provide a period of vibration in the range appropriate to actual steel and concrete buildings. Still, these 8-kip loads produce dead load girder stresses under 9 ksi. The girders and columns both have f_y = 45.9 ksi (mill test report). Evidently, this test frame is greatly overdesigned for the resistance of lateral loads. Estimated weights of the steel components and measured weights of the concrete blocks are listed in table 3.1.1.

Figure 3.1.3 and 3.1.4 show how the frame was mounted on the rubber bearings. The heavy W10x49 base floor girders ensure that the rubber bearings will have little tendency to undergo bending deformations. Figure 3.1.5 shows how the energy-absorbing device was connected to the base floor. The device is effective only for motion of the frame in the same direction as the motion of the shaking table.

A large number of transducers was used in the testing program to collect the time history data presented in this report. Horizontal floor accelerations and displacements were monitored with linear potentiometers

and accelerometers. Load cells were placed under each rubber bearing to measure shear forces at the base level. Accelerometers and potentiometers were used to check the uplift tendencies of the rubber bearings due to vertical ground motion. Strain gages recorded most girder and column axial forces and bending moments. A load cell recorded all forces through the energy-absorbing devices.

The output of these transducers and load cells was recorded by a Neff System 620 Analog Digital Processor and a Diablo Model 30 magnetic disk cartridge drive controlled by a NOVA 1200 computer. The data was scanned at approximately 50 samples per channel per second and ultimately stored on magnetic tape. Phase I and Phase II of these tests incorporated 58 and 96 channels of data respectively.

3.2 Experimental Test Program

Phase I of the test program was conducted to (1) determine the feasibility of rubber bearings in earthquake isolation systems, (2) examine the design of low damping rubber bearings, and (3) to study the effects of large amounts of damping in an isolation system. The test results of the Phase I program are reported in reference 20. The Phase II tests to be reported here were conducted to (1) test newly designed high damping rubber bearings, (2) to check the response of the isolation system to vertical motion, (3) to test the effect of simple breaking fuses that 'tie down' the structure under wind loading, and (4) to study the use of energy-absorbing devices coupled with the rubber bearings to produce a workable 'soft story' isolated structure.

The two phases of the experimental test program incorporated over 130 separate earthquake tests. Four different types of foundations

were used for the model, representing a fixed (rigid) foundation and three types of isolation systems. A simple rubber foundation was used which incorporated rubber bearings beneath each column, with no wind restraint. A rubber bearing and shear pin foundation was used that had steel pins that kept the model structure rigid under wind loads, while breaking under large earthquake loading, after which the model was isolated. A rubber bearing and energy-absorbing device foundation was used that causes the model to behave as a building with a soft first story. In another paper by these authors (21), detailed results are presented for the isolated structure on a rubber foundation with and without wind restraints. In this paper, reference will be made to the fixed foundation (FIX), rubber bearing with no wind restraint foundation (RUBBER), and the soft story foundation (ENERGY ABSORBER or EA).

Three earthquake records were used in the testing program: (1) the El Centro N-S (1940), (2) Parkfield N65E (1966), and (3) Pacoima Dam S16E (1971). Different amplitudes of these earthquakes were used. The span setting associated with a particular amplitude earthquake defined the maximum displacement of the input motion. In the current tests, a span 1000 test porduced an earthquake with maximum table displacement of ±5 inches. A span 500 test produced a maximum displacement of about ±2.5 inches. The maximum associated table acceleration did not depend on the span setting, but on the nature of the earthquake motion. Table 3.2.1 shows the peak displacements and accelerations of the three earthquakes used at various span settings. No Pacoima Dam tests were run for the FIX base foundation.

The three different types of energy-absorbing devices used will be designated EA1, EA2, and EA3. Table 3.2.2 shows which devices were used for the different earthquake motions, and the properties of the devices.

4. Reduction of Test Data

The following descriptions apply to the plots presented in this report. Positive results represent responses to the North. Negative responses represent responses to the South.

Response Spectra

Response Spectra were generated using a computer program by Nigam and Jennings (22). The input to this program is the recorded table acceleration for a given earthquake test run. Each response spectra was calculated at 1, 3, 10, 25, 30, 35, 40, and 45 per cent damping ratios. At periods close to the natural periods of the experimental structure, responses were calculated at 0.01 second intervals. In all, a total of 98 responses were calculated at each damping level. As the spectra are not presented on four way log paper, the actual (not the pseudo) accelerations and velocities are plotted. The pseudo velocities obtained from displacement x ω are within 15% of the actual velocities. Pseudo and actual accelerations are almost identical.

Table Displacement

Actual recorded table motion during the test.

Rubber Pad Displacement Relative to Table

The two traces plotted, solid and dash, respectively represent the lateral deflections of the rubber bearings (pads) on the west and east frames (A and B) of the model. Discrepancies between these traces would indicate torsional response of the structure. Positive indicates relative motion North of the table displacement.

First, Second and Third Floor Displacement Relative to Table

This data is obtained by subtracting the recorded table displacement from the absolute motion of each floor.

Table Acceleration

Actual recorded table acceleration.

Base, First, Second and Third Floor Absolute Acceleration

Recorded accelerations of the concrete blocks on each floor. The accelerometers were mounted 8-1/4 inches above the centerlines of the floor girders, and thus were 2 inches below the center of mass of each floor.

Energy Absorber Force

The lateral force exerted between the base floor and the energy-absorbing device.

Energy Absorber Displacement

The pin displacement at the inner arms of the energy-absorbing device. This data is obtained by averaging the rubber bearing displacements along frames A and B.

First Story Drift

First floor displacement relative to table minus rubber pad displacement relative to table. Positive represents the first story drifting North of the base floor.

Second and Third Story Drifts

Second minus first and third minus second relative floor displacements, respectively.

First, Second and Third Floor Shear

The inertia force at each floor level was determined from the product of the story mass and the measured story acceleration. The first story shear represents the summation of the first, second and third story inertia forces. This is equivalent to the total shear force in the four columns between the first and base level floors.

Base Shear

The base shear represents the summation of the base, first, second and third floor inertia forces. This same shear was also recorded by the load cells beneath the rubber bearings and energy-absorbing device. The difference between these two forms of data was negligible.

Base, First, Second and Third Floor Overturning Moments

The floor overturning moment is the summation of the floor inertia forces about the floor level in question. Base shears and overturning moments are not meaningful for the fixed foundation model.

All tests of a particular earthquake, regardless of span setting or base fixity condition, have been shifted in time so that the peak table displacement occurs at the same instant. This is to allow for easy comparison between tests.

5. Test Results

In this section the results obtained from the first 18 seconds of ten selected test runs are presented in the following sequence:

1 - El Centro 400	Rubber	Foundation
2 - El Centro 900	Fix	"
3 - El Centro 750	EA1	"
4 - El Centro 750	EA3	"
5 - Parkfield 500	Fix	"
6 - Parkfield 500	EA1	"
7 - Parkfield 500	EA2	"
8 - Parkfield 500	EA3	"
9 - Pacoima Dam 500	EA1	"
10 - Pacoima Dam 500	EA3	"

The minima and maxima results of six additional test runs are presented in tabular form. The largest load-deflection curves for each type of energy-absorbing device are also presented.

5.1 El Centro Tests

El Centro span 750 was the largest El Centro test performed during Phase II of the test program, and had a peak ground (table) acceleration of 0.627g. The actual El Centro N-S component had a peak ground acceleration of 0.32g. However, it was found that the acceleration intensity of the shaking table could not be compared with that of the original earthquake record. Clough and Tang (19) report that the velocity spectrum of their El Centro 900 test (peak table acceleration 0.61g) was only about 30% greater than the true El Centro velocity spectrum, while the peak accelerations varied by 90%. Therefore, peak acceleration intensity of a table motion must be interpreted carefully.

The El Centro 900 test on the model with a fix foundation was performed by Tang in 1974. This table motion is almost identical in

magnitude to the Phase II El Centro 750 test performed in 1977. The response spectra for these two tests are very similar in shape and intensity. The span settings differ due to modifications in the shaking table control systems.

The response spectra for El Centro 750 are shown in Figure 5.1. Tables 5.1 and 5.2 give the minimum and maximum response values for the El Centro tests.

5.1.1 El Centro 400/350 Rubber Foundation

This medium intensity test is presented to demonstrate the behavior of the model structure on a simple rubber bearing isolation system. No energy-absorbing devices are used, and energy dissipation arises mostly from the viscous damping action of the rubber bearings.

First mode damping was evaluated by logarithmic decrement from free vibration decay to be 10%.

Both a horizontal table motion (span 400) and a vertical table motion (span 350) were used. The vertical motion is taken from the recorded El Centro 1940 vertical acceleration.

Figures 5.1.1.1 and 5.1.1.2 show that while the simply isolated structure sustained peak accelerations of about 0.10g to this 0.30g earthquake, it also underwent a large base floor displacement of nearly 3 inches. There was almost no story drift in the structure. Figure 5.1.1.3 shows that there was no amplification of the vertical table motion in the structure. There was no frame rocking action or rubber bearing uplift during the test. This is important, because rubber has low tensile strength. In all, the simple rubber bearing isolation tests were very successful.

Some soft story EA foundation tests were run with horizontal and

vertical earthquake components. As expected, the structure's horizontal and vertical responses were uncoupled, and in no case was the vertical response significant. For these reasons no vertical response data will be presented for the EA foundation tests contained in this report.

5.1.2 El Centro 900 Fix Foundation

This test was performed in 1974 by Tang on essentially the same model structure as was used in the current soft story isolation tests, except that it had no base floor. Fixed foundation tests on the model with and without the base floor indicated first mode natural frequencies of 2.05 and 2.25 Hz respectively. The softening of the model with base floor is attributed mostly to the reduced fixity of the first floor column connections to the base floor.

The El Centro 900 FIX foundation test produced a modest amount of yielding in the frame members. The dynamic first floor girder moments exceeded the 333 kip-inch yield level. The dynamic first floor column bottom end moment also exceeded its 393 kip-inch yield level. Significant first floor girder and column post-yield end rotations occured. The first floor girder sustained a permanent end rotation of about 1/4 of its yield end rotation. More detailed results can be obtained in (19).

The first floor overturning moment and shear shown in Figure 5.1.2.3 of 457 kip-feet and 33.3 kips were calculated from floor inertia forces and are in excellent agreement with shears calculated by strain gage data.

Peak first floor story drift of 1.33 inches was 1.8% of first story height. A large amount of damage to partition walls would be expected.

5.1.3 El Centro 750 EA1 Foundation

The total length of the El Centro input table motion is 31 seconds. There is mostly small amplitude vibration after 13 seconds, and the plotted results are arbitrarily cut-off at 18 seconds.

The rubber pad displacement shift of -0.25 inches after time 13 seconds is the same as the final shift at the end of the test. This shift is due to the plastic deformations of the device.

The device's displacement of 2.56 inches during this test was the most severe loading of any device during the entire test program. Even after this test, the mild steel device showed no signs of deterioration.

Figure 5.1.3.1 shows the two distinct types of response characteristics of the soft story EA foundation. The table displacement between 2 and 7 seconds is the strongest part of the El Centro motion, and the structure responds at an effective frequency of 1.0 Hz. The table displacement between 7 and 12 seconds is relatively small, and the structure responds at a frequency of 1.6 Hz.

Figure 5.1.3.5 shows that between 2 and 7 seconds, the energy-absorbing device is almost always well beyond its 4 kip yield point. Between 7 and 12 seconds, the device rarely yields. The change in the structure's frequency is due to the large change of stiffness by the device. Figure 5.1.3.6 shows that the elastic stiffness of device EA1 is near 15 kips/inch and the post-yield stiffness ranges between 0.2 and 1.3 kips/inch. By adding to these values the near constant rubber bearing stiffness of 1.2 kips/inch, we obtain an "elastic" base stiffness of 16 kips/inch, and a "post-yield" base stiffness of about 2 kips/inch. This change in base stiffness accounts for the observed frequency shift. Section 8 discusses frequency and mode shape changes in more detail.

The first, second and third floor displacements are all similar to the base floor (rubber pad) displacements, indicating that there should be small story drifts. However, Figure 5.1.3.2 shows that the second mode accelerations are dominant on the base and third floors. In fact, maximum first mode accelerations are less than one half the peak table accelerations of -0.627g. The second mode response causes a significant amount of story drift, as shown in Figure 5.1.3.5. Peak drifts do not always occur at the same instant as peak displacements. Still, the peak first story drift of 0.73 inches is only 0.95% of first story height, or half that of the fixed foundation test's peak drift. A small or moderate amount of damage to partition walls would be expected.

There was no yielding in any of the frame members. The maximum dynamic bending moment in the first floor girder was just 66 kip-inches, or 20% of its yield value.

5.1.4 El Centro 750 EA3 Foundation

From 2 to 7 seconds, the structure responds at about 1.1 Hz, and from 7 to 12 seconds the structure responds at 1.6 Hz. The post-yield stiffness of the EA3 device is between 2.5 and 7.3 kips/inch. This accounts for the higher post-yield frequency of the EA3 versus EA1 foundation.

Unlike what occured in the EA1 test, there is almost no permanent shift in the rubber pad displacement at the end of this test. The peak rubber pad displacements were +1.93 and -1.62 inches. This is smaller than the +1.79 and -2.56 inches that occured with the EA1 device. Closer observation shows that the EA1 device deflects and shifts more, due to its increased tendency to undergo large one-way plastic deformations. This is due to EA1's lower post-yield stiffness.

This test caused the most severe motion (1.93 inches) of the EA3 device. Small fatigue cracks appeared in the torsion bar. These cracks did not appreciably degrade the device's capacity.

The structure with the EA3 foundation responds more severely than the structure with the EA1 foundation - peak third floor acceleration of 0.987g versus 0.625g and peak first story drift of 0.97 inches versus 0.73 inches. The peak EA3 force of 16 kips is more than double the EA1 force. The peak EA3 base shear of 18.9 kips is 1.73 times the EA1 base shear of 10.9 kips. Still, these EA3 response values are well below those of the fixed foundation.

5.2 Parkfield Tests

The response spectra for the Parkfield table motion are shown in Figure 5.2. The spectra reveal that this table motion has significant energy at periods near the elastic base period of the soft story structure, but relatively little energy at its post-yield period. Table 5.3 gives the extreme value results.

5.2.1 Parkfield 500 Fix Foundation

This table motion did not cause any yielding in the frame members, although peak third floor accleration was 0.85g. The small amount of normal structural damping (under 1%) allows the structure to oscillate for many cycles after its initial response. This moderate earthquake still produces maximum first story drift of 0.98 inches (1.3% of first story height). Maximum overturning moment and first floor shear are 264 kip-feet and 18.9 kips. The structure has greater response in this test than in any of the soft story foundation tests.

5.2.2 Parkfield 500 EA1 Foundation

The peak third floor acceleration of 0.315g is only 1.33 times this 0.237g earthquake, and is just 37% that of the fixed foundation test.

The only significant yielding of the energy-absorbing device takes place between 3 and 6 seconds. The frequency shift at this time is not as great as it is with the El Centro motions, due to the shorter time intervals when the device is yielded. There is a rubber pad displacement shift of +0.28 inches at the end of the test.

5.2.3 Parkfield 500 EA2 Foundation

The response of the structure with the EA2 device and the EA1 device is similar, the major difference being that the EA2 device tends to shift less. The final rubber pad displacement shift is just -0.09 inches. Otherwise, the EA2 tests exhibit about a 15% increase in most other response parameters. The slightly increased yield force level and post-yield stiffness of the EA2 device (see Figure 5.3.3) accounts for this.

5.2.4 Parkfield 500 EA3 Foundation

The response of the structure with the EA3 device is more intense than with the EA1 or EA2 devices. In particular, the post-yield type oscillation at 5 to 6 seconds is greatly increased. It is also observed that the elastic-type vibration occuring after 6 seconds exhibits a longer period of vibration than in the EA1 or EA2 tests. During this time, there was no corresponding yielding of the device.

It was noticed in this test that the jaws of the moment arms holding the torsion bar had opened up slightly due to cracked welds. This allowed the torsion bar to rotate freely a small amount at the peak of

each half cycle. This accounts for the observed lengthening of the elastic base frequency. Still, there is only a final rubber pad displacement shift of -0.16 inches.

The torsion bar showed considerable fatigue cracks at the beginning of this test. These cracks reduced the stiffness of this trip steel device somewhat, but did not significantly reduce its energy-absorbing capability.

5.3 Pacoima Dam Tests

The response spectra in Figure 5.3 indicate that the Pacoima Dam table motion is very severe for periods between 0.1 and 0.5 seconds, dips low at the elastic period of the soft story structure, and increases again near the post-yield period of the structure. Inspection of the table displacement time history shows that between 3.5 and 5.5 seconds, the motion is almost a perfect sine wave, very close to the post-yield frequency of the structure. In fact, the structure acts almost 90^{0} out of phase with the input motion during this time interval. Table 5.4 gives the extreme value data for the Pacoima Dam tests.

5.3.1 Pacoima Dam 500 EAl Foundation

The rubber pad displacement plot in Figure 5.3.1.1 seems to show three types of basic response frequencies: 1) A post-yield frequency of 0.85 Hz, 2) An elastic frequency of 1.5 Hz, and 3) An even higher frequency response between time 5.5 to 6.7 seconds, and 7.4 to 8.6 seconds.

The energy absorber force plot in Figure 5.3.1.3 shows that during the two high frequency time intervals, the device is almost always in its elastic range. The first, second and third floor displacement plots indicate that this high frequency response is in fact the elastic first mode

response with a strong second mode response superimposed. The floor acceleration plots also show this clearly.

This severe table motion produced no yielding in the frame members. Maximum first floor girder dynamic bending moment was only 53 kip-inches. Maximum first story drift was only 0.50 inches, or 0.65% of first story height. Maximum base shear and overturning moment are 11.2 kips and 123 kip-feet. Little or no damage to the structure and its contents would be expected. This accompanies a large rubber pad peak displacement of 2.49 inches.

The rubber pad displacement time history indicates that large one-way displacement shifts occured three times during the test. The final rubber pad displacement shift was +0.48 inches. Between 7.5 and 8.7 seconds, the shift was +0.94 inches. Some authors (23) suggest that subsequent earthquakes tend to cause additional shifts in the same direction as the original shift. This is not so with the soft story EA foundation.

This Pacoima Dam 500 test was immediately followed by an identical test with reversed table motion. Peak table motion of this second test was +2.38, -2.78 inches, as compared to the first test's peaks of +2.77, -2.37 inches. The initial rubber pad displacement shift was +0.48 inches, due to the previous test. The results of the second test were almost identical to the first test results, except in sign. The final rubber pad displacement shift was -0.20 inches, or a net shift of -0.68 inches.

This 'overshift' result is explained by the increased post-yield stiffness of the device with increased deflection, as shown in Figure 5.3.1.6. If the device is deflected a large amount to one side, it takes less force to reduce the device's deflection than to continue increasing it. Thus the device always tends to oscillate about zero deflection, where it is softest.

When the device's inner arms deflect enough, the changed geometry of the device causes the input force to be resisted partly by torsion and partly by bending in the torsion bar. If the inner arms rotated a full 90^0, representing a horizontal deflection of about 4-1/2 inches, then the input force is resisted only by bending action of the torsion bar. Since the rectangular torsion bar has much higher stiffness in bending than in torsion, the device's post-yield stiffness increases with increasing inner arm deflection.

5.3.2 Pacoima Dam 500 EA3 Foundation

The peak base floor displacement for the EA3 test was 1.81 inches versus the 2.49 inches of the EA1 test. The EA3 test shows very little shifting during the test, with a final shift of +0.20 inches. This small shifting is attributed to the increased post-yield stiffness of the EA3 device.

However, the EA3 first story drift of 0.89 inches was 80% larger than the EA1 first story drift. The base floor shear and overturning moment for the EA3 foundation were 16.1 kips and 222 kip-feet, much larger than in the EA1 test. Maximum first floor girder dynamic bending moment was 83 kip-inches, although still much lower than its 333 kip-inch yield moment.

As with the Parkfield 500 EA3 test, the connection of this device's moment arms to the torsion bar had degraded, causing a lengthening of the elastic base frequency.

5.3.3 Pacoima Dam 400 EA2 Foundation

The only figure shown is the load-deflection curve for the EA2 device.

Its post-yield stiffness ranges from 0.66 to 2.82 kips/inch.

Table 5.4 gives comparitive data of the Pacoima Dam 400 EA1 and EA2 tests. As with the Parkfield tests, the EA2 Pacoima Dam 400 foundation test caused slightly greater structural response than did the EA1 test.

The EA1 test had a peak shift of +0.47 inches and a final shift of +0.12 inches. The corresponding EA2 shifts were +0.59 inches and +0.56 inches. Thus, the EA2 device shifted slightly more after the first major pulse of the earthquake, but shifted much less due to the second smaller pulse.

Both the EA1 and the EA2 devices were made of the same mild steel. However, the EA1 device's post-yield stiffness was lower, only ranging from 0.2 to 1.3 kips/inch. The EA2 device's inner moment arms were shorter than those of the EA1 device. As explained in section 5.3.1, the torsion bar of the EA2 device acted as a bending element at lower deflections than did that of the EA1 device, thus increasing its post-yield stiffness.

Since the EA2 device had shorter moment arms, it required higher forces to produce the yield torque in the torsion bar element. The EA2 device yielded at about 5 kips, while the EA1 device yielded at about 4 kips.

6. Discussion of Results

6.1 Effect of Increasing Earthquake Intensity

Since the model structure behaved in two very distinct ways depending upon the shaking intensity, we may expect that linearly increasing input motion may cause extremely nonlinear changes in the structure's response. To test this hypothesis three input motions of three intensities each were run. These motions and respective foundaton conditions were;

El Centro 450,600,750 on EA1 foundation

El Centro 450,600,750 on EA3 foundation

Pacoima Dam 200,400,500 on EA1 foundation

In none of these nine tests did any yielding occur in the frame members.

6.1.1 El Centro Motion with EA1 Foundation

Figure 6.1.1.1 shows that the energy absorber displacement plots were very similar in frequency content for the increasing El Centro input motion. This is because the smallest test, El Centro 450, was not small enough to keep the device below its yield point during the test. But it is noted that peak values for the three tests did not increase in a linear correspondance with increasing table motion. In fact, the peak displacements increased 9% and 80% for table displacement increases of 33% and 66% respectively. Table 6.1.1.1 lists the peak values of various response parameters versus input motion intensity.

The three energy absorber displacement peaks occur at different times due to the amount of shifting that took place during the tests. These tests were not run in successive order, so that conclusions based upon past behavior cannot be made directly. However, it can be concluded that increased shifting is likely to occur with increased displacement. This is due to the increasingly unsymmetrical directional stiffness characteristics the devices

assume with increased deflection.

A better comparison between energy absorber deflections is the maximum peak to peak displacement the device goes through in one cycle. This would cancel out the effects due to shifting. The results for this analysis are:

	Max. Peak to Peak Displacement	Δ%
El Centro 450	2.50 inches	
El Centro 600	2.95 inches	+18%
El Centro 750	3.69 inches	+48%

Figures 6.1a-f graphically display that all response parameters for the EA1 El Centro foundation tests rise in a linear fashion, except for energy absorber displacements. First story drift and third floor acceleration response parameters rise at a much faster rate than the other parameters due to their very strong dependence upon second mode participation.

It is concluded from these results that once the input motion is large enough to produce significant yielding in the energy absorber soft foundation, further increases of the input motion produce only small increases in the first mode response of the structure, but may produce large increases in higher mode response of the structure.

6.1.2 El Centro Motion with EA3 Foundation

As with the EA1 El Centro test, the EA3 El Centro 450 test was still large enough to cause significant yielding in the EA3 device. Thus there is little difference in the shape of the time history response for the EA3 foundation to either El Centro 450, 600 or 750 motions.

As expected, Figure 6.1.2.1 shows that the EA3 foundation has little tendency to shift, even with the increasing magnitude El Centro motions.

6.1.3 Pacoima Dam Motion with EA1 Foundation

Unlike the El Centro 450 tests, the Pacoima Dam 200 test was small enough to keep the EA1 device from yielding during a portion of the test when the large span Pacoima Dam tests did yield the device. Figure 6.1.3.1 shows this happening between 3.5 and 5.5 seconds.

Table 6.1.3.2 gives the comparative data for the first 6.5 seconds of the Pacoima Dam motion. This table shows that the yielding soft story is very effective in keeping the structure from responding to the input motion. The jump from span 200 to span 400 (a 101% increase in table displacement and a 108% increase in table acceleration) produces only a 30% to 70% increase in the structural response parameters. First story drift and third floor accelerations do not follow this pattern as they are strongly dependent upon higher mode response.

As discussed in section 6.2.2, the effective change in the first mode frequency shifts the structure to another portion of the response spectra, and the energy absorption by the device effectively increases the structure's damping ratio to a very high value. These two factors explain the nonlinear increases in response parameters as the base condition yields. Unlike the El Centro tests, the maximum peak to peak displacement of the device changes in a nonlinear fashion. A similar analysis as done for the El Centro tests yields the following:

	Max. Peak to Peak Displacement	Δ%
Pacoima Dam 200	1.42 inches	
Pacoima Dam 400	3.18 inches	+124%
Pacoima Dam 500	4.62 inches	+225%

It is concluded from these results that by doubling the input motion so that the base does yield, deflections may increase by double or more, depending upon shifting, change in period, and energy absorption by the device. However, the forces in the structure will only moderately increase, due to these same factors.

6.2 Comparison of Base Conditions

6.2.1 Rubber Foundation

There is no doubt that a structure on a simple rubber foundation will experience very little destructive motion during a severe earthquake. The basic problem with using a simple rubber bearing isolation system is that a large earthquake may require lateral deflections of the rubber bearings of one foot or more. While rubber bearings for a full scale structure can be designed to easily accept such deflections, it is undesirable to have a typical structure moving so much during an earthquake. Utility connections pose restrictions on allowable base floor deflections. For special structures such as hospitals and nuclear power plants, the additional costs of special foundation details may well be a small cost to pay for the very low forces and damage experienced by such an isolated structure.

6.2.2 Fix Foundation Versus Soft Story Energy Absorber Foundation

Figures 6.2a-d show that all soft story foundation structures had lower accelerations, story drifts, shears and moments than fixed foundation structures. This was independent of the type of energy-absorbing device. This result was also independent of earthquake intensity or earthquake motion.

The soft story foundation structures differ from fixed foundation structures in three major attributes; normal condition (elastic base) first mode frequency, earthquake condition (yielded base) first mode frequency, and earthquake condition damping value. The fixed and elastic base frequencies were kept as nearly equal as possible so that comparisons would be made more valid. The fact that they differ (T_1 = 0.6 versus 0.5 seconds) is not very important, as the peak response of the soft story foundation structure is almost independent of its elastic base frequency.

The two important factors affecting the response of the highly nonlinear soft story system are the energy absorption by the device and the change in the first mode period due to the softening of the device. There has been much discussion by engineers as to which of these two factors is most important. In fact, for this structural isolation system, both factors are very important, and when combined will almost always reduce the structure's response much lower than that of a conventionally fixed foundation structure.

Both the elastic analysis presented in section 8 and the test results show that peak displacement response is strongly dependent upon the effective first mode period that the structure vibrates at maximum displacement. For earthquakes similar in frequency content to those in California, structures with first mode periods over one second will typically be past the acceleration dominated high frequency end of the response spectrum. The three earthquake motions used during the tests all roughly follow this fact. Thus, the large decrease in base stiffness due to the yielding of the energy absorber, which increases the model structure's first mode period from 0.6 to about one second, tends to move the structure out of the range of most of the earthquake's energy. Then, the yielded base

condition effectively isolates the structure from the typical earthquake.

Also discussed in section 8 is the fact that the hysteretic action by the energy-absorbing device proves equivalent to about 30% to 35% of critical viscous damping. This is clearly a very beneficial effect in strongly reducing the large displacements associated with long period structures.

True, it is difficult to compare the response of two different frequency structures to the same earthquake. However, it is interesting to note that of the three input motions used in the tests, Parkfield decreases a lot in intensity from 0.6 to 1 second, Pacoima Dam decreases slightly, and El Centro increases substantially. (This is qualitative, based upon all acceleration, velocity and displacement response spectra.) Yet there were significantly lower forces in the soft story foundation structures versus fixed foundation in response to all three earthquakes.

We can conclude that the lengthening of first mode period past one second of any structure will be beneficial for most California earthquakes. This, coupled with viscous damping values over 30%, almost ensures that soft story foundation structures will have less damage than corresponding fixed foundation structures.

6.2.3 Effect of Yield Force and Post Yield Stiffness of Energy-Absorbing Devices

The effect of increasing the device's yield force and post yield stiffness are threefold: a) There will be reduced amount of shifting; b) The post yield frequency will decrease slightly less; c) Shears, moments, accelerations and drifts, and hence damage, will increase in the structure. Figures 6.2.3.1, 2 and 3 all display the shifting and frequency differences. Figures 6.2a-d show the other response parameter differences.

From the experimental data alone, it is difficult to differentiate the response effects of yield force and post-yield stiffness. Simple analyses conducted by Clough, Clough and Chopra (11) for a soft story eight story shear-type building indicated that the lowest possible yield force along with almost zero post-yield stiffness will produce the best results. Actually, this limit state approaches putting the structure on rollers or a simple rubber bearing system. The problems for this are already mentioned in section 6.2.1.

It is obvious from the results that the EA1 foundation fared better than either EA2 or EA3 foundations. The post-yield stiffness of the EA1 foundation of about 1 kip/inch, or about 5% of the elastic stiffness, is about as low as obtainable using low carbon steel energy-absorbing devices. Since the shifting associated with low post-yield stiffness does not directly cause excitation of the structure, and the geometry of the devices puts a positive limit to maximum base displacement, designing for the lowest possible post-yield stiffness is probably best.

A yield force close to zero is not practical, as it is not advisable to have the building swaying in the wind. Depending upon the climate and location of the site, 50 or 100 year return wind forces may reach 2% to 4% of a structure's weight. The associated base shear with these static wind loads may be 3% to 6% of the structure's weight.

The EA1 foundation had a yield force of about 4 kips, or 10% of the model structure's weight. The sturctural responses with the EA1 foundation were quite small. Due to the nature of second mode response plus the fact that lower yield forces means smaller energy absorber loops and hence lower effective damping, further reduction in yield force may or may not always result in lower structural response. Analytical studies currently

being carried out are investigating this problem.

From the test results, and practical considerations, a post-yield stiffness near 5% of elastic stiffness coupled with yield forces between 5% and 10% of the structure's weight should provide an optimal soft story foundation isolation system.

7. Nonlinear Analyses

The test results showed that there were significant nonlinearities in the energy-absorbing devices, and these strongly affected the response of the structure. The force-displacement figures in section 5 indicate that a bilinear hysteretic nonlinear element might well describe the EA1 energy-absorbing device. A computer program DRAIN-2D (24) was used to analyse the time history response of a twelve d.o.f. elastic structure with a bilinear energy-absorbing foundation. A modified truss-element was used to describe the devices.

The elastic and post-yield stiffnesses of the energy absorber used in the nonlinear analysis, as taken from the experimental data, were 15 k/in and 0.85 k/kn. First and second mode critical damping values were 3% and 1%.

Figures 7.1, 7.2 and 7.3 show the comparison of the analytical and experimental results in response to the El Centro, Parkfield and Pacoima Dam earthquake inputs. Table 7.1 compares the maximum results. The analytical model predicts the highly nonlinear displacement response within 10% for the El Centro test, 18% for the Parkfield test, and 9% for the Pacoima Dam test. The model accurately predicts the change in effective first mode frequency due to yielding of the energy-absorbing device. The shifting effects that the analytical model predicts are reasonably accurate.

The nonlinear model gives floor shears typically within ±15% of the experimental results. The computed first story drifts are 25% to 50% lower than experimental results. This indicates that the analytical model is not adequately describing second mode response. It is strongly suspected that the bolted column-girder connection on the first floor level was not sufficiently rigid, and allowed small but significant rotations to occur

at these connections. These rotations strongly excited the model structure into a higher mode response. This did not strongly affect the relative floor displacements, but did affect floor accelerations and story drifts.

The bilinear element was modified to model the EA3 device. As with the EA1 analyses, the EA3 analytical time history results were very close to experimental results. As with the EA1 results, maximum floor displacements and shears were in good accordance, while first floor drift was not.

The nonlinear analyses give a good approximation of the basic behavior of the experimental model. It does not give good results for higher mode behavior, but this is a problem with approximations of assumed joint rigidity, and may easily be refined. Then, on at least a general scale, this model can be used to test the sensitivity of the structure's response to changes in the assumed behavior of the energy-absorbing device.

It is easy to analyse the beneficial effects of hysteretic energy absorption by the device. A nonlinear analysis was done using the same bilinear element for the El Centro 750 test (as in Figure 7.1), except that the bilinear element was modified to always remain elastic. The force displacement behavior of the original and the modified elements are shown in Figures 7.4 a and b.

The comparison of the results is shown in Figure 7.5. As expected, until the first yielding of the device, the analytical models are identical. After three seconds, the device does yield, and the elastic model shows oscillations of +4.79 and -4.14 inches, 102% larger than the hysteretic model. Maximum base shear for the elastic model was 14.5 kips, 58% larger than for the hysteretic model. Thus the damping effect of the device is extremely beneficial in reducing structural response. Table 7.1 gives the full comparison between the analyses.

The elastic model dies out very quickly after 6 seconds. This was not due to energy absorption or damping effects. Closer inspection of the input El Centro displacement motion shows a pulse 180^{o} out of phase with the structure's motion between 6 and 6.5 seconds. To determine the effect of this pulse, the structure was further analysed, using the bilinear elastic element, in response to just the first 6 seconds of the El Centro input motion. Without the motion arresting pulse, the structure continued in free vibration after 6 seconds with 62% larger displacement. It was finally damped out by the 3% viscous damping of the rubber bearings.

8. Elastic Analysis and Design Methods

8.1 Mode Shapes and Frequencies

The frequency and mode shape values given in table 8.1.1 for fixed foundation models are taken from free vibration tests. For the three floor model this was done by putting a small shaker on the first floor. The results are considered to be very accurate. For the four floor model, the results are taken from free vibrations following forced vibration earthquake tests. The results are considered to be reasonable.

The analytical results in this table for the rubber foundation model are in excellent agreement with observed responses of the structure. The analysis used was a twelve degree of freedom system representing four horizontal floor displacements and eight joint rotations. The joint rotation d.o.f. are eliminated using static condensation. The accuracy of the higher mode shapes indicated that simple changes to the base member's stiffnesses in this analysis would give good analytical results for the soft story EA foundation models.

It is clearly understood that the nonlinear action of the soft story foundation cannot be completely described by an elastic analysis. However, the test results showed that there are distinct and major frequency shifts occuring when the energy-absorbing device yields. The simple eigenvalue analyses presented in table 8.1.2 are used only as a tool to help explain the observed behavior of the model.

The stiffness used in the yielded energy absorber analyses is an average post-yield stiffness of the device. This stiffness value was varied to test the sensitivity of the results. By changing the assumed post-yield stiffness from 0.8 k/in to 1.1 k/in (38%), the first mode frequency only changed from 0.68 Hz to 0.73 Hz (7%). Thus the use of an average post-yield

stiffness is reasonable in trying to describe the model's behavior.

8.2 Elastic Analysis

The elastic energy absorber analyses are an accurate description of the model except for the seven seconds of the El Centro tests, three seconds of the Parkfield tests and five seconds of the Pacoima Dam tests, when significant base yielding occurs. Logarithmic damping taken from the free vibration decay at the end of the Pacoima Dam test gives elastic first mode damping ratio between 3% and 4%. This is larger than the 0.5% observed with the fixed foundation model due to the hysteresis loops of the rubber bearings. It does not equal the 10% damping ratio observed on tests with rubber bearings alone due to the strain energy of the EA device.

If the energy absorber yields in both directions during one cycle, then there are four major transitions of base stiffness during this cycle. This causes the base floor to behave as if sudden forces were being applied to it at each transition. These initial conditions do cause significant higher mode response in the structure. Neglecting them, consider the basic behavior of the structure in each mode.

For the elastic EA1 foundation, the mass and stiffness matrices (after static condensation) used were

$$\underline{M} = \begin{bmatrix} .02438 & 0 & 0 & 0 \\ 0 & .02438 & 0 & 0 \\ 0 & 0 & .02514 & 0 \\ 0 & 0 & 0 & .02832 \end{bmatrix} \text{ kip-sec}^2/\text{inch}$$

$$\underline{K} = \begin{bmatrix} 46.28 & -66.21 & 22.89 & -2.96 \\ -66.21 & 143.5 & -97.38 & 20.07 \\ 22.89 & -97.38 & 129.8 & -55.35 \\ -2.96 & 20.07 & -55.35 & 54.24 \end{bmatrix} \text{ kips/inch}$$

For the post-yield EA1 foundation, the stiffness matrix was

$$\underline{K} = \begin{bmatrix} 46.28 & -66.21 & 22.89 & -2.96 \\ -66.21 & 143.5 & -97.38 & 20.07 \\ 22.89 & -97.38 & 129.8 & -55.35 \\ -2.96 & 20.07 & -55.35 & 40.24 \end{bmatrix} \text{ kips/inch}$$

If $L_n = \underline{\phi}_n \underline{M} (\underline{1})$, then the mode superposition method gives

$$\underline{v}(t) = \sum_n \underline{\phi}_n \frac{L_n}{M_n \omega_n} V_n(t)$$

where

$\underline{v}(t)$ = floor displacement vector

$M_n = \underline{\phi}_n^t \underline{M}_n \underline{\phi}_n$

ω_n = circular frequency for mode n

$V_n(t)$ = pseudo-velocity response for SDOF system of frequency ω_n.

If the $\underline{\phi}$ vectors are normalized so that the maximum value in each modal vector is unity, then M_n and L_n are

Foundation	M_1	M_2	L_1	L_2
EA1 elastic	.0616	.0505	.0764	.0188
EA1 post-yield	.0922	.0579	.0970	.0034
EA2 elastic	.0581	.0509	.0733	.0217
EA2 post-yield	.0873	.0564	.0942	.0053
EA3 elastic	.0540	.0534	.0692	.0259
EA3 post-yield	.0791	.0540	.0893	.0088

Allowing

$$V_n(t) = \omega_n D_n(t)$$

and

$$A_n(t) = \omega_n^2 D_n(t)$$

the floor displacements and acceleration responses can be written as

$$\underline{v}(t) = \underline{\phi}_1 P_1 D_1(t) + \underline{\phi}_2 P_2 D_2(t) + \ldots .$$

$$\ddot{\underline{v}}(t) = \underline{\phi}_1 P_1 A_1(t) + \underline{\phi}_2 P_2 A_2(t) + \ldots .$$

where $P_n = \frac{L_n}{M_n}$ is the mode participation factor.

The values of P_n are

Foundation	P_1	P_2
EA1 elastic	1.24	0.372
EA1 post-yield	1.05	0.059
EA2 elastic	1.26	0.426
EA2 post-yield	1.08	0.094
EA3 elastic	1.28	0.485
EA3 post-yield	1.13	0.163

Thus, the mode superposition response of the EA1 foundation would be

$$\underline{v}(t) = \underline{\phi}_{1e}\ (1.24)\ D_{1e}(t) + \underline{\phi}_{2e}\ (0.372)\ D_{2e}(t) + \ldots \text{(elastic)}$$

$$\underline{v}(t) = \underline{\phi}_{1y}\ (1.05)\ D_{1y}(t) + \underline{\phi}_{2y}\ (0.059)\ D_{2y}(t) + \ldots \text{(post-yield)}$$

and the acceleration response is similar, substituting $A_{1e}(t)$ for $D_{1e}(t)$, etc.

This simple analysis shows that second mode participation of the structure is strongly decreased when the base condition is yielded. In effect, observed second mode response results when the base condition is elastic, or from changes in base stiffness. The net effect is that a soft story structure of similar proportions to the model structure may experience smaller second (and higher) mode response than the same structure on a conventional rigid base. This is in keeping with results given by Veletsos (25) where he says that the closer the first mode shape is to rigid body translation of the floor masses, the smaller the higher mode contributions. Inspection of the analyses' first mode shapes shows that the first mode shape does approach rigid body translation after the base condition is yielded.

For the yielded base condition, the second mode shape varies almost linearly from +1.00 to -1.00 from the top to bottom of the structure. This result is not far different when the base is elastic. Thus, as the floor masses of this structure were almost equal, second mode response column shears will cancel at the base level, and be greatest at the first and second floor levels. This was observed in the test results.

If the stiffness of the model had tapered significantly with height, as is typical with tall buildings, second mode shears will not necessarily be small at the base of the structure.

To see how accurate this analysis is by substituting maximum

values from response spectra for $D_{1e}(t)$, etc., modal viscous damping values must be assumed.

As mentioned earlier, the rubber bearings provide about 10% first mode viscous damping when no EA devices are used. Second mode damping values of about 1% are appropriate for both the elastic and post-yield base conditions. However, it is difficult to assign a viscous damping value to the post-yield base condition.

The energy dissipation mechanism for the energy-absorbing device is clearly stiffness dependent, and varies with peak displacements of the device.

Let w_d be the area under the force-displacement diagrams of the devices and rubber bearings, i.e., the energy loss per cycle. Then

$$w_d = 4 \gamma d F_{EA} + 2\xi_R \pi k_R d^2$$

where

d = one-half of maximum peak to peak displacement of the energy absorber

F_{EA} = one-half of maximum peak to peak force of the energy absorber

γ = shape factor of the energy absorber

ξ_R = % critical damping of structure on rubber bearings alone

k_R = horizontal shear stiffness of rubber bearings

For a rigid-plastic system, $\gamma = 1$. Figure 8.2.1 describes how γ varies with d. While ξ_R for rubber varies with displacement and frequency in general, it is nearly constant for the range of values observed during the tests.

To equate the actual hysteretic energy behavior with viscous damping, a spring stiffness k_{EA} must be assumed. A simple assumption that

proves to give good analytical results is

$$k_{EA} = F/d$$

the secant stiffness at maximum deflection. Figure 8.2.2 describes this relationship for the EA1 device. The data for Figures 8.2.1 and 8.2.2 are derived from the EC 750 and Pacoima Dam 500 EA1 foundation tests. Since the hysteretic energy loss by the devices is not frequency dependent, these results should apply for any type of structural system above the base.

The associated strain energy is

$$w_s = \frac{k_{EA} d^2}{2} + \frac{k_R d^2}{2}$$

The viscous damping ratio is defined as

$$\xi = \frac{w_d}{4\pi w_s}$$

Substituting values for w_d and w_s gives

$$\xi_{1\ eff} = \left(\frac{2\gamma}{\pi} - \xi_R\right)\left[\frac{k_{EA}}{k_{EA} + k_R}\right] + \xi_R$$

The test results showed that maximum displacements always occured when the base condition was yielded. This indicates that displacement response may be described by

$$\underline{v}(t) = \underline{\phi}_{1eff} P_{1eff} D_{1eff}(t) + \underline{\phi}_{2eff} P_{2e} D_{2eff}(t) + \ldots$$

and

$$\underline{\ddot{v}}(t) = \underline{\phi}_{1eff} P_{1eff} A_{1eff}(t) + \underline{\phi}_{2eff} P_{2e} A_{2eff}(t) + \ldots$$

where the subscript 1eff, 2eff, etc. denotes $\underline{\phi}$, P, D and A values associated with the effective natural frequencies the structure is vibrating at (f_{1eff}, f_{2eff}, etc.) after the base has yielded.

Since the base is changing from elastic to yield and yield to elastic conditions four times every large displacement cycle, neither the elastic nor yielded base analyses (as in table 8.1.2) will accurately predict the actual $f_{n\ eff}$. One expects that the further the device yields, the lower will be f_{1eff}, as the structure will be at the yielded frequency, f_{1y}, for a longer duration of time. Figure 8.2.3 describes this phenomenon. The data for this figure are taken from the experimental data for the EA1 foundation tests. The correlation coefficient for the linear regression equation for this data

$$T_{1eff} = 0.271\ d + 0.582$$

where

$$T_{1eff} = \frac{1}{f_{1eff}}$$

is

$$r = 0.969$$

If we assume that $\underline{\phi}_{1e}$ changes to $\underline{\phi}_{1y}$ and P_{1e} changes to P_{1y} in a linear fashion depending upon f_{1eff}, then

$$C = \frac{T_{1eff} - T_{1e}}{T_{1y} - T_{1e}}$$

and

$$\underline{\phi}_{1eff} = \underline{\phi}_{1e} + C(\underline{\phi}_{1y} - \underline{\phi}_{1e})$$

and

$$P_{1eff} = P_{1e} + C(P_{1y} - P_{1e})$$

The experimental tests showed that the second mode shape is much closer to $\underline{\phi}_{2y}$ than $\underline{\phi}_{2e}$. Since C is directly proportional to the amount of

yielding in the base, then

$$\underline{\phi}_{2eff} = \underline{\phi}_{2e} + C(\underline{\phi}_{2y} - \underline{\phi}_{2e})$$

and

$$T_{2eff} = \frac{1}{f_{2eff}} = T_{2e} + C(T_{2y} - T_{2e})$$

To account for second mode participation by elastic and yield base transitions, P_{2e} is used in the analysis. The may be conservative as P_{2eff} is typically very small.

A simple preliminary design technique based upon response spectra can be developed using these formulas. Since the structure actually undergoes frequency changes during the test, the SDOF response spectra values may not give the true maximum response of the structure, but should provide an upper bound on the response.

8.3 Elastic Design I - Design Building

Do a normal design based upon code vertical loads and wind loads. The structure should be completely elastic.

II - Design Rubber Bearings

Vertical strength of the bearings = F.S. x W, where W = maximum dead load + live load. F. S. = factor of safety and should exceed 2. If we assume that there will be no tension forces in the pads due to overturning moments, then the maximum possible vertical load on one-half the bearings will be the total weight of the building (this will depend on the configuration of the columns of course).

Minimum vertical stiffness of the bearings, k_{vert}

$$k_{vert} = 4\pi^2 f_{vert}^2 W/g$$

where f = minimum desirable vertical frequency to minimize rocking motion. (f_{vert} during the tests was near 9 Hz. Preliminary analyses indicate that

values as low as 6 Hz may still be sufficient.)

Lateral stiffness, k_R, should be chosen to provide in combination with the energy-absorbing devices a suitable post-yield base stiffness (high for small base shifts, low for small base shears).

III - Design Energy-Absorbing Devices

The yield level should be above the maximum base shear due to maximum wind loading and small earthquakes. The ideal yield force is a function of the cost to replace the devices, and possible utility repairs, and the benefit of reduced building damage and lower initial construction cost.

IV - Do Analyses

Do eigenvalue analyses for both the elastic and yielded base conditions.

V - Evaluate Damping Values

Assume a peak displacement of the energy absorber. As explained in Section 6.1.1, this should be one-half the maximum peak to peak displacement. Calculate $f_{n\ eff}$, $\underline{\phi}_{n\ eff}$, and $P_{1\ eff}$. From the properties of the device, get the equivalent first mode damping value, $\xi_{1\ eff}$. Assume $\xi_{2\ eff}$, $\xi_{3\ eff}$, etc., to be appropriate with higher mode damping values for normal structures. Figure 8.3.1 gives the response spectra for the Pacoima Dam motion for 30, 35, 40 and 45% critical damping.

VI - Evaluate Response

From the appropriate design spectra, get

$$\underline{v}_{max} = \underline{\phi}_{1\ eff}\, P_{1\ eff}\, D(f_{1\ eff}, \xi_{1\ eff}) + \underline{\phi}_{2\ eff}\, P_{2e}\, D(f_{2\ eff}, \xi_{2\ eff}) + \cdots$$

$$\underline{\ddot{v}}_{max} = \underline{\phi}_{1\ eff}\, P_{1\ eff}\, A(f_{1\ eff}, \xi_{1\ eff}) + \cdots \qquad j \text{ modes}$$

Base shears and overturning moments are then evaluated by

$$V_o = \sum_{j=1}^{n} m_i\, \ddot{v}_{ji\ max}$$

$$M_o = \sum_{j=1}^{n} m_i \ddot{V}_{ji\ max}\ x_i$$

where

m_i = floor i mass

x_i = height of floor mass i above base.

If the computed base displacement is not equal to the assumed displacement, new values for $\xi_{n\ eff}$ and $f_{n\ eff}$ should be assumed and step VI repeated.

The results for these elastic analyses are in Table 8.3.1 a and b. The experimental floor displacment values are different from those in Table 5.1 as thay are one-half peak to peak displacements. The assumed base displacement was taken from the experimental data.

In general, the elastic analysis first mode displacement and acceleration results are very good. Since these results are fairly dependent upon the assumed damping value, the initial decision to use secant stiffness for k_{EA} seems reasonable.

The second mode accelerations and shears are not as well correlated to the experimental data. There are two reasons for this. First, there is the somewhat arbitrary (and from the results, conservative), choice for $P_{2eff} = P_{2e}$. Second, as pointed out in section 7, the experimental second mode vibration may have been increased due to the non rigid first floor beam-column connections.

The root mean square combination of the first two modes gives excellent displacement correlation between experiment and elastic analysis. However, the elastic analysis gives no indication of the true peak displacements, as it does not take into account nonlinear base shifting.

9. Conclusions

9.1 Soft Story Energy-Absorbing Foundation Structure versus a Fixed Foundation Structure

It is difficult to make direct comparisons between fixed base and soft story based structures due to their inherently different frequencies. However, for a single structure designed with a soft story EA foundation rather than a conventional fixed foundation, the following can be expected:

- The soft story structure will respond at a frequency one half or less than that of the fixed base structure.

- The soft story sturcture will respond with effective first mode critical damping of 30% or more.

- The soft story structure will exhibit localized yielding in the energy-absorbing device. A mild steel device has an expected low-cycle fatigue life well over 300 cycles and need not be replaced after every earthquake. There may be no yielding in any of the frame members.

- The soft story structure will require foundation level utility connections capable of a few inches of drift.

- The design cost of the special foundation is easily offset by the structure's lower cost due to decreased lateral loads. In addition, the soft story structure's long term cost is much less due to reduced earthquake caused damages.

- Since a soft story structure requires less lateral bracing and shear walls, it is architecturally more flexible. Due to the reduced number of lateral support systems, the structure has increased floor space than a conventional fixed foundation structure.

9.2 Response of the Soft Story Structure

For wind loading and small earthquakes, the soft story structure behaves as a stiff rigid foundation structure.

A large earthquake will cause the soft story to yield. This is accompanied by an increase in first mode period and a large increase in first mode damping. Thus the yielding of the energy-absorbing device will strongly reduce the first mode response of the soft story structure.

The second and higher mode response of the soft story structure is not greatly changed by the yielding of the devices.

The combination of first, second and higher mode responses may give maximum floor level shears above the base level for regularly proportioned structures.

9.3 Energy-Absorbing Device Performance

The two mild steel energy-absorbing devices performed well in over 20 earthquake tests. Neither showed fatigue or weld cracks.

The special TRIP steel device did show fatigue cracks after a large number of cycles. These did not seriously decrease its capacity. However, TRIP steel's high alloy content makes it a poorly weldable material. The cracked welds between torsion bar and moment arms did significantly reduce the device's performance. To date, soft mild steel is the best material for these devices.

The torsion devices are ideally suited to earthquake isolation systems as their two way plastic behavior is unaffected by tension-compression buckling problems; they provide a positive limit to the maximum deflections of the base floor; they have long life under low-cycle large plastic strains; they can easily be adapted for displacements in two directions.

9.4 Natural Rubber Bearings

The rubber bearings performed well during over 130 earthquake tests.

The vertical stiffness of the bearings should be as high as possible to reduce possible frame rocking.

The horizontal stiffness of the bearings should be as low as possible to reduce the post-yield stiffness of the soft story EA foundation systems.

Natural rubber is an excellent material for the bearings.

9.5 Base Floor Shifting

The nonlinear nature of the soft story foundation allows the base floor to have permanent shifts at the end of an earthquake. The amount of final shift is not necessarily proportional to the magnitude of the earthquake. The amount of shift is a function of both the soft story's post-yield stiffness and the peak deflections of the energy-absorbing devices. Shifting will not tend to increase in the same direction with subsequent earthquakes.

9.6 Effects of Energy-Absorbing Device Yield Force and Post-Yield Stiffness

The device's yield force should be chosen so that maximum base shears due to wind loads (3% to 6% of the structure's weight) will not cause the device to yield. The best performing device during the tests had a yield force of 10% of the model structure's weight. In general, the lower this yield force is, the lower the structural response will be.

A large post-yield stiffness (greater than 20% of elastic stiffness) will reduce the tendency for base floor shifting. This will in general increase the structure's response. The best performing device during the

test had a post-yield stiffness of 5% of its elastic stiffness. As deflections are limited by the device's geometry, the post-yield force should be as low as possible.

9.7 Analysis and Design

A nonlinear analysis was shown to give reasonable prediction of structural response for the soft story foundation system. The properties of the nonlinear torsion device element were varied to show that the energy absorption by the device reduces structural response by a large amount.

The elastic analysis described shows that the highly nonlinear system can be reasonably modelled as the root-mean-square combination of effective first and higher mode responses.

Based upon the elastic analysis, an approximate design method is suggested. This design method gives good results for the actual earthquake tests performed, with the aid of simple elastic SDOF response spectra.

10 References

1. Derham, C. J., Wootton, L. R., and Learoyd, S. B. B., "Vibration Isolation and Earthquake Protection of Buildings by Natural Rubber Springs," Natural Rubber Technology, Vol 6, part 2, 1975.

2. Ikonomu, A. S., "The Earthquake Guarding System," Technica Chronica, Vol 41, 1972.

3. Derham, C. J. and Learoyd, S. B. B., "The Use of Natural Rubber Springs for Earthquake Protection," Proceedings, 4th South East Asian Conference on Soil Engineering, Kuala Lampur, April, 1975.

4. Plichon, C. "Hooped Rubber Bearings and Frictional Plates: A Modern Antiseismic Engineering Technique," Proceedings, Specialist Meeting on the Anti-Seismic Design of Nuclear Installations, OECD, Paris, December 1975.

5. Delfosse, G. C., "The GAPEC System; A New Highly Effective Aseismic Design," Centre National de la Recherche Scientifique, France.

6. Matsushita, K., and Izumi, M., "Studies on Mechanisms to Decrease Earthquake Forces Applied to Buildings," Proceedings of 4th World Conference on Earthquake Engineering, Santiago, January 1969, Vol II.

7. Martel, R. R., "The Effects of Earthquakes on Buildings with a Flexible First Story," Bulletin of the Seismological Society of America, Vol. 19, No. 3, Septermber 1929.

8. Green, N. B., "Flexible 'First Story' Construction for Earthquake Resistance," Transactions, ASCE, Vol 100, 1935, p. 645.

9. Fintel, M., and Khan, F. R. "Shock Absorbing Soft Story Concept for Multistory Earthquake Structures," ACI Journal, Vol. 66, May 1969.

10. Caspe, M. S., "Earthquake Isolation of Multistory Concrete Structures," ACI Journal, November 1970.

11. Clough, R. W., Clough, D. P., and Chropra, A., "Earthquake Resistance of Buildings with a Soft First Story," Earthquake Engineering and Structural Dynamics, Vol. I, P. 347, 1973.

12. Lee, D. M., and Medland, I. C., "Base-Isolation for Earthquake Protection of Multi-Story Shear Structures," Proceedings, 6th Australian Conference on Mechanics of Structures and Materials, Christchurch, New Zealand, 1977.

13. Priestly, M. J. N., Crosbie, R. L., and Carr, A. J., "Seismic Forces in Base Isolated Structures," Bulletin of the New Zealand Society for Earthquake Engineering, Vol. 10, No. 2, June 1977.

14. Kelly, J. M, Skinner, R. I., and Heine, A. J., "Mechanisms of Energy Absorption in Special Devices," Bulletin of the New Zealand Society for Earthquake Engineering, Vol 5, p. 63, 1972.

15. Kelly, J. M., Skinner, R. I., and Heine, A. J., "Hysteretic Dampers for Earthquake Resistant Structures," International Journal of Earthquake Engineering and Structural Dynamics, Vol 3, pp. 287-297, 1975.

16. Kelly, J. M, and Tsztoo, D., "Earthquake Simulation Testing of a Stepping Frame with Energy-Absorbing Devices," EERC-77-17, 1977.

17. Natural Rubber in Bridge Bearings, Brochure, Malayan Rubber Fund Board.

18. Derham, C. J., Plunkett, A. P., "Fire Resistance of Steel-Laminated Natural Rubber Bearings," Natural Rubber Technology, Vol 7, Part 2, pp. 113-123, 1976.

19. Clough, R. W., and Tang, D. T., "Earthquake Simulator Study of a Steel Frame Structure, Volume I, Experimental Results," Report No. EERC 75-6, Earthquake Engineering Research Center, U. C. Berkeley, April, 1975.

20. Kelly, J. M. and Eidinger, J. M., "Earthquake Isolation Systems - Experimental Results," CANCAM, Vancouver, May 1977.

21. Kelly, J. M., Eidinger, J. M., Derham, C. J., et al, "Natural Rubber Bearings for Earthquake Isolation, to appear in NR Technology, (1977).

22. Nigam, N. C., and Jennings, P. C., "SPECEQ-SPECUQ - Digital Calculations of Response Spectra from Strong Motion Earthquake Records," NISEE, June 1968, Cal Tech.

23. Bertero, V. V., and Bresler, B., "Failure Criteria (Limit States)," Panel on Design and Engineering Decisions, 6WCEE, New Delhi, January 1977.

24. Powell, G. H., and Kanaan, A. E., "DRAIN-2D - A General Purpose Computer Program for Dynamic Analysis of Inelastic Plane Structures," EERC 73-6 and EERC 73-22, April 1973, revised August 1975.

25. Veletsos, A. S., and Vann, W. P., "Response of Ground-Excited Elastoplastic Systems," Journal of the Structural Division, ASCE, April 1971.

	BASE FLOOR	1ST FLOOR	2ND FLOOR	3RD FLOOR
Concrete Blocks	8100	8250	8000	8160
Columns	203	358	310	155
Girders	1780	288	288	288
Cross Beams	0	360	360	360
Misc.	740	460	460	460
Rubber Bearings	120	0	0	0
TOTAL (In Lbs.)	10,943	9,716	9,418	9,423
TOTAL, ALL FLOORS	39,500 pounds			

TABLE 3.1.1. Weight of Structural Components and Concrete Blocks

EARTHQUAKE	SPAN	DISPLACEMENT		ACCELERATION	
		Max. (inch)	Min. (inch)	Max. (inch)	Min. (inch)
EL CENTRO	450	2.47	-1.92	.270	-.325
	600	3.28	-2.56	.348	-.445
	750	4.11	-3.21	.486	-.627
PACOIMA DAM	200	1.10	-0.94	.254	-.243
	400	2.21	-1.90	.529	-.504
	500	2.77	-2.37	.628	-.616
PARKFIELD	500	2.45	-1.31	.161	-.237

TABLE 3.2.1. Input Earthquake Records

DEVICE	EA1	EA2	EA3
TYPE	Mild Steel	Mild Steel	Trip Steel
ELASTIC STIFFNESS	15 Kip/in	19 Kip/in	27 Kip/in
POST-YIELD STIFFNESS	0.2-1.3 k/in	.66-2.8 k/in	2.5-7.3 k/in
POST YIELD STIFFNESS - % OF ELASTIC STIFFNESS	1.3-8.7%	3.5-15%	9.3-27%
EARTHQUAKE AND SPAN			
EL CENTRO			
450	X	X	X
600	X		X
750	X		X
PACOIMA DAM			
200	X		
400	X	X	
500	X		X
PARKFIELD			
500	X	X	X

TABLE 3.2.2. Tests Performed On Energy Absorbers and Energy Absorber Characteristics

		EC 900-II Fix Base		EC 750 EA1		EC 750 EA3		EC 400-350 Rubber	
		Max.	Min.	Max.	Min.	Max.	Min.	Max.	Min.
Floor Disp. Rel. To Table (Inches)	3RD	3.05	-3.24	2.77	-3.31	3.71	-2.77	3.09	-2.25
	2ND	2.34	-2.42	2.60	-3.19	3.36	-2.58	3.05	-2.22
	1ST	1.33	-1.30	2.31	-2.93	2.84	-2.27	3.02	-2.15
	BASE			1.79	-2.60	1.94	-1.62	2.88	-2.15
Table Disp. (Inches)		4.18	-2.50	4.11	-3.21	4.12	-3.22	2.19	-1.71
Absolute Floor Acceleration (G)	3RD	1.95	-1.56	.57	-.63	.99	-.79	.11	-.11
	2ND	1.28	-1.37	.36	-.52	.61	-.64	.10	-.11
	1ST	1.02	-1.02	.40	-.52	.84	-.55	.10	-.10
	BASE			.48	-.37	.86	-.50	.09	-.09
Table Acceleration (G)		.61	-.57	.49	-.63	.57	-.54	.27	-.29

TABLE 5.1 Extreme Values El Centro 900, 750, 400

		EC 450 Fix Base		EC 450 EA1		EC 450 EA2		EC 450 EA3	
		Max.	Min.	Max.	Min.	Max.	Min.	Max.	Min.
Floor Disp. Rel. To Table (Inches)	3RD	2.64	-2.56	1.86	-1.40	2.07	-1.40	2.48	-2.01
	2ND	2.09	-2.07	1.76	-1.34	1.94	-1.29	2.24	-1.82
	1ST	1.24	-1.27	1.56	-1.26	1.72	-1.17	1.88	-1.59
	BASE			1.42	-1.09	1.40	-0.96	1.28	-1.06
Table Disp. (Inches)		2.38	-1.77	2.47	-1.92	2.46	-1.92	2.47	-1.92
Absolute Floor Acceleration (G)	3RD	1.29	-1.10	.31	-.39	.48	-.49	.62	-.59
	2ND	.99	-.96	.21	-.29	.35	-.42	.41	-.49
	1ST	.67	-.70	.27	-.25	.42	-.37	.59	-.41
	BASE			.33	-.30	.42	-.41	.59	-.38
Table Acceleration (G)		.30	-.36	.27	-.33	.30	-.35	.26	-.33

TABLE 5.2 Extreme Values El Centro 450

		PARKFIELD 500 Fix Base		PARKFIELD 500 EA1		PARKFIELD 500 EA2		PARKFIELD 500 EA3	
		Max.	Min.	Max.	Min.	Max.	Min.	Max.	Min.
Floor Disp. Rel. To Table (Inches)	3RD	1.99	-1.52	1.99	-1.05	1.50	-1.33	1.92	-1.79
	2ND	1.58	-1.22	1.92	-0.97	1.37	-1.25	1.76	-1.64
	1ST	0.98	-0.75	1.77	-0.85	1.19	-1.15	1.48	-1.41
	BASE			1.60	-0.66	0.96	-0.92	1.04	-0.98
Table Disp. (Inches)		2.48	-1.30	2.45	-1.31	2.45	-1.31	2.45	-1.32
Absolute Floor Acceleration (G)	3RD	.78	-.85	.30	-.32	.39	-.38	.33	-.37
	2ND	.58	-.63	.24	-.25	.30	-.35	.29	-.36
	1ST	.44	-.52	.22	-.26	.29	-.39	.27	-.35
	BASE			.27	-.29	.35	-.33	.33	-.28
Table Acceleration (G)		.19	-.25	.16	-.24	.21	-.21	.16	-.18

TABLE 5.3 Extreme Values Parkfield 500

		PACOIMA DAM 400 EA1		PACOIMA DAM 500 EA1		PACOIMA DAM 400 EA2		PACOIMA DAM 500 EA3	
		Max.	Min.	Max.	Min.	Max.	Min.	Max.	Min.
Floor Disp. Rel. To Table (Inches)	3RD	2.19	-2.08	3.23	-2.76	2.58	-1.73	3.30	-2.79
	2ND	2.03	-2.01	3.10	-2.66	2.40	-1.61	3.00	-2.55
	1ST	1.80	-1.89	2.82	-2.48	2.12	-1.45	2.51	-2.14
	BASE	1.57	-1.67	2.49	-2.15	1.72	-1.18	1.48	-1.81
Table Disp. (Inches)		2.21	-1.89	2.77	-2.37	2.21	-1.89	2.78	-2.3
Absolute Floor Acceleration (G)	3RD	.43	-.51	.58	-.59	.59	-.55	.60	-.67
	2ND	.34	-.36	.45	-.42	.40	-.46	.48	-.57
	1ST	.28	-.35	.34	-.49	.38	-.42	.45	-.41
	BASE	.33	-.42	.51	-.44	.51	-.46	.58	-.43
Table Acceleration (G)		.53	-.47	.63	-.62	.53	-.50	.69	-.57

TABLE 5.4 Extreme Values Pacoima Dam 400, 500

	SPAN 450	AT TIME (SEC.)	SPAN 600	AT TIME (SEC.)	Δ%	SPAN 750	AT TIME (SEC.)	Δ%
Table Displacement	2.47 inch	3.65	3.28	3.65	+33%	4.11	3.65	+66%
Energy Absorber Disp.	1.42 inch	2.72	1.55	12.37	+ 9%	2.56	5.23	+80%
Energy Absorber Force	5.85 kip	2.70	6.74	2.70	+15%	7.91	5.21	+35%
First Floor Shear	7.60 kip	2.64	9.35	2.64	+23%	10.80	2.66	+42%
Base Floor Shear	8.20 kip	2.70	9.23	2.70	+13%	10.90	5.21	+33%
Overturning Moment	104. k-ft	2.64	112.	2.62	+ 8%	117.	2.68	+13%
First Floor Drift	.24 inch	2.66	.42	2.64	+74%	.73	2.68	+205%
Third Floor Accl.	.39 g	2.62	.45	2.58	+16%	.63	2.72	+62%

TABLE 6.1.1.1. Effect of Increasing El Centro Input Motion to EA1 Foundation

	SPAN 450	AT TIME (SEC.)	SPAN 600	AT TIME (SEC.)	Δ%	SPAN 750	AT TIME (SEC.)	Δ%
Table Displacement	2.47 inch	3.65	3.29	3.65	+33%	4.12	3.65	+66%
Energy Absorber Disp.	1.27 inch	2.70	1.58	2.68	+24%	1.93	2.70	+52%
Energy Absorber Force	11.7 kip	2.68	13.7	2.66	+17%	15.8	2.68	+35%
First Floor Shear	11.7 kip	2.62	13.6	2.64	+16%	15.2	2.72	+30%
Base Floor Shear	14.0 kip	2.68	16.6	2.66	+19%	18.9	2.68	+35%
Overturning Moment	153. k-ft	2.66	183.	2.66	+20%	202.	2.66	+32%
First Floor Drift	.61 inch	12.74	.75	2.72	+23%	.97	2.74	+59%
Third Floor Accl.	.63 g	3.12	.88	3.10	+40%	.99	3.12	+58%

TABLE 6.1.2.1. Effect of Increasing El Centro Input Motion to EA3 Foundation

	SPAN 200	AT TIME (SEC.)	SPAN 400	AT TIME (SEC.)	Δ%	SPAN 500	AT TIME (SEC.)	Δ%
Table Displacement	1.10 inch	4.25	2.21	4.25	+101%	2.77	4.25	+152%
Energy Absorber Disp.	1.09 inch	7.21	1.66	3.90	+52%	2.44	4.53	+124%
Energy Absorber Force	5.09 kip	7.19	6.70	4.47	+32%	7.91	4.51	+55%
First Floor Shear	6.37 kip	7.13	8.81	7.15	+38%	9.44	9.41	+48%
Base Floor Shear	6.91 kip	7.21	8.99	4.47	+30%	11.2	4.51	+62%
Overturning Moment	100. k-ft	7.15	133.	7.15	+33%	137.	9.39	+ 3%
First Floor Drift	.26 inch	3.84	.34	9.76	+30%	.50	9.43	+49%
Third Floor Accl.	.33 g	9.23	.51	7.11	+52%	.59	9.78	+76%

TABLE 6.1.3.1. Effect of Increasing Pacoima Dam Input Motion to EA1 Foundation

	SPAN 200	AT TIME (SEC.)	SPAN 400	AT TIME (SEC.)	Δ%	SPAN 500	AT TIME (SEC.)	Δ%
Table Displacement	1.10 inch	4.25	2.21	4.25	+101%	2.77	4.25	+152%
Energy Absorber Disp.	0.44 inch	3.86	1.66	3.90	+277%	2.44	4.53	+454%
Energy Absorber Force	4.84 kip	3.80	6.70	4.47	+38%	7.91	4.51	+63%
First Floor Shear	5.53 kip	4.02	7.33	4.65	+33%	8.51	4.49	+54%
Base Floor Shear	5.73 kip	4.06	8.99	4.47	+57%	11.2	4.51	+95%
Overturning Moment	86.5 k-ft	3.80	116.	4.43	+34%	135.	4.47	+16%
First Floor Drift	.26 inch	3.84	.24	5.35	- 7%	.43	5.13	+77%
Third Floor Accl.	.24 g	3.80	.41	6.47	+69%	.36	5.35	+49%

TABLE 6.1.3.2. Effect if Increasing Pacoima Dam Input Motion (Just First 6.5 Seconds) to EA1 Foundation

	EL CENTRO 750 EA1			PARKFIELD 500 EA1		PACOIMA DAM 500 EA1		EL CENTRO 750 EA3	
	Experi-mental	Analytical Hysteretic[1]	Elastic[2]	Exper.	Anal.[1]	Exper.	Anal.[1]	Exper.	Anal.[1]
Floor Disp.									
3RD	3.31 inch	2.90	5.41	1.99	2.31	3.23	3.14	3.71	3.50
2ND	3.19	2.70	5.34	1.92	2.26	3.10	3.05	3.36	3.27
1ST	2.93	2.52	5.13	1.77	2.11	2.82	2.88	2.84	2.89
BASE	2.60	2.37	4.80	1.60	1.89	2.44	2.65	1.94	2.41
Floor Shear									
3RD	5.89 Kip	6.18	8.16	2.97	4.56	5.54	7.60	9.30	7.78
2ND	7.06	8.42	10.50	5.18	5.80	8.15	9.02	11.67	10.64
1ST	10.83	10.20	12.50	6.79	6.48	9.44	9.44	15.23	14.82
BASE	10.85	9.17	14.50	8.31	7.65	11.16	10.66	18.89	19.81
Story Drift									
3RD	.22 inch	.23	.31	.14	.16	.24	.30	.36	.26
2ND	.35	.33	.42	.25	.19	.34	.32	.53	.44
1ST	.73	.39	.47	.30	.23	.50	.35	.97	.57

NOTES
1 - Using Bilinear Hysteretic Element
2 - Using Bilinear Elastic Element to Show Effect of Energy Absorption

TABLE 7.1. Nonlinear Analysis Comparisons

	FIX FOUNDATION 3 Floor Model		FIX FOUNDATION 4 Floor Model		RUBBER FOUNDATION 4 Floor Model		
	1ST[1] Mode	2ND[1] Mode	1ST[1] Mode	2ND[1] Mode	1ST[2] Mode	2ND[2] Mode	3RD[2] Mode
FREQUENCY	2.27 Hz	7.83 Hz	2.05 Hz	7.33 Hz	0.58 Hz	3.84 Hz	8.89 Hz
MODE SHAPE							
3RD FLOOR	1.00	1.00	1.00	1.00	1.00	1.00	1.00
2ND FLOOR	0.77	-0.62	0.78	-0.25	0.98	0.42	-0.85
1ST FLOOR	0.41	-1.23	0.46	-1.00	0.96	-0.33	-1.10
BASE FLOOR	--	--	--	--	0.92	-1.02	0.88

1 - Experimental Results. 2 - Analytical Results

TABLE 8.1.1. Frequencies and Mode Shapes for FIX and RUBBER Foundations

	ELASTIC ENERGY ABSORBER		YIELDED ENERGY ABSORBER	
	1ST MODE	2ND MODE	1ST MODE	2ND MODE
EA1 FOUNDATION	ELASTIC STIFFNESS = 15 K/IN		YIELDED STIFFNESS = 0.8 K/IN	
FREQUENCY	1.56 Hz	4.64 Hz	0.682 Hz	3.84 Hz
3RD FLOOR	1.000	-0.773	1.000	-0.969
2ND FLOOR	0.883	-0.161	0.977	-0.398
1ST FLOOR	0.696	0.529	0.939	0.336
BASE FLOOR	0.461	1.000	0.889	1.000
EA2 FOUNDATION	ELASTIC STIFFNESS = 19 K/IN		YIELDED STIFFNESS = 2.0 K/IN	
FREQUENCY	1.66 Hz	4.86 Hz	0.846 Hz	3.91 Hz
3RD FLOOR	1.000	-0.755	1.000	-0.941
2ND FLOOR	0.869	-0.114	0.965	-0.370
1ST FLOOR	0.658	0.578	0.907	0.356
BASE FLOOR	0.397	1.000	0.831	1.000
EA3 FOUNDATION	ELASTIC STIFFNESS = 27 K/IN		YIELDED STIFFNESS = 4.5 K/IN	
FREQUENCY	1.79 Hz	5.23 Hz	1.08 Hz	4.05 Hz
3RD FLOOR	1.000	-0.751	1.000	-0.890
2ND FLOOR	0.849	-0.039	0.943	-0.318
1ST FLOOR	0.609	0.669	0.848	0.394
BASE FLOOR	0.313	1.000	0.727	1.000

TABLE 8.1.2. Frequencies and Mode Shapes for EA Foundations

	EL CENTRO 750	PACOIMA DAM 500
Assumed Energy Absorber Displacement (Inches)	1.85	2.28
T_{1eff} (Seconds)	1.08	1.21
f_{1eff} (Hz)	0.923	0.826
γ	0.65	0.70
ξ_R	0.10	0.10
K_{EA} (K/IN)	3.30	3.00
K_R (K/IN)	1.20	1.20
ξ_{1eff}	0.33	0.35
P_{1eff}	1.14	1.18
ϕ_{1eff}	1.000 0.933 0.825 0.689	1.000 0.947 0.861 0.751
T_{2eff} (Seconds)	0.239	0.246
f_{2eff} (Hz)	4.18	4.06
ξ_2	0.01	0.01
P_2	0.372	0.372
ϕ_{2eff}	-0.877 -0.287 0.426 1.000	-0.906 -0.322 0.398 1.000
$D_1(f_{1eff}, \xi_{1eff})$ (Inch)	2.17	2.78
$D_2(f_{2eff}, \xi_2)$ (Inch)	0.897	1.35
$A_1(f_{1eff}, \xi_{1eff})$ (G)	0.291	0.277
$A_2(f_{2eff}, \xi_2)$ (G)	1.54	2.39

TABLE 8.3.1a. Elastic Analysis Calculations

EL CENTRO 750 EA1				
	Experimental	Analytical		
		1ST Mode	2ND Mode	R M S
3RD Flr Disp	2.72 inch	2.47	.29	2.49 inch
2ND Flr Disp	2.56	2.31	.10	2.31
1ST Flr Disp	2.32	2.04	.14	2.04
Base Flr Disp	1.85	1.70	.33	1.74
3RD Flr Accl	.63 g	.33	.50	.60 g
2ND Flr Accl	.52	.31	.16	.35
1ST Flr Accl	.52	.27	.24	.37
Base Flr Accl	.48	.23	.57	.62
3RD Flr Shear	5.89 kip	3.13	4.73	5.67 kip
2ND Flr Shear	7.06	6.05	6.27	8.71
1ST Flr Shear	10.83	8.71	3.90	9.54
Base Flr Shear	10.85	11.21	-2.35	11.45
1ST Flr Drift	.73 inch	.34	.19	.39 inch

PACOIMA DAM 500 EA1				
	Experimental	Analytical		
		1ST Mode	2ND Mode	R M S
3RD Flr Disp	3.02 inch	3.28	.46	3.31 inch
2ND Flr Disp	2.89	3.11	.16	3.11
1ST Flr Disp	2.72	2.83	.20	2.84
Base Flr Disp	2.31	2.47	.50	2.52
3RD Flr Accl	.59 g	.33	.80	.87 g
2ND Flr Accl	.45	.31	.29	.42
1ST Flr Accl	.49	.28	.35	.45
Base Flr Accl	.51	.25	.89	.92
3RD Flr Shear	5.54 kip	3.08	7.58	8.18 kip
2ND Flr Shear	8.15	6.00	10.28	11.90
1ST Flr Shear	9.44	8.73	6.84	11.09
Base Flr Shear	11.16	11.41	-2.89	11.77
1ST Flr Drift	.50 inch	.36	.30	.47 inch

TABLE 8.3.1b Elastic Analysis Comparisons

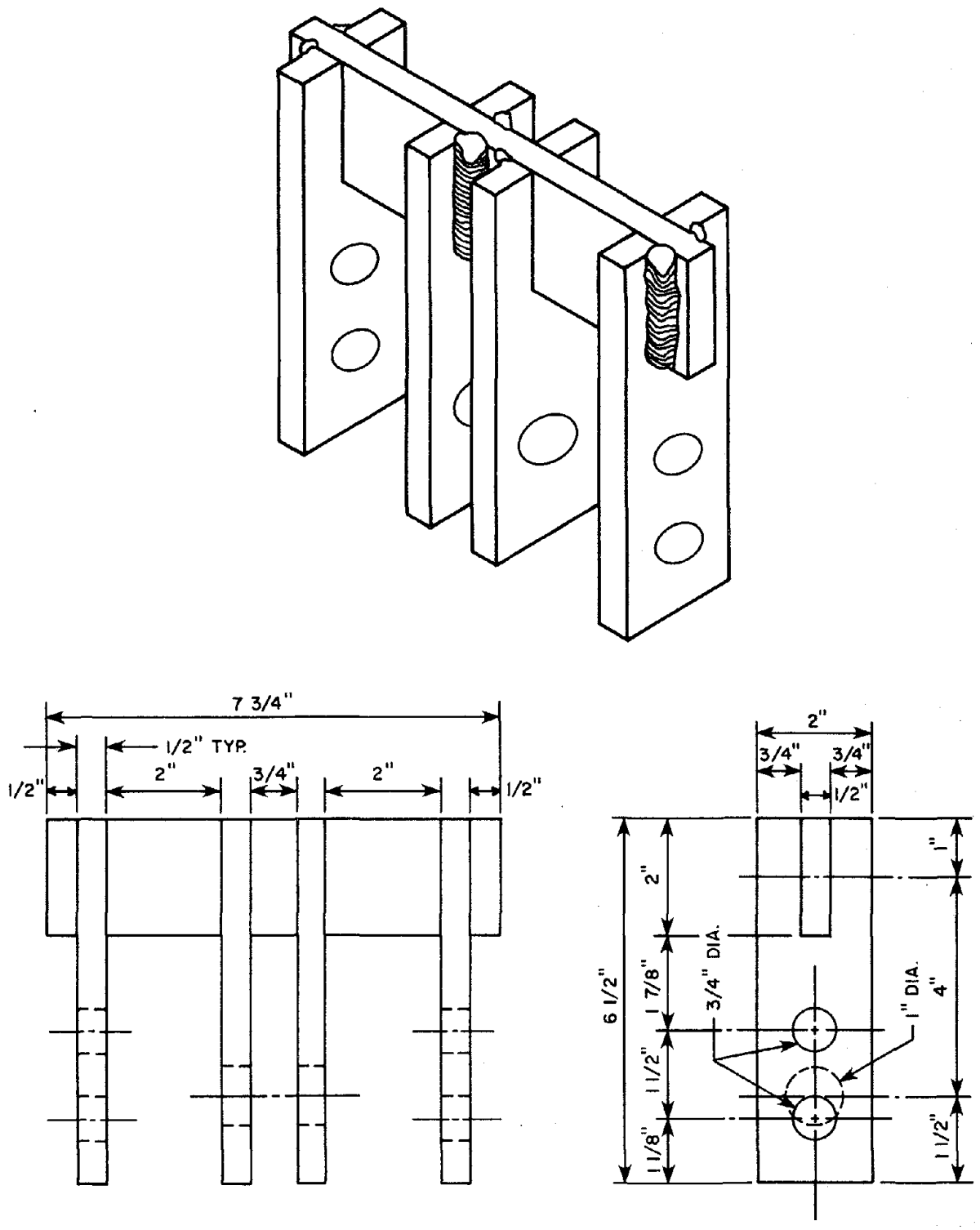

FIGURE 2.1.1 DIMENSIONS OF ENERGY-ABSORBING DEVICES

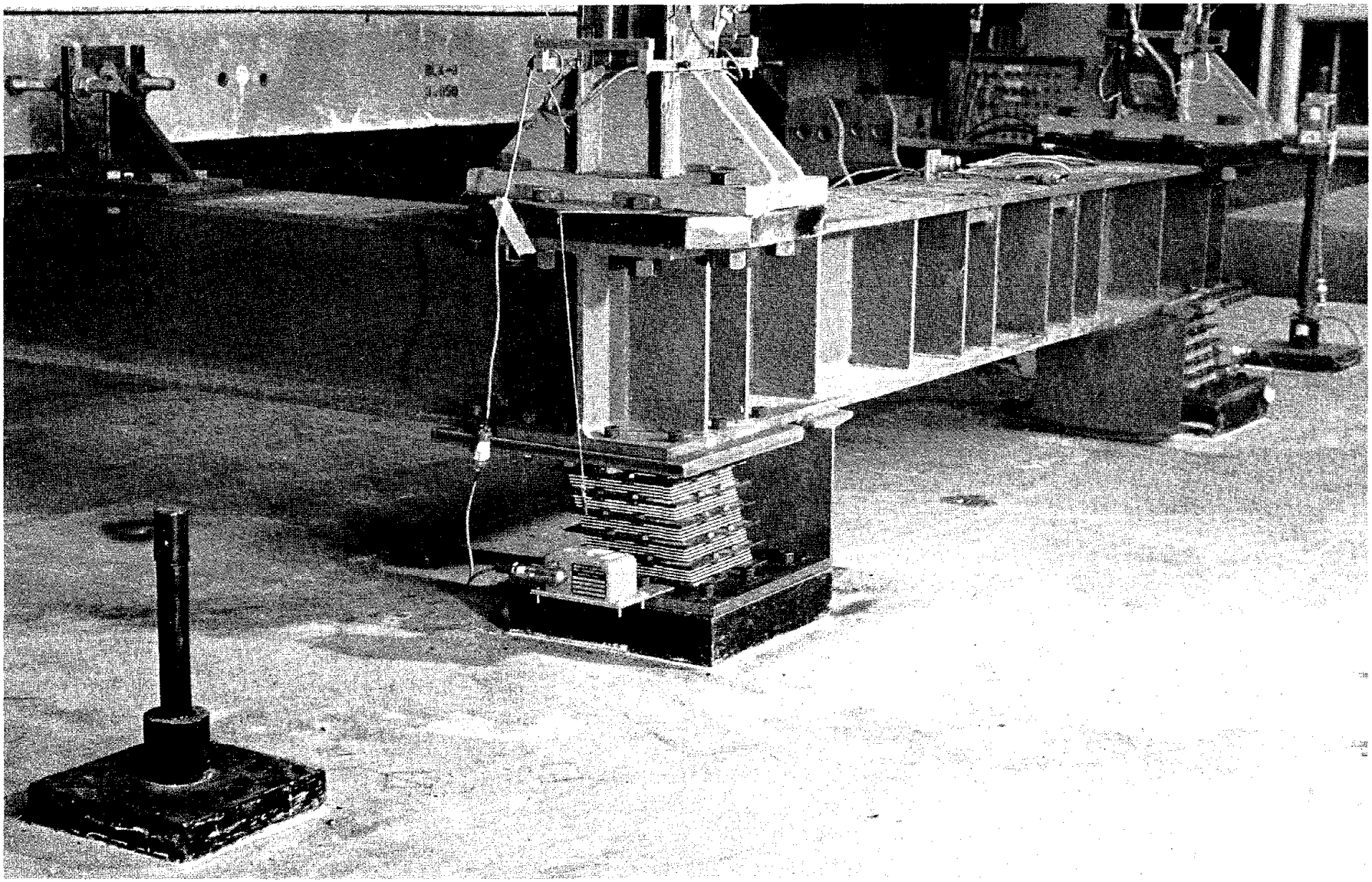

FIGURE 2.2.1 SHEAR DEFLECTION OF RUBBER BEARINGS

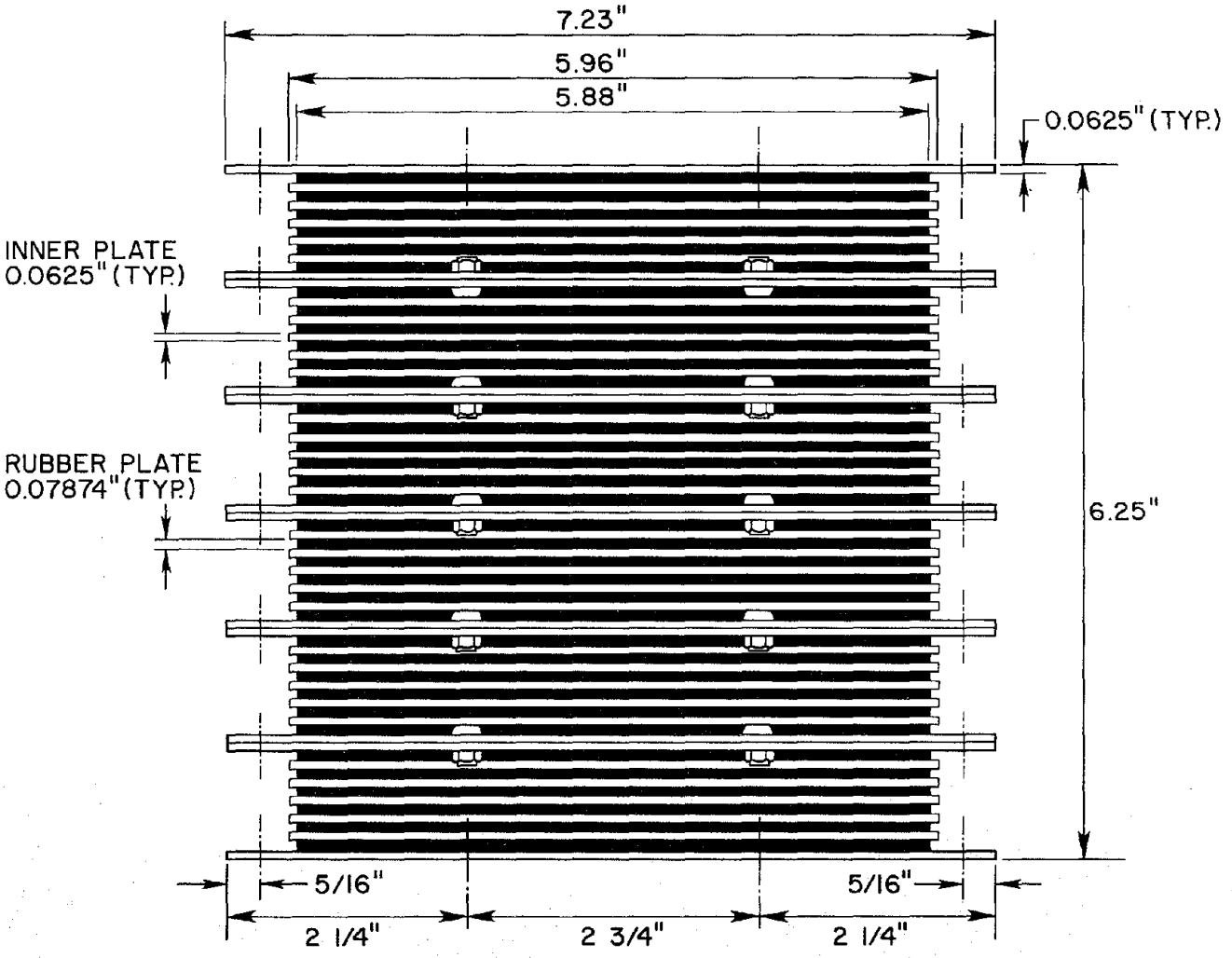

FIGURE 2.2.2 DIMENSIONS OF NATURAL RUBBER BEARINGS

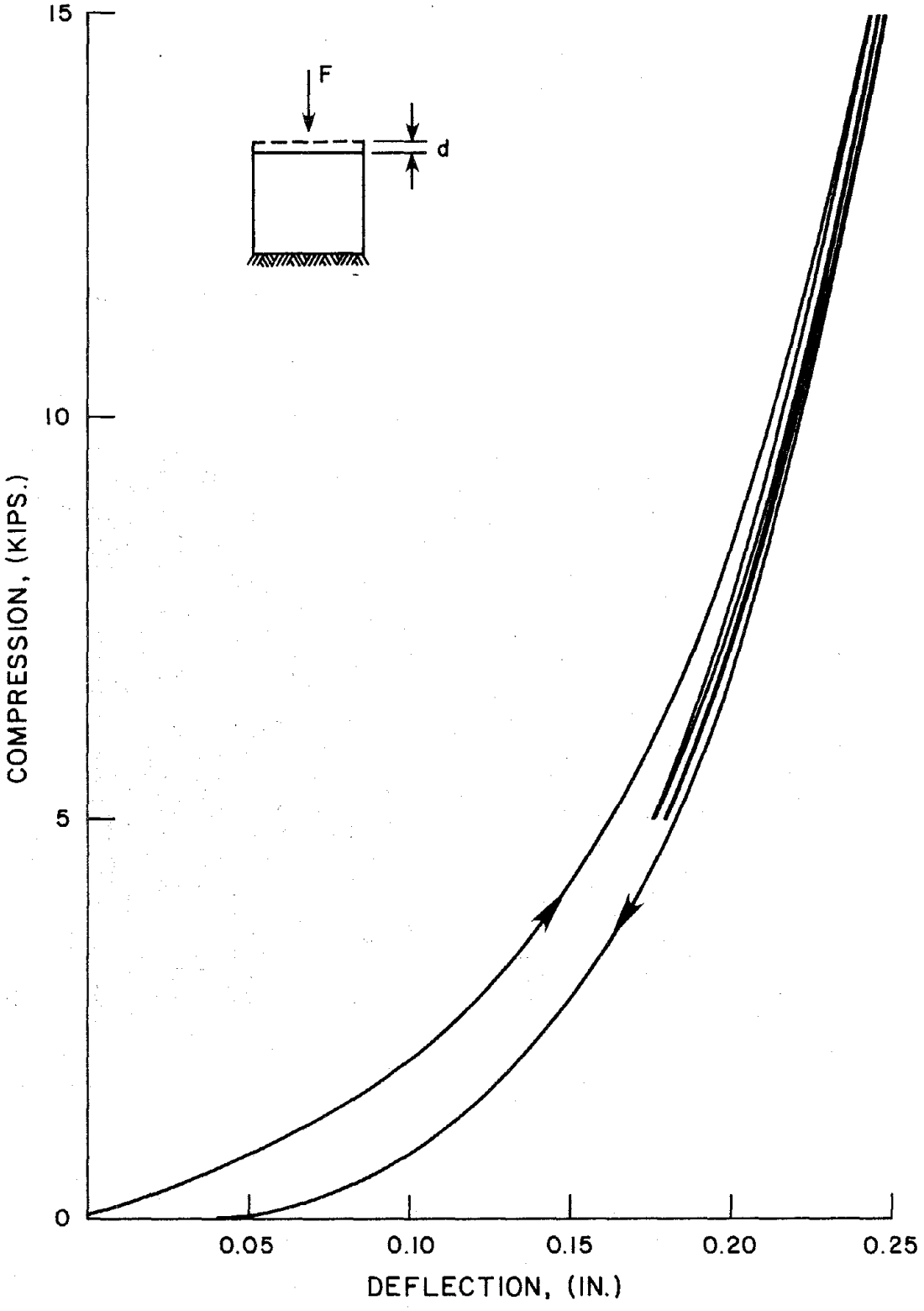

FIGURE 2.2.3 VERTICAL STIFFNESS OF BEARINGS

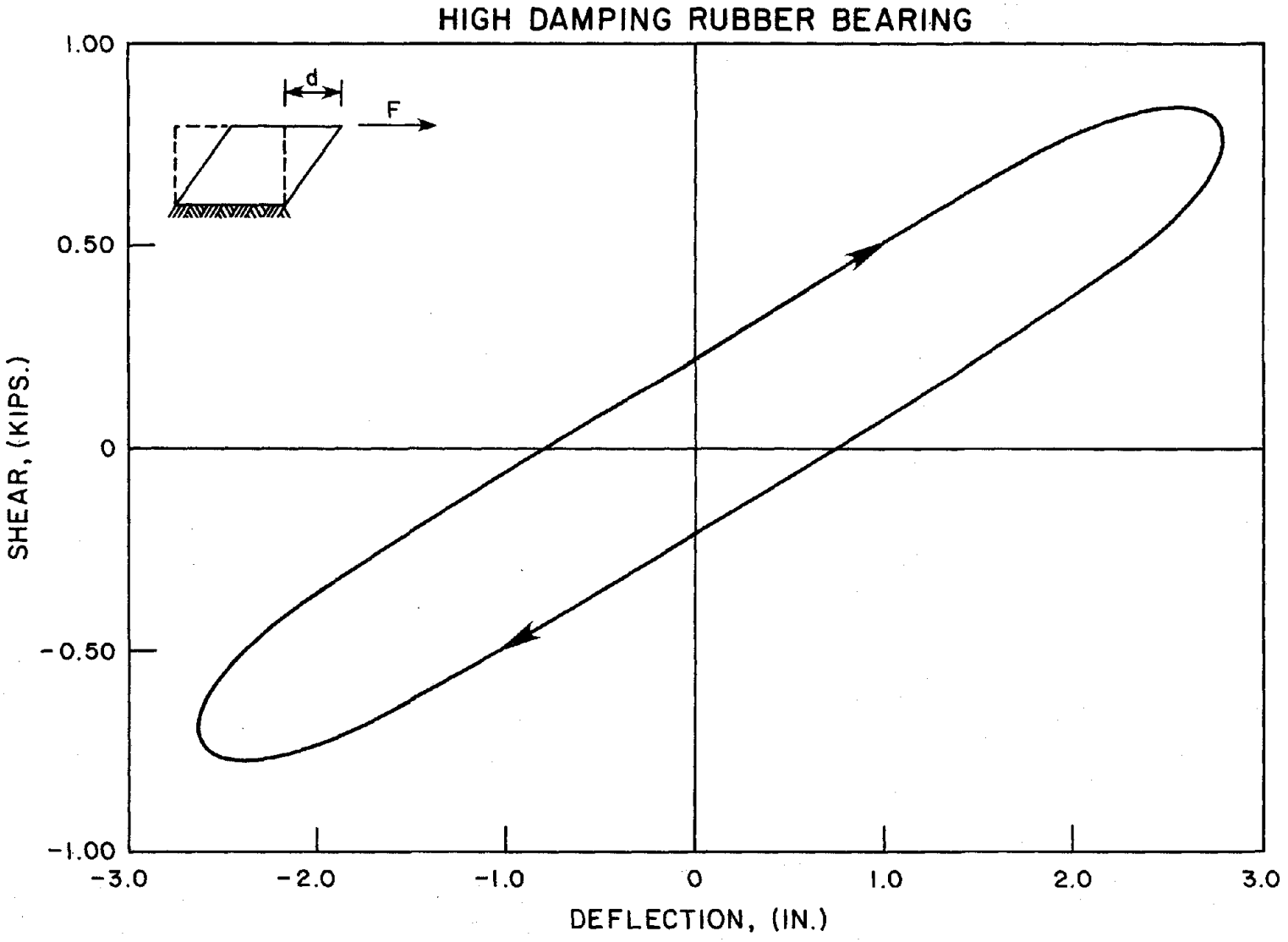

FIGURE 2.2.4 HORIZONTAL STIFFNESS OF BEARINGS

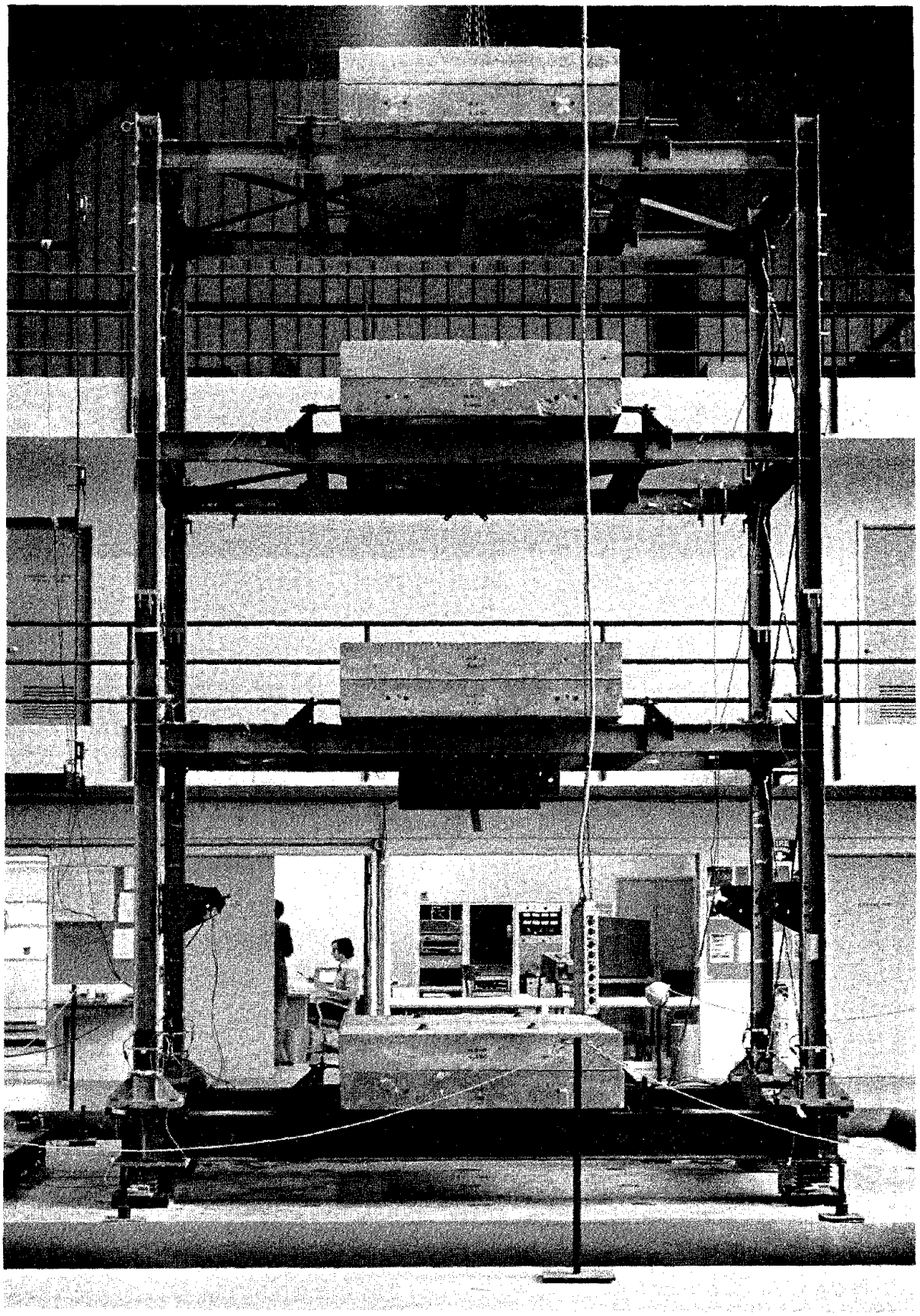

FIGURE 3.1.1 MODEL STRUCTURE

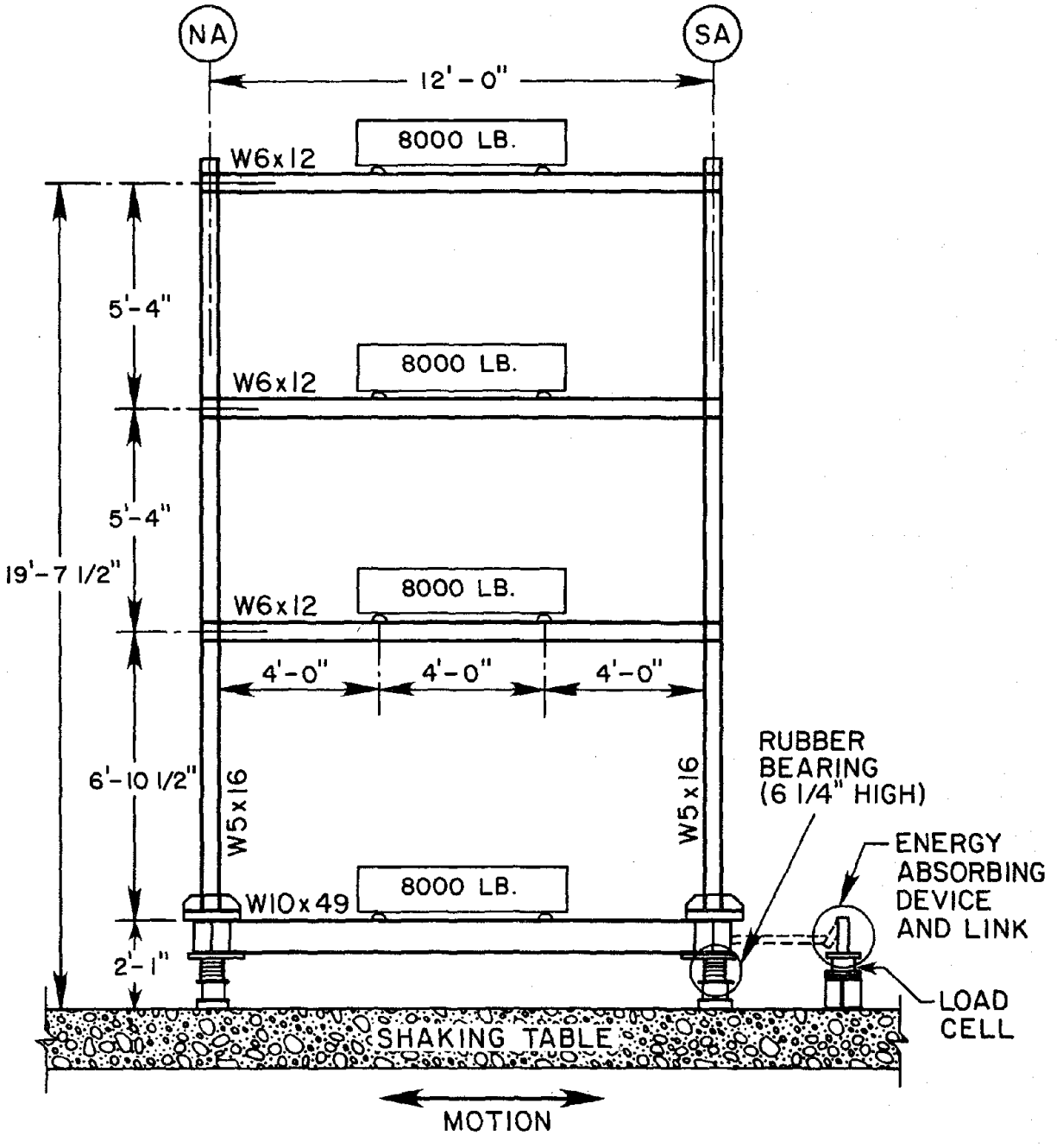

FIGURE 3.1.2 DIMENSIONS OF STRUCTURE

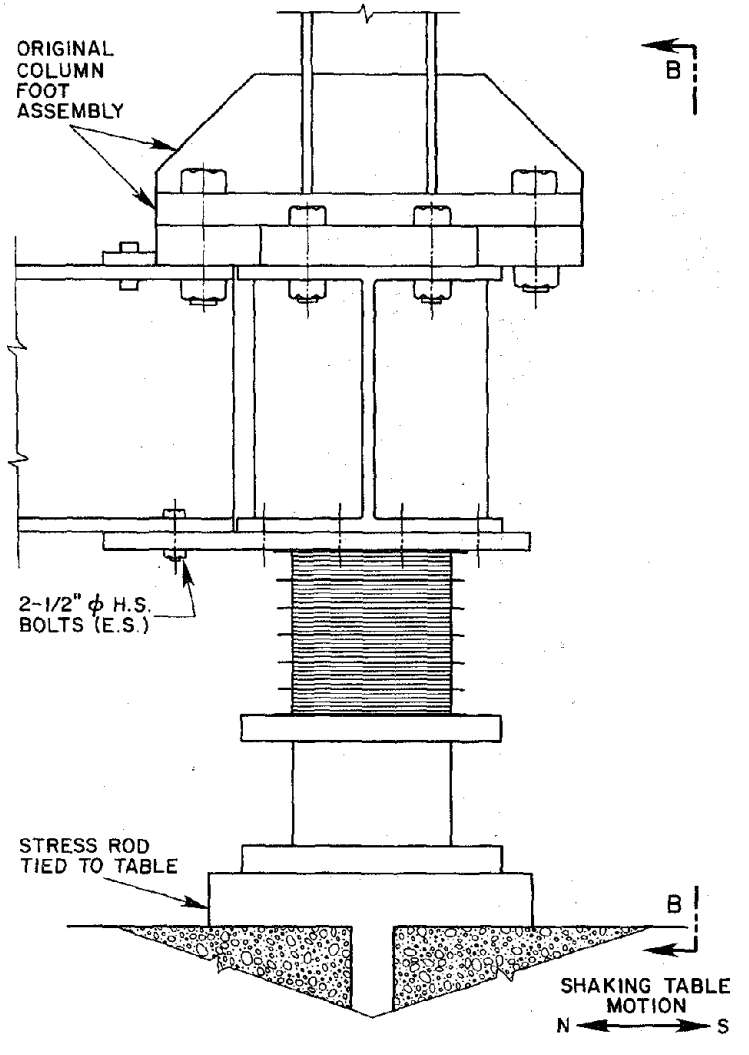

SECTION A-A

FIGURE 3.1.3 RUBBER BEARING CONNECTION - DETAIL

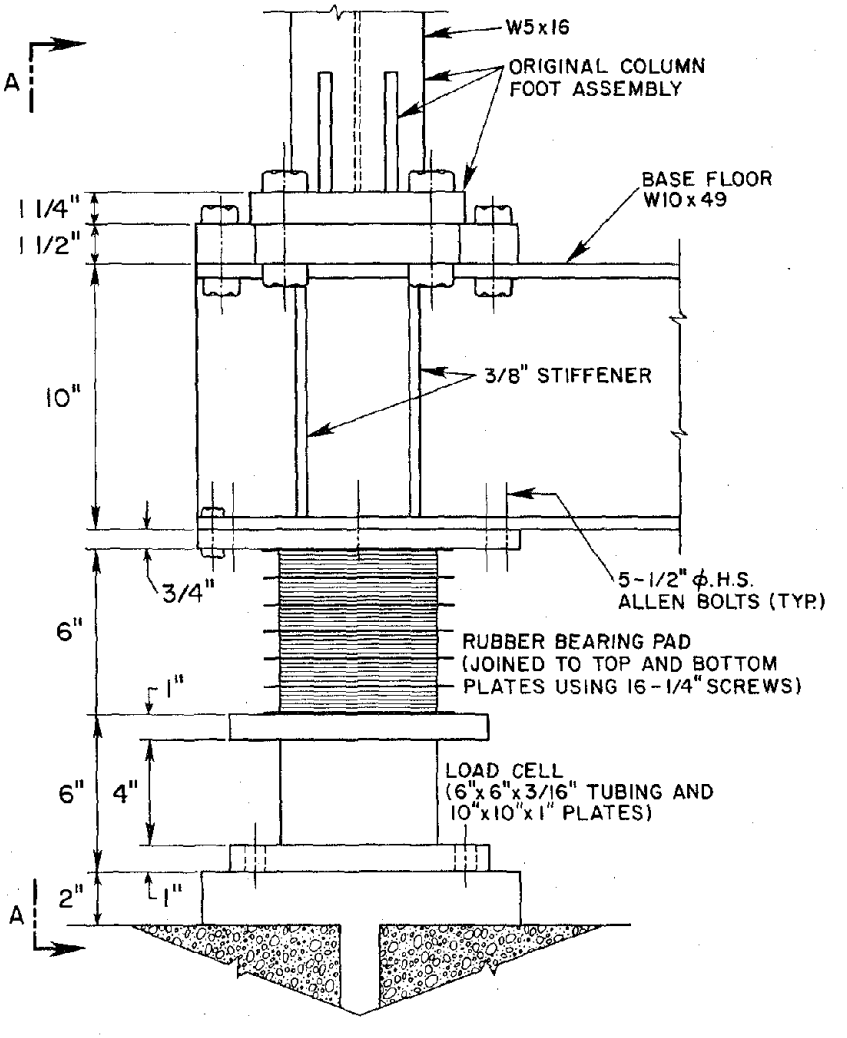

SECTION B-B

FIGURE 3.1.4 RUBBER BEARING CONNECTION - DETAIL

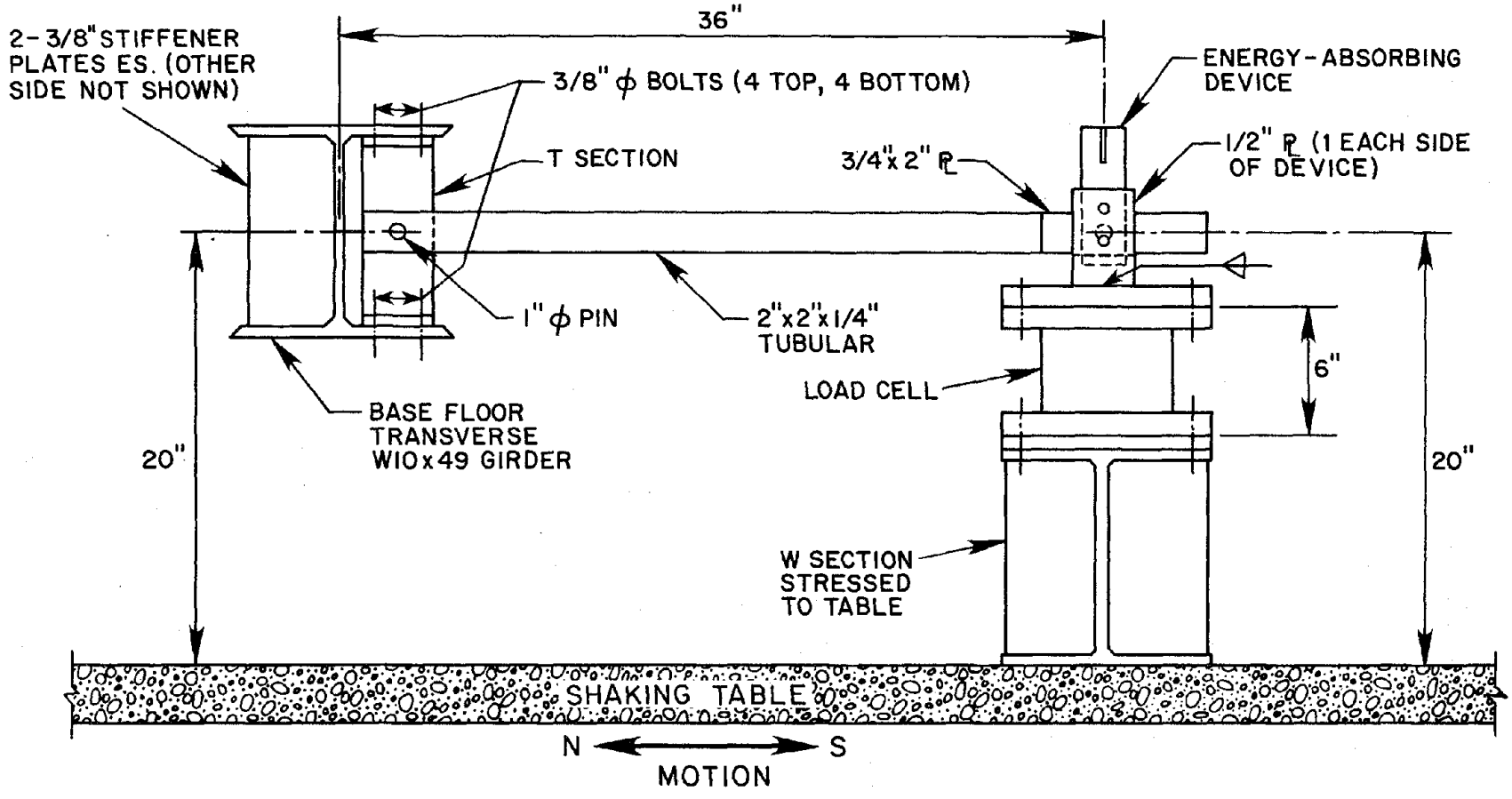

FIGURE 3.1.5 ENERGY-ABSORBING DEVICE CONNECTION - DETAIL

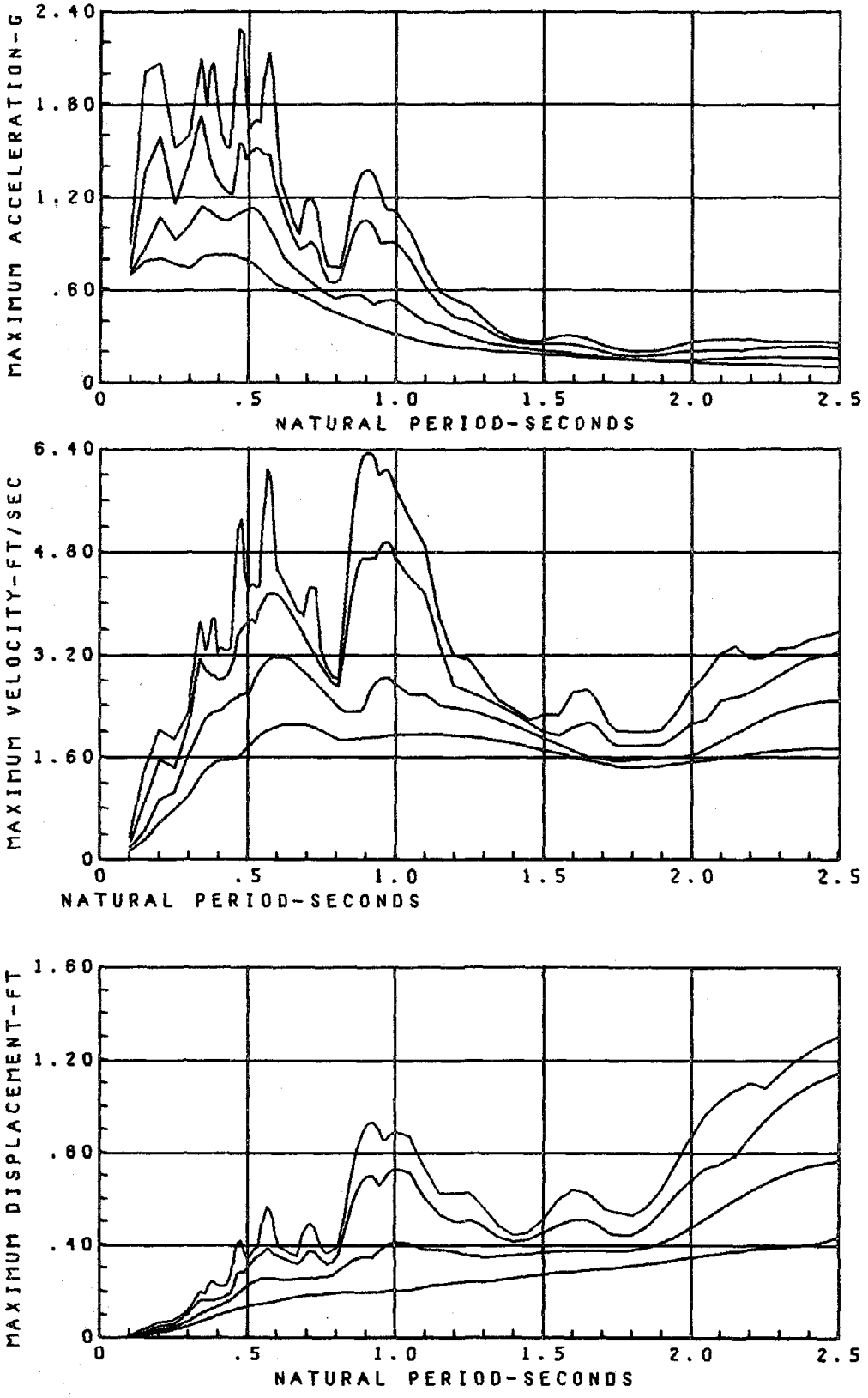

FIGURE 5.1 EL CENTRO 750 RESPONSE SPECTRA
ξ = 1, 3, 10, 25%

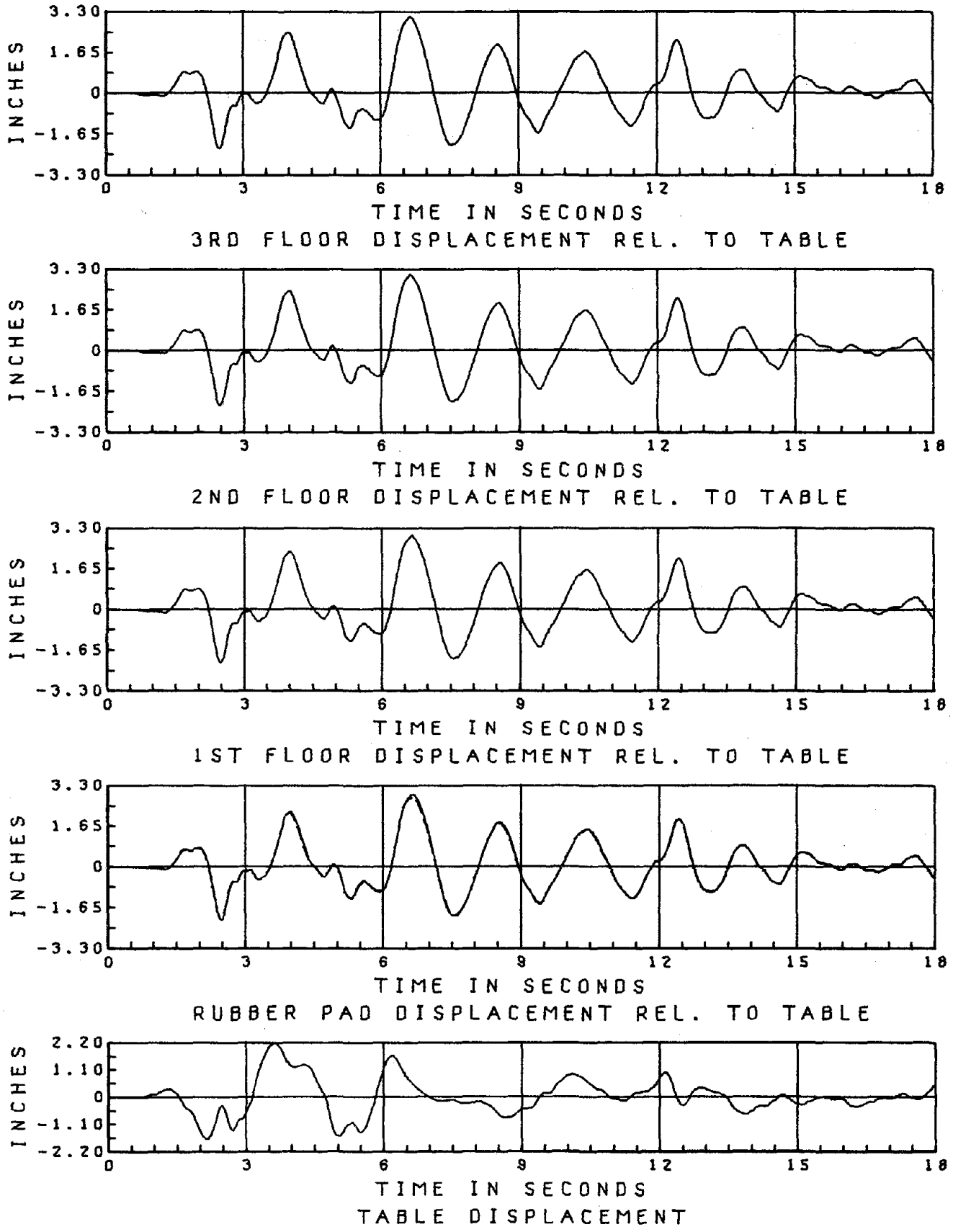

FIGURE 5.1.1.1 EC 400/350 RUBBER, DISPLACEMENT

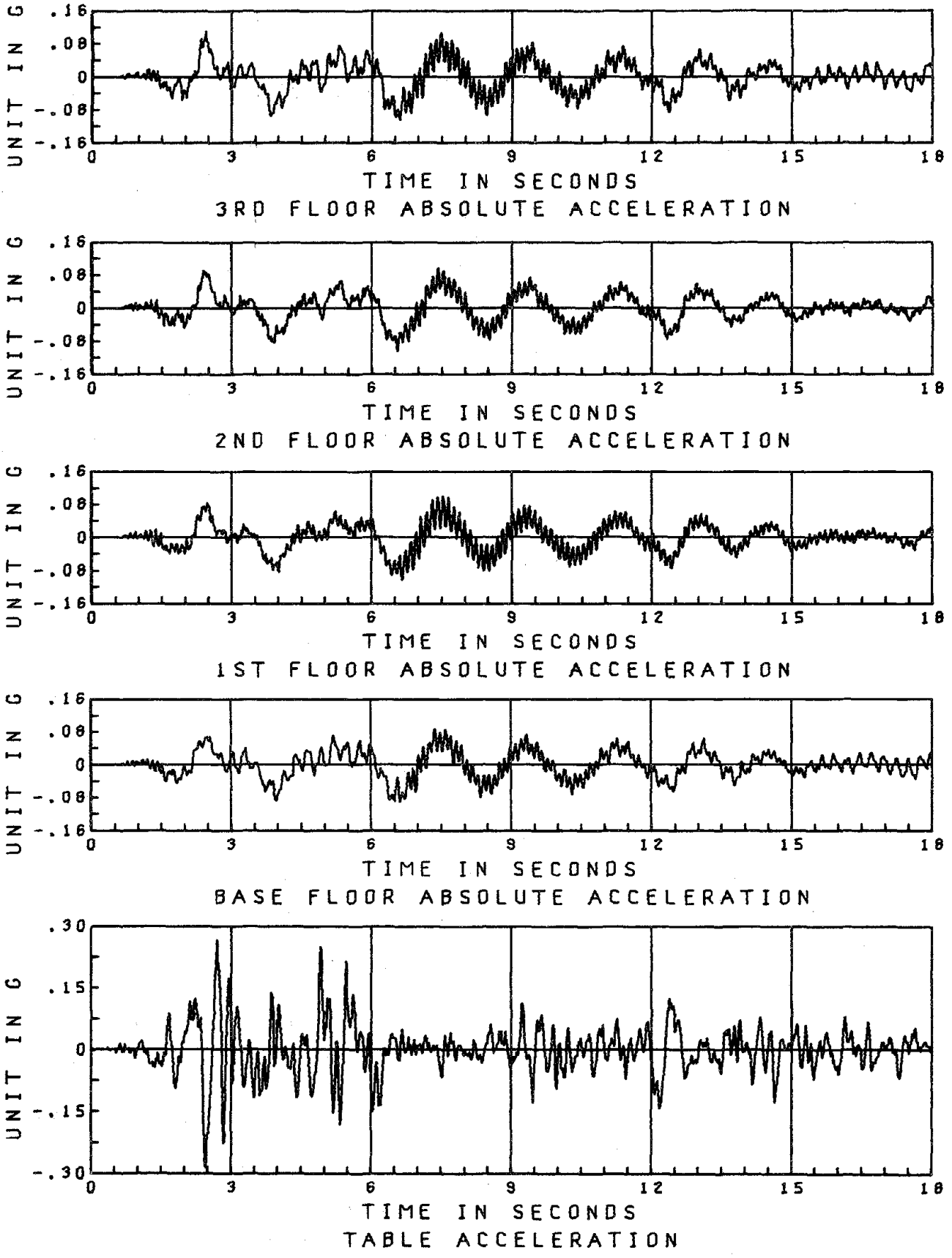

FIGURE 5.1.1.2 EC 400/350 RUBBER, HORIZONTAL ACCELERATIONS

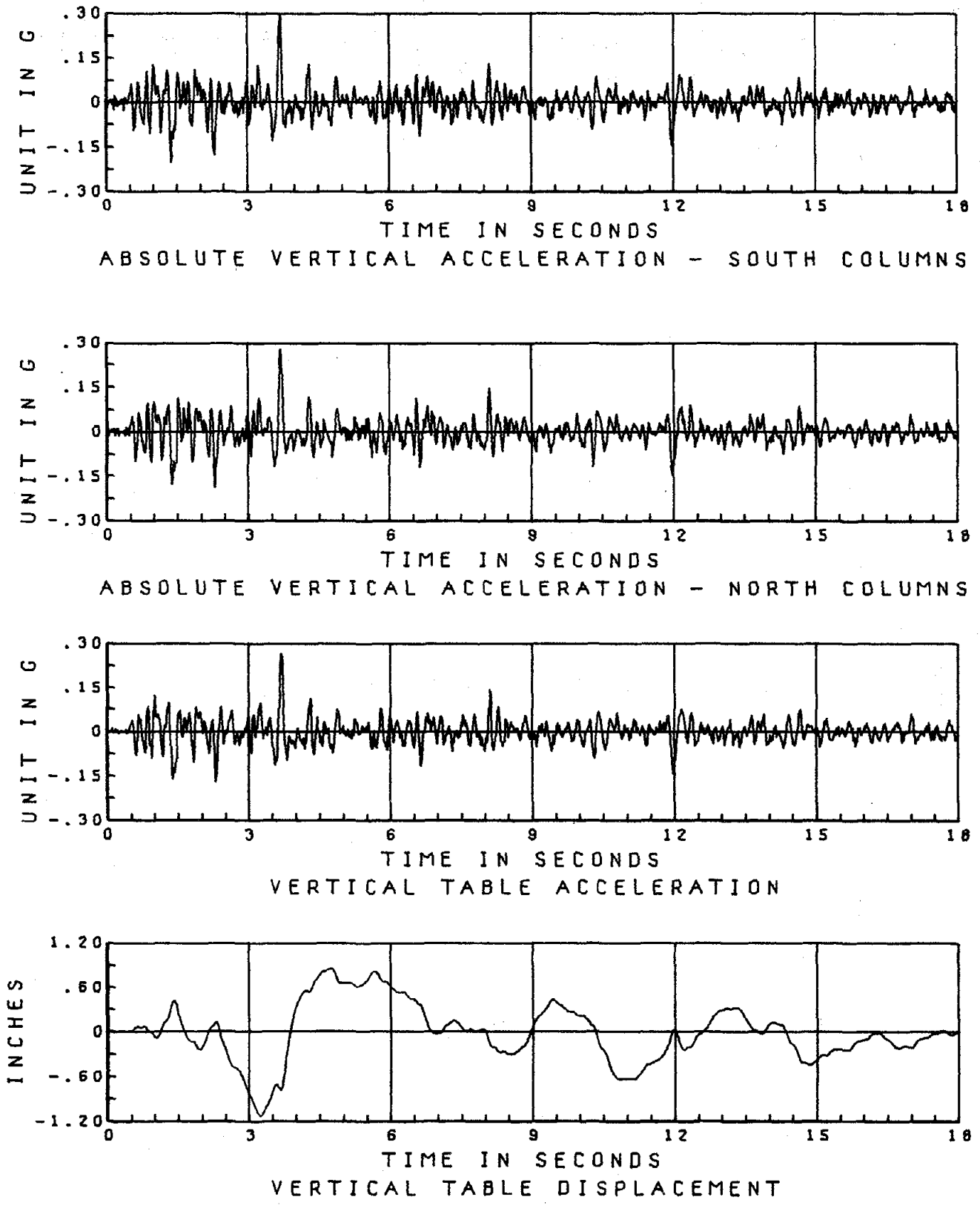

FIGURE 5.1.1.3 EC 400/350 RUBBER, VERTICAL MOTIONS

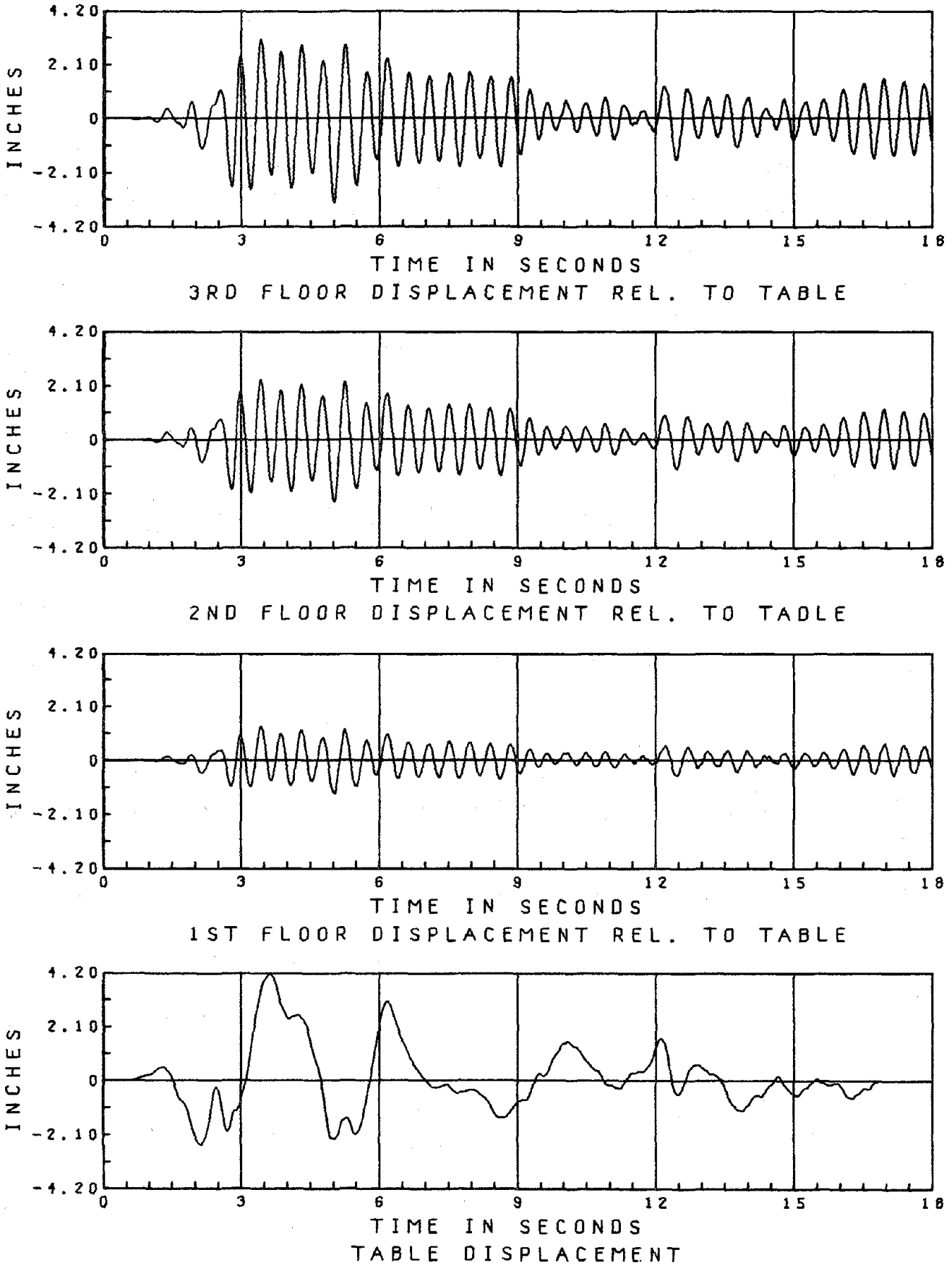

FIGURE 5.1.2.1 EC 900 FIX, DISPLACEMENTS

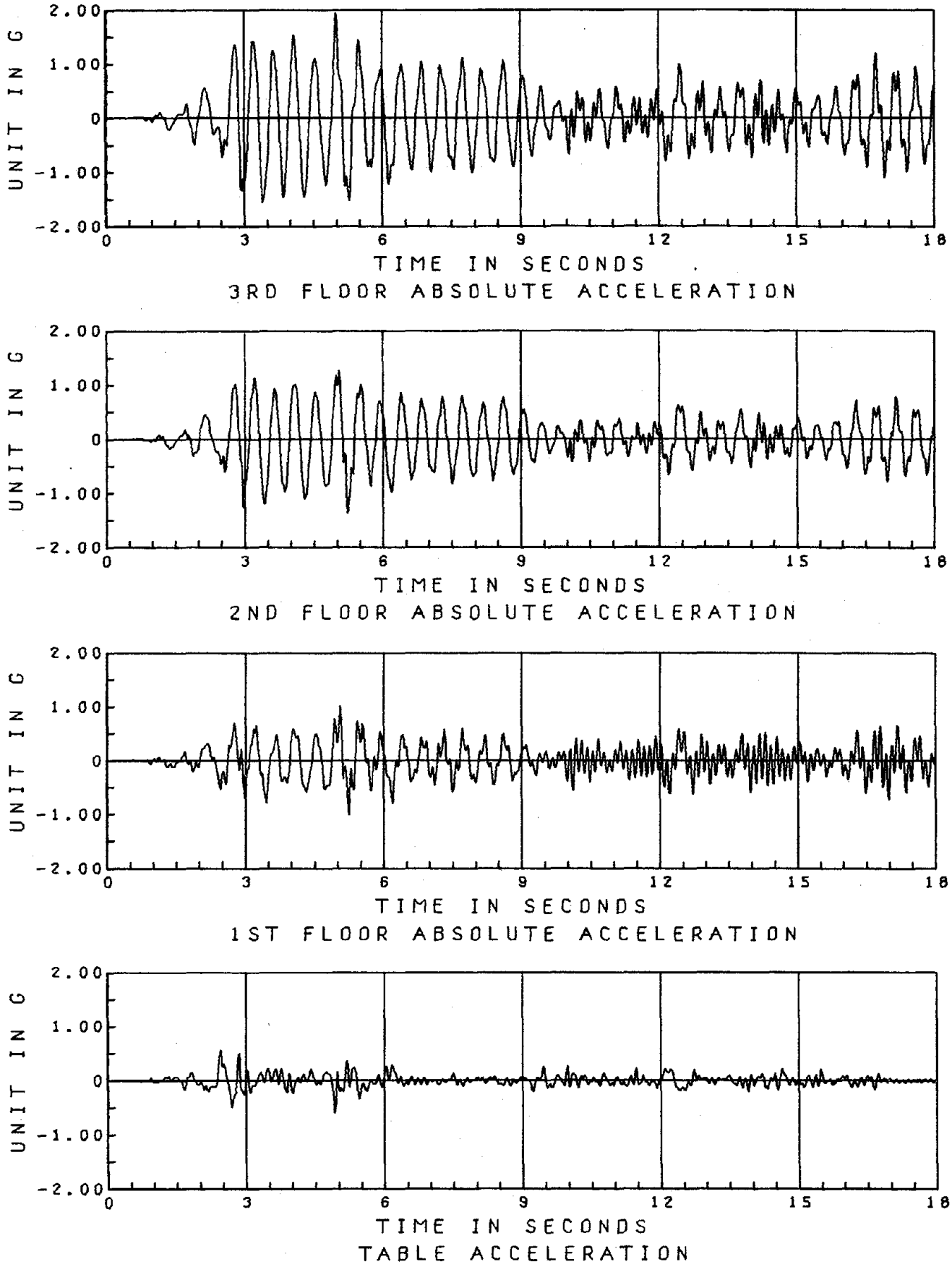

FIGURE 5.1.2.2 EC 900 FIX, ACCELERATIONS

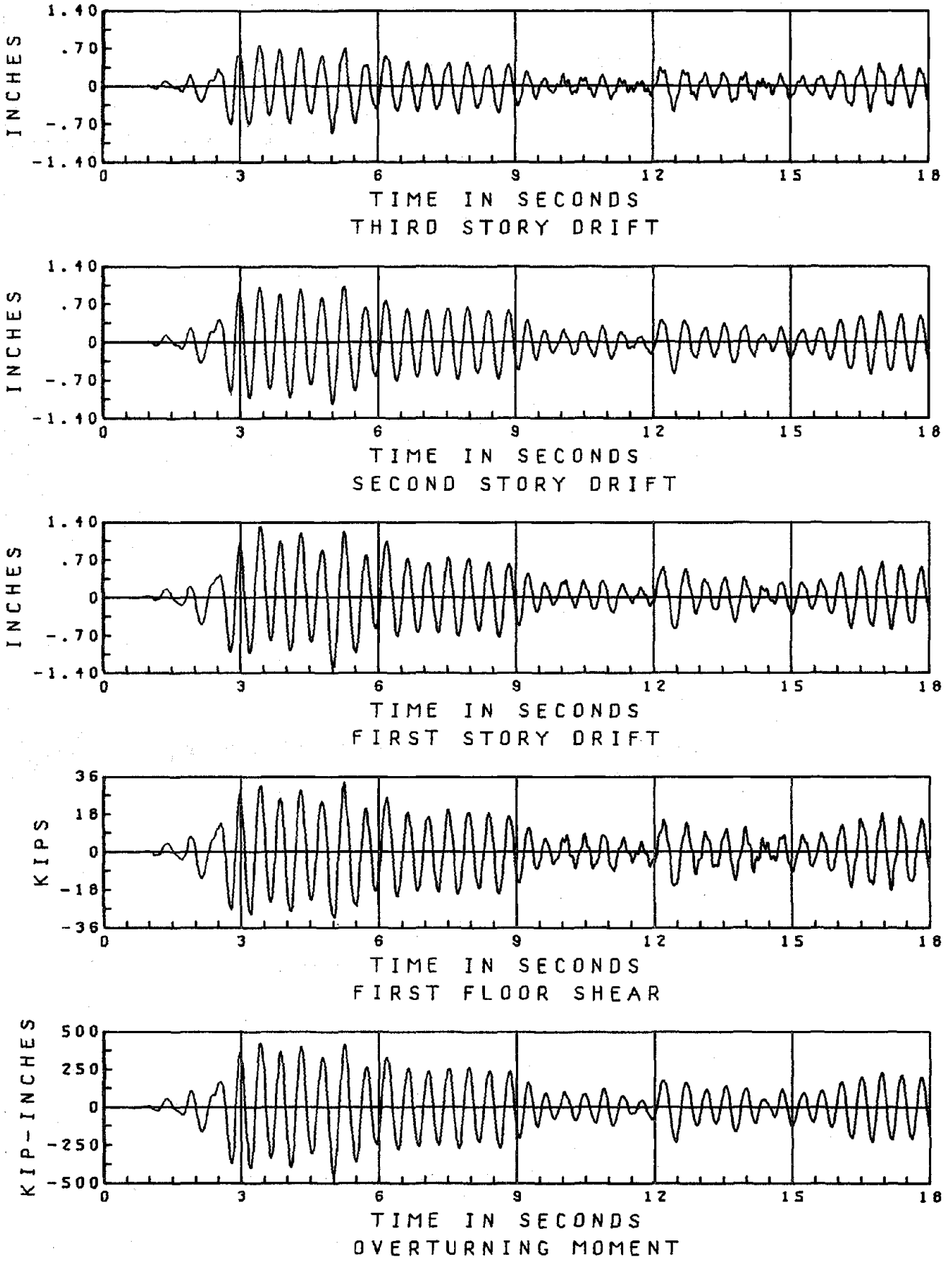

FIGURE 5.1.2.3 EC 900 FIX, DRIFTS, SHEAR, OTM

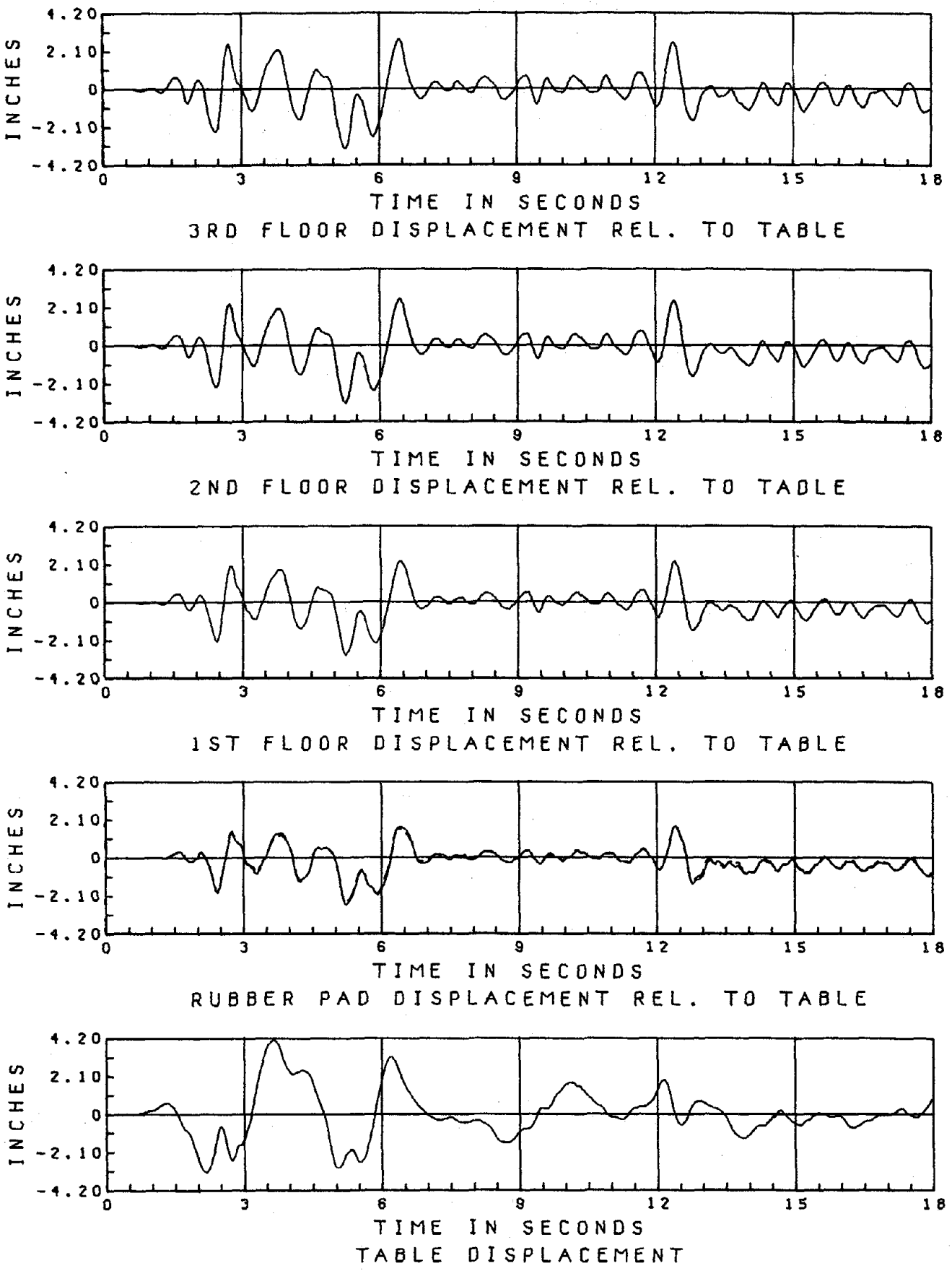

FIGURE 5.1.3.1 EC 750 EA1, DISPLACEMENTS

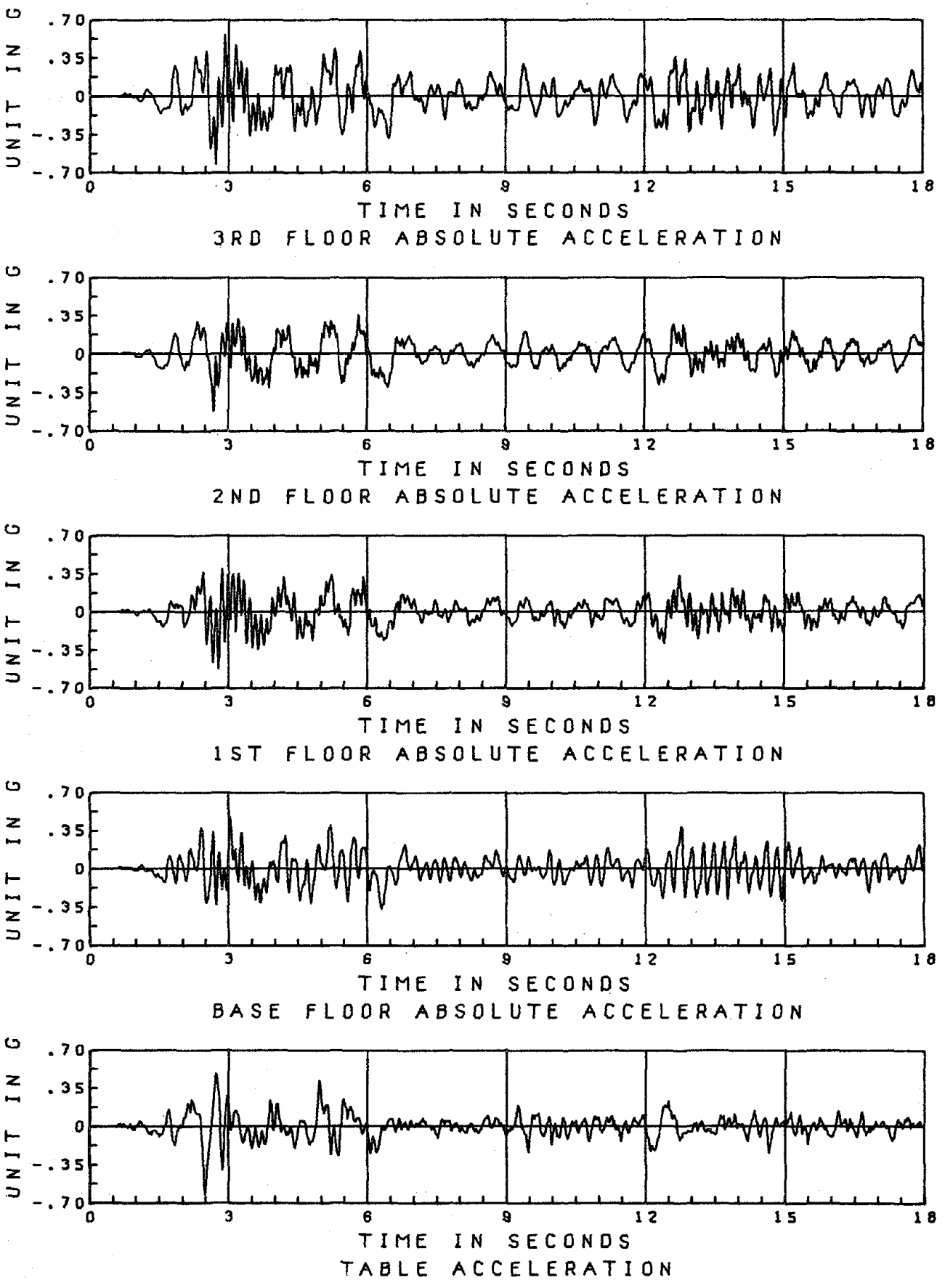

FIGURE 5.1.3.2 EC 750 EA1, ACCELERATIONS

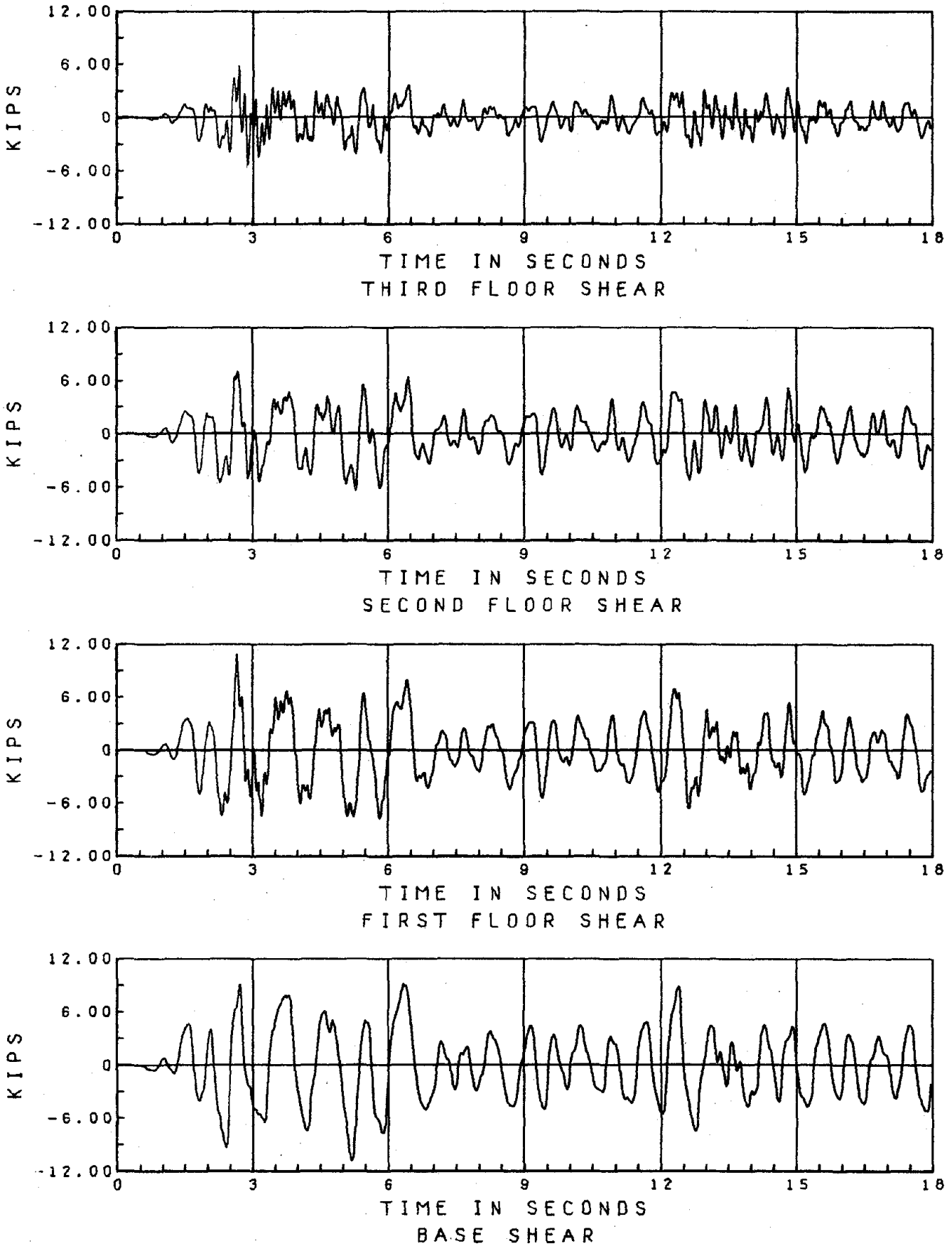

FIGURE 5.1.3.3 EC 750 EA1, SHEARS

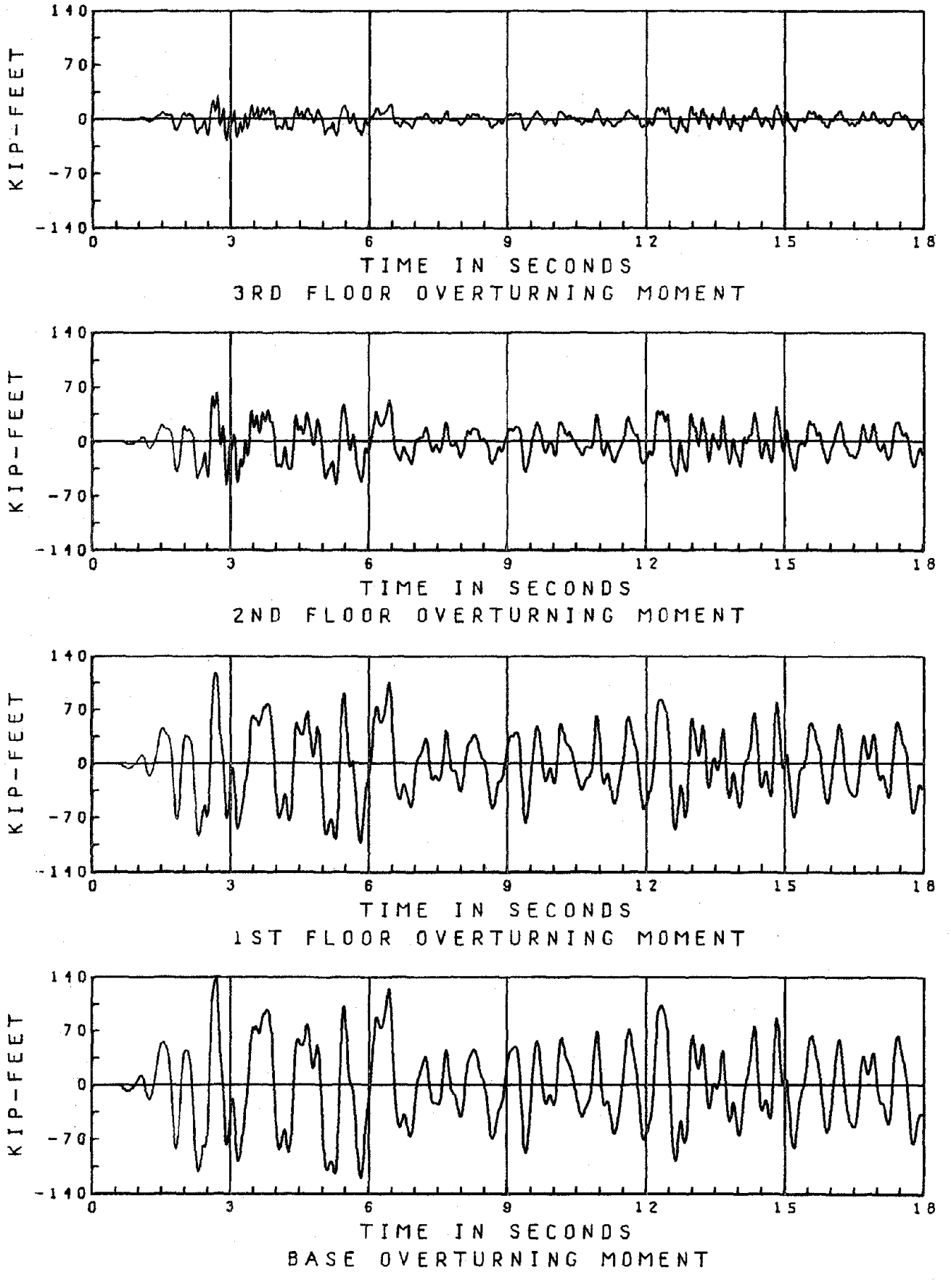

FIGURE 5.1.3.4 EC 750 EA1, OVERTURNING MOMENTS

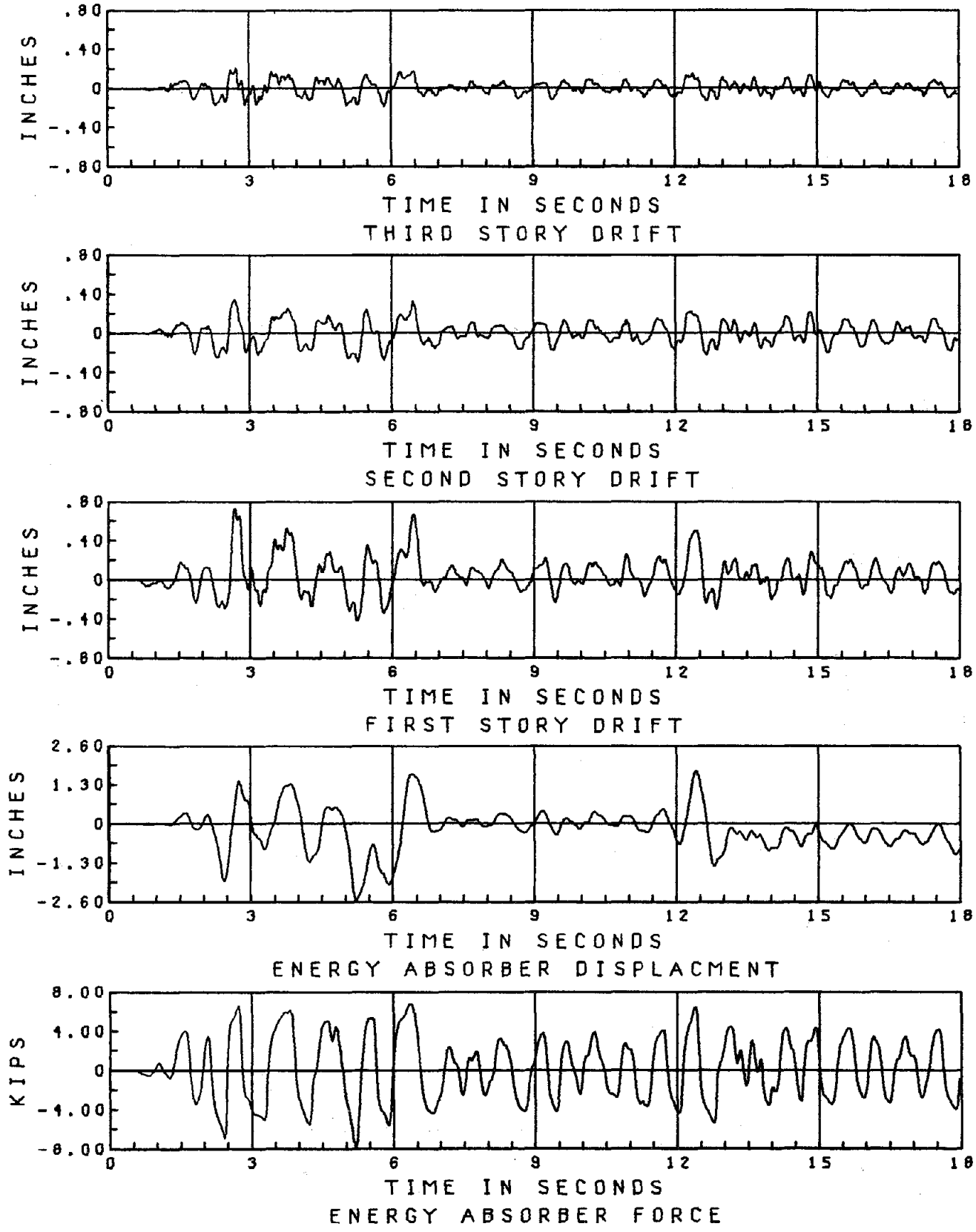

FIGURE 5.1.3.5 EC 750 EA1, DRIFT, DEVICE RESPONSE

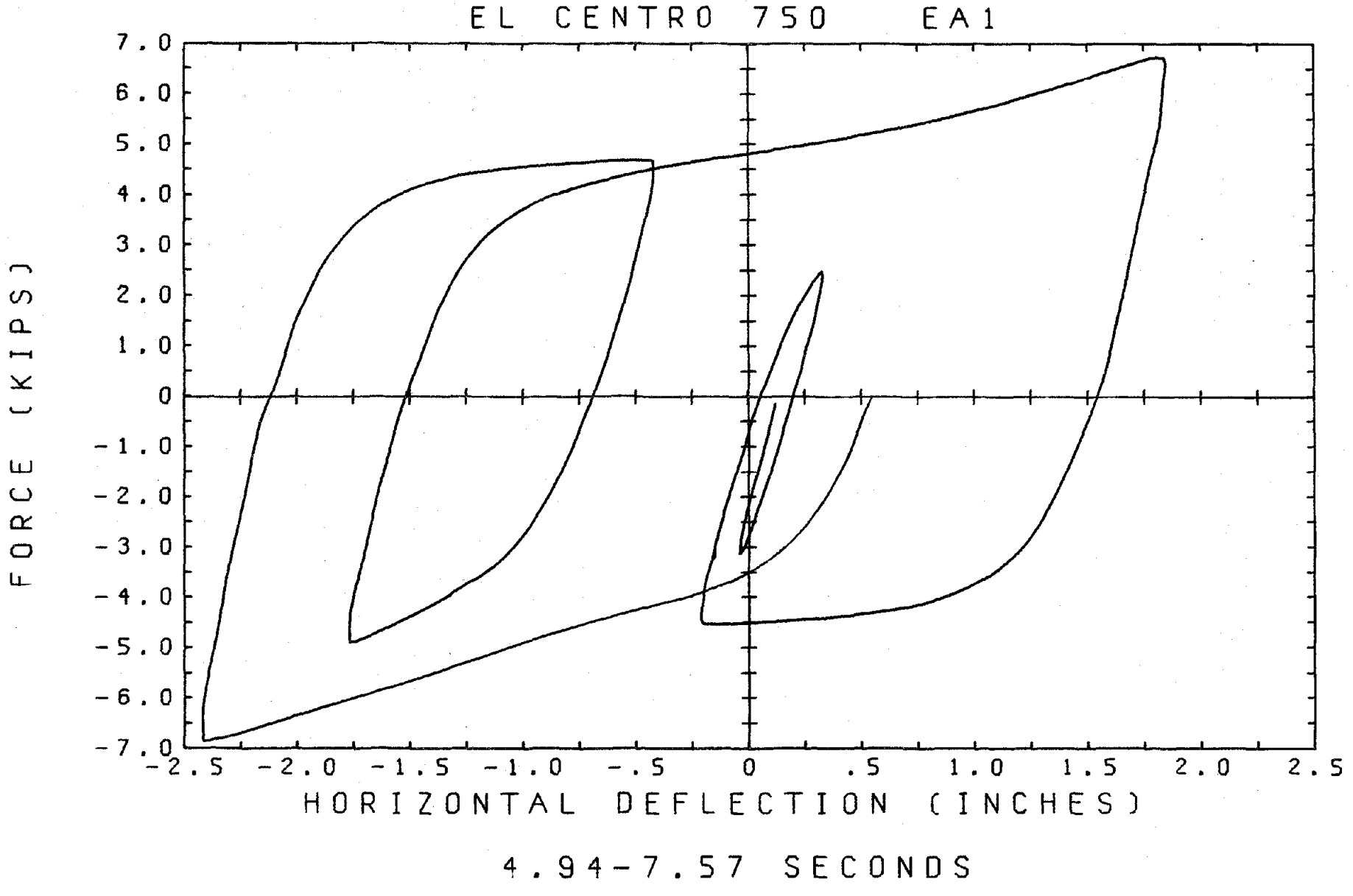

FIGURE 5.1.3.6 EC 750 EA1, ENERGY-ABSORBER EA1 LOOPS

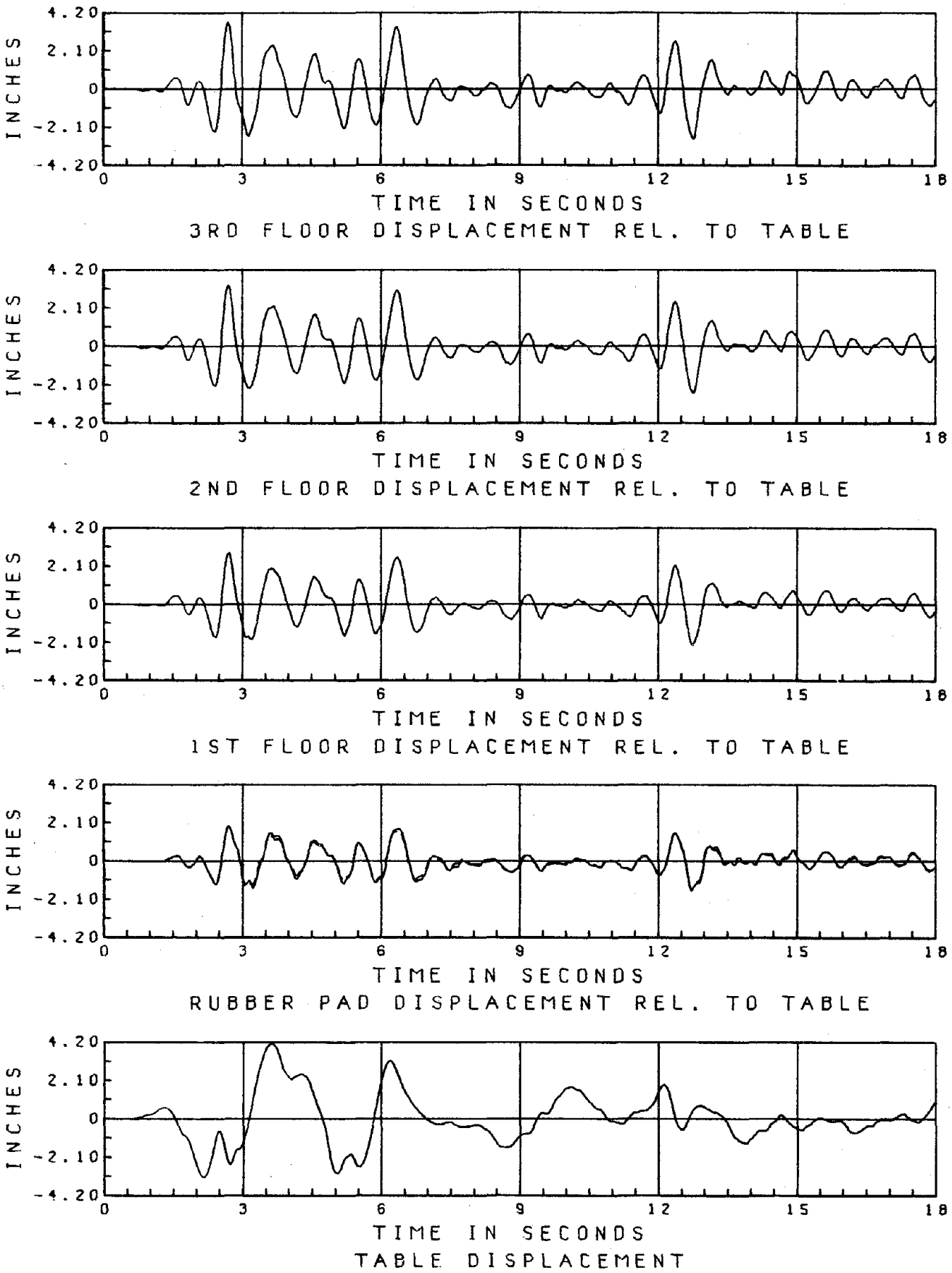

FIGURE 5.1.4.1 EC 750 EA3, DISPLACEMENTS

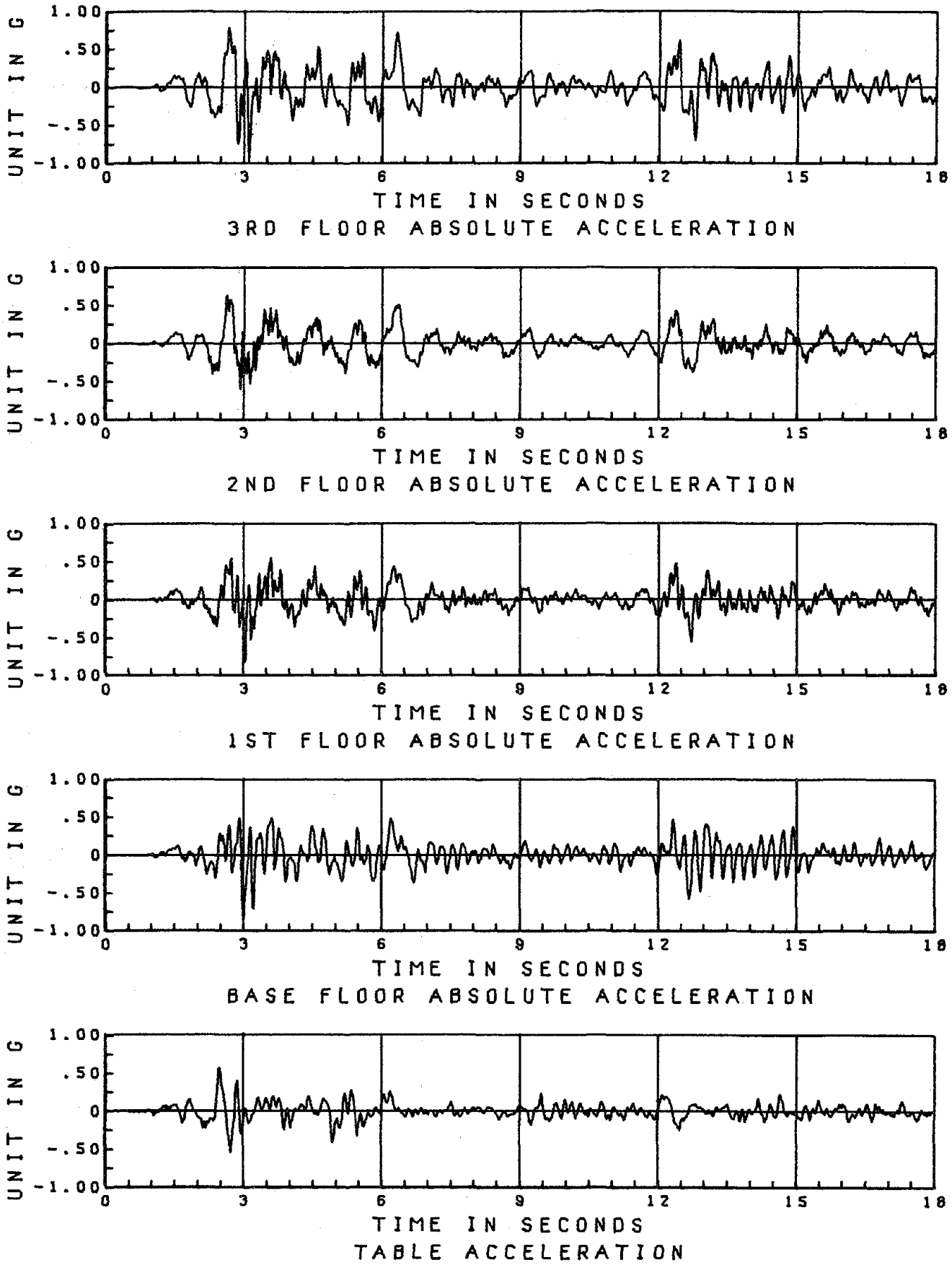

FIGURE 5.1.4.2 EC 750 EA3, ACCELERATIONS

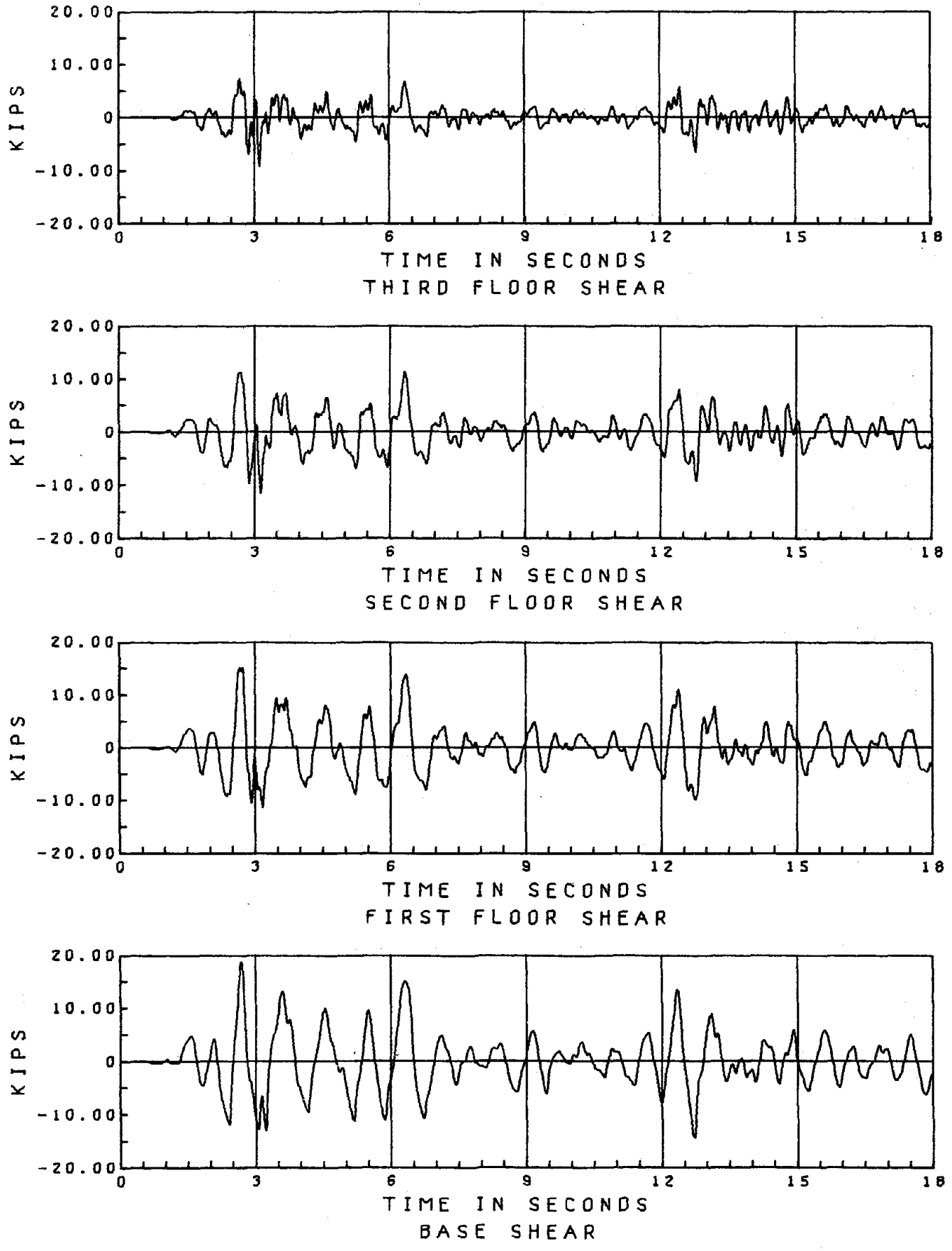

FIGURE 5.1.4.3 EC 750 EA3, SHEARS

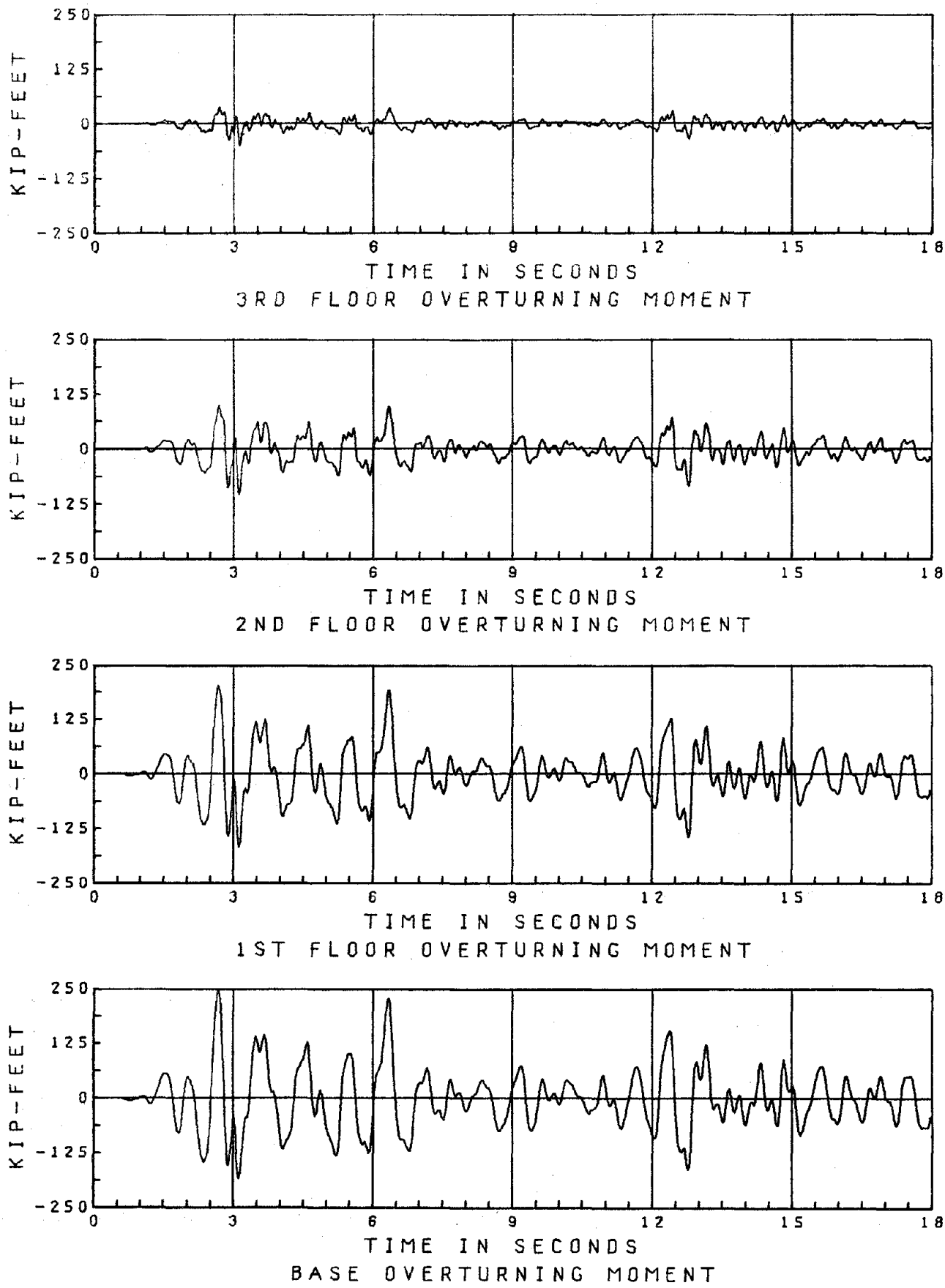

FIGURE 5.1.4.4 EC 750 EA3, OVERTURNING MOMENTS

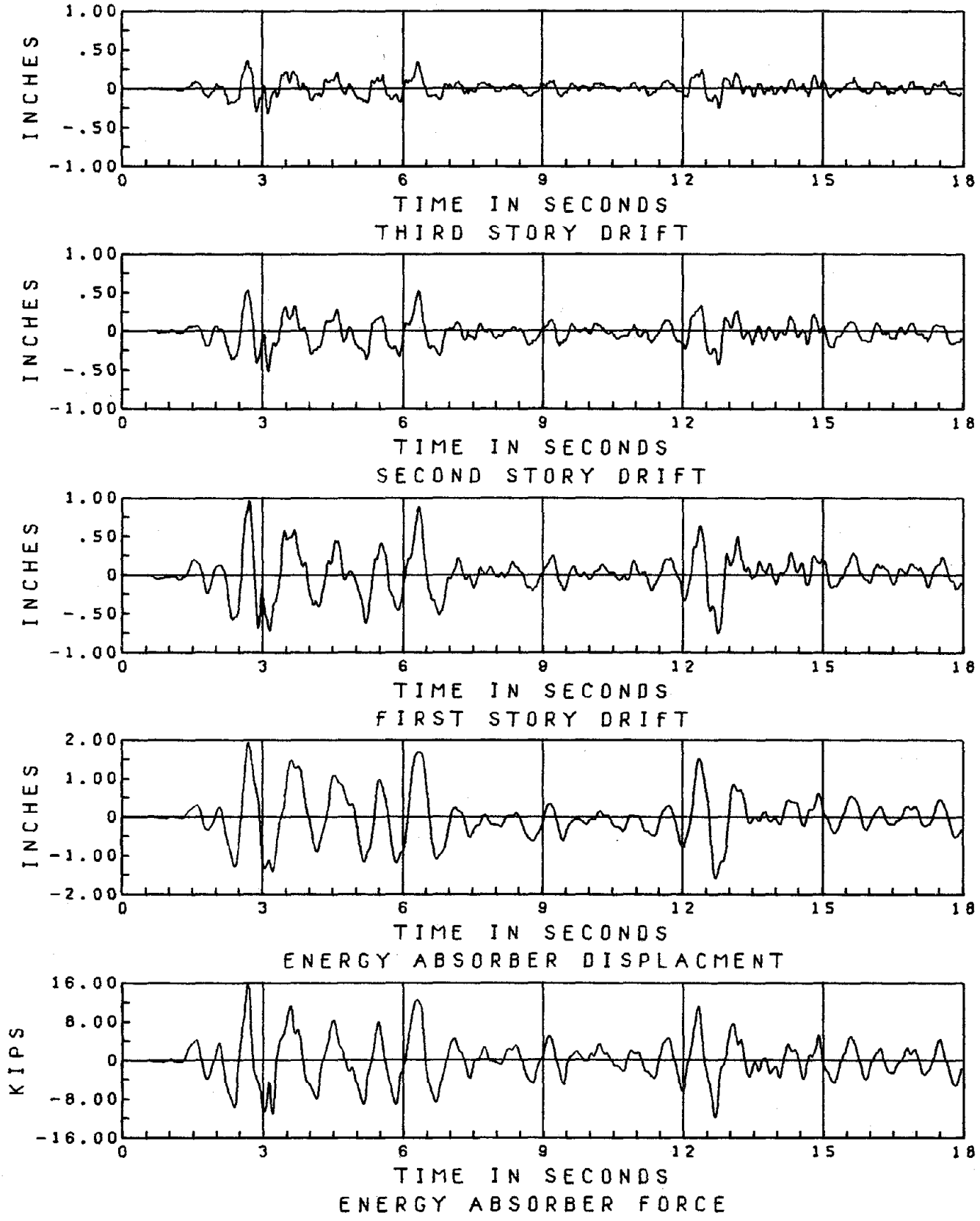

FIGURE 5.1.4.5 EC 750 EA3, DRIFTS, DEVICE RESPONSE

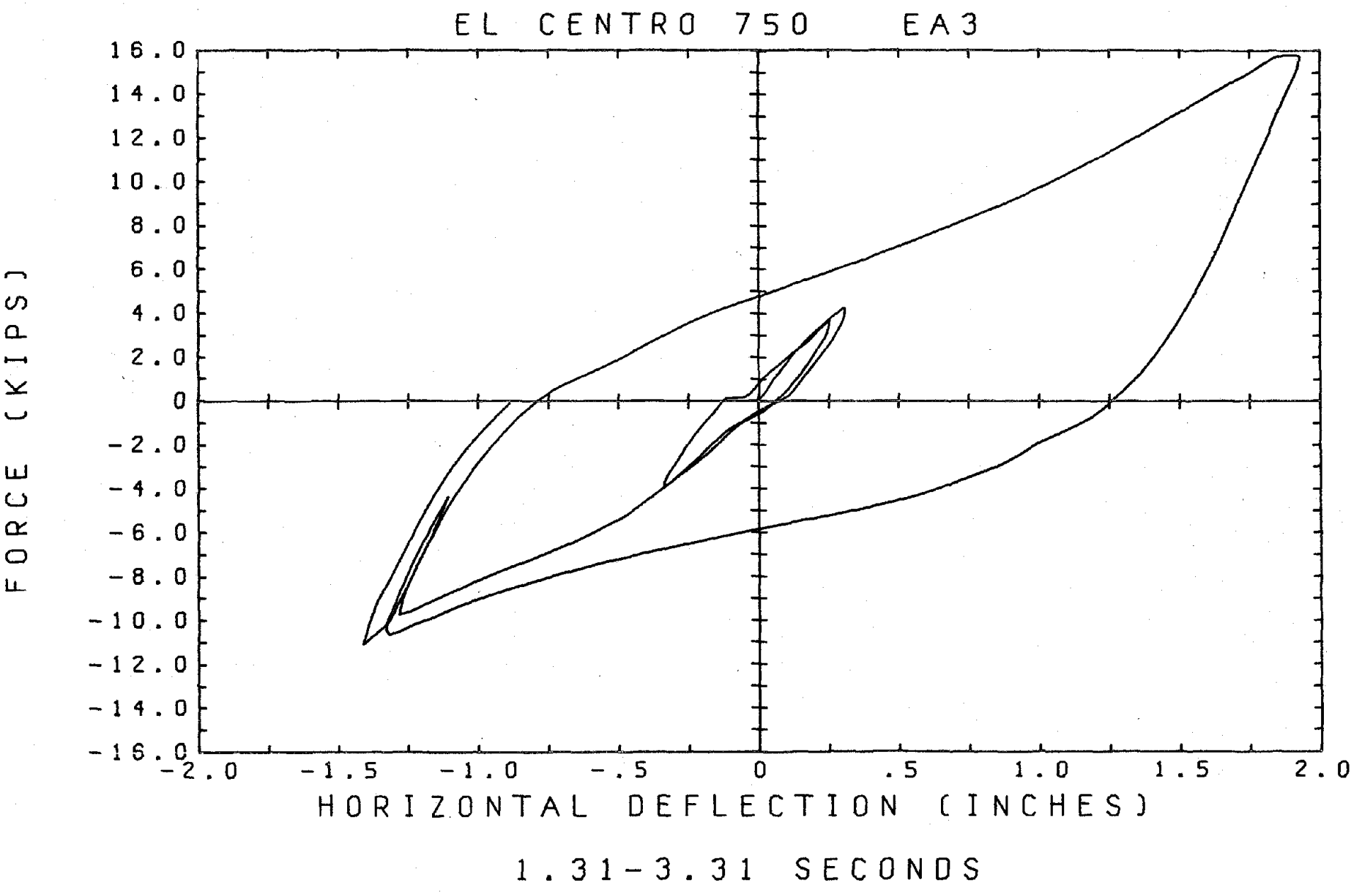

FIGURE 5.1.4.6 EC 750 EA3, ENERGY-ABSORBER EA3 LOOPS

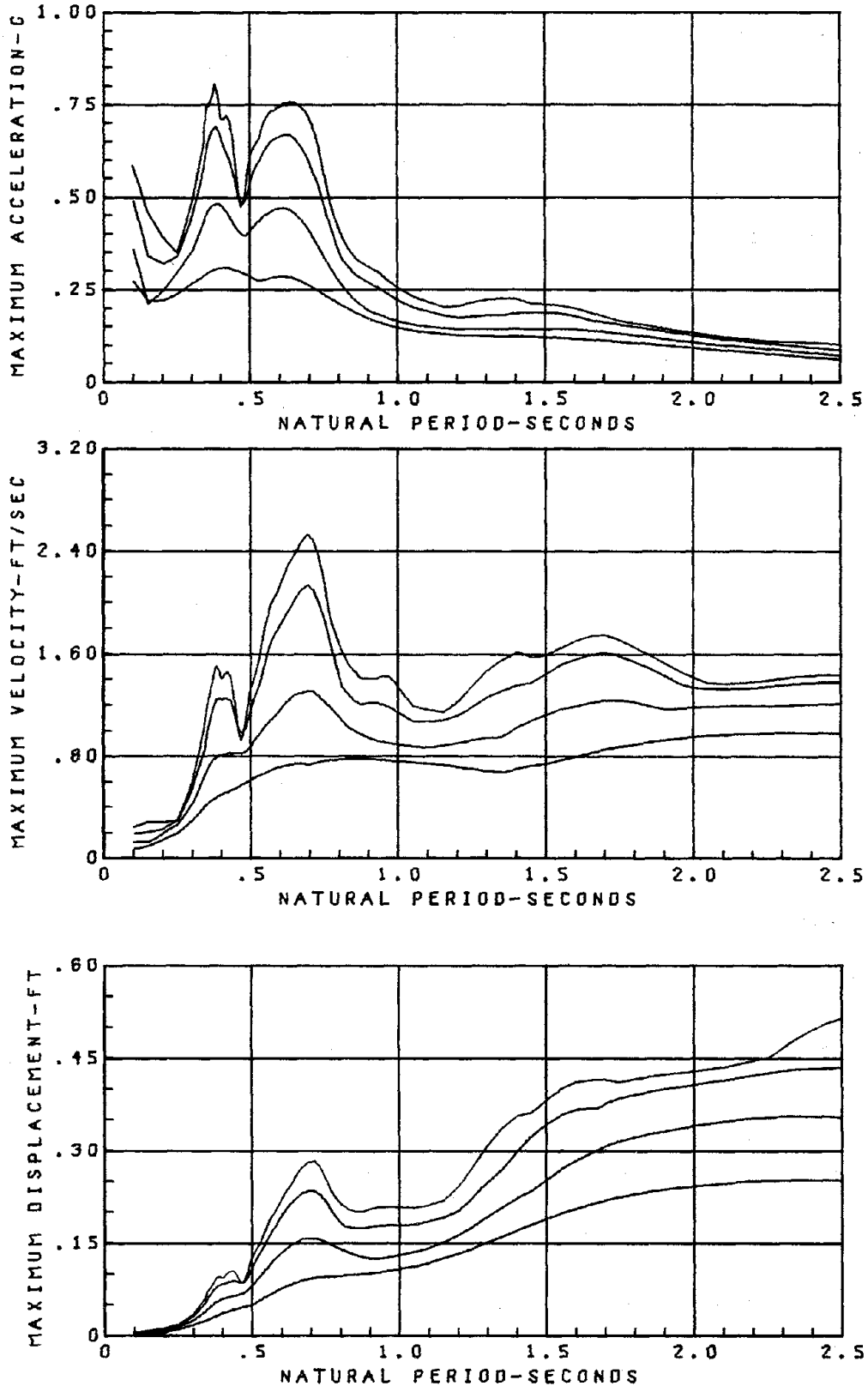

FIGURE 5.2 PARKFIELD RESPONSE SPECTRA
ξ = 1, 3, 10, 25%

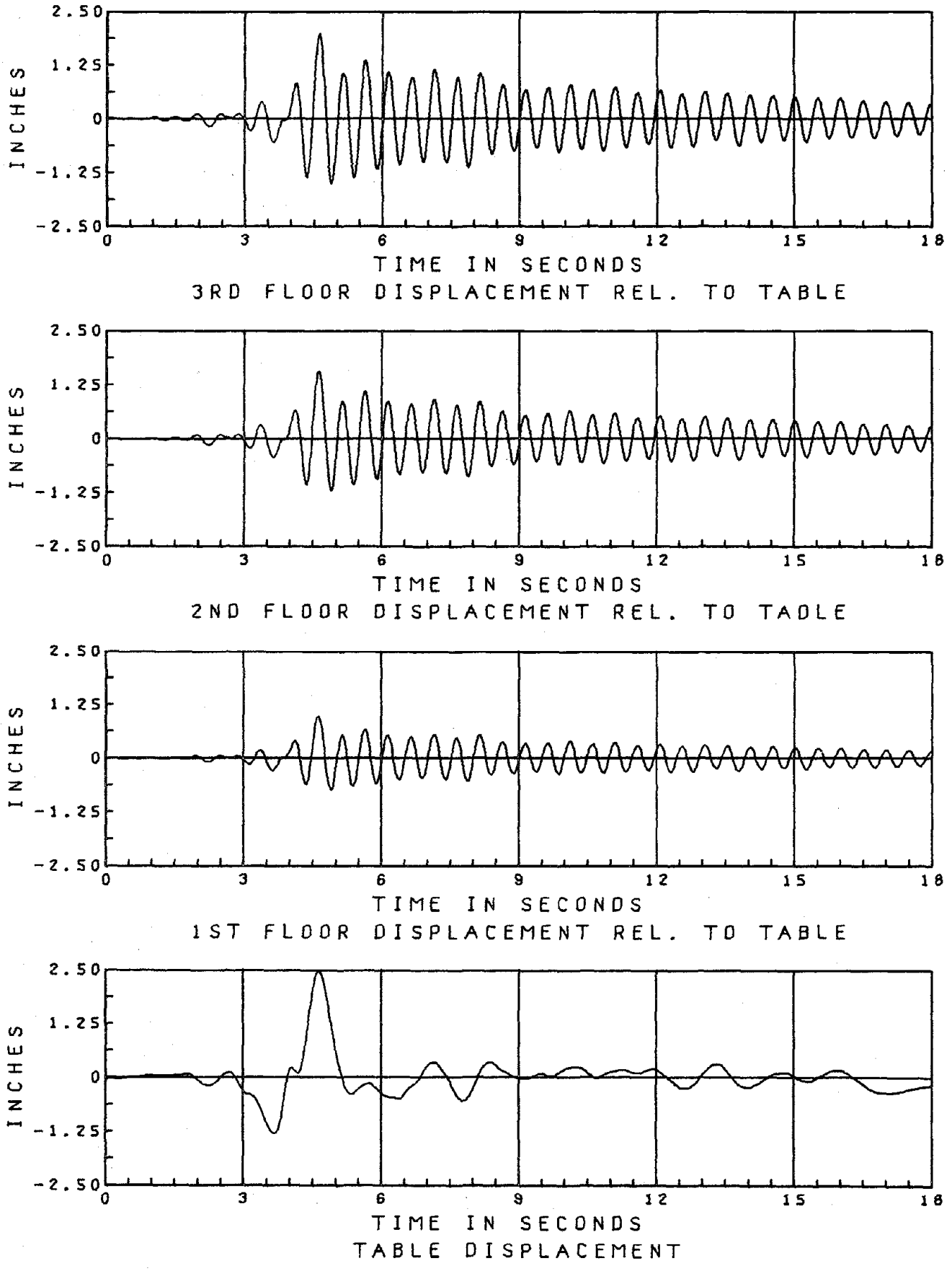

FIGURE 5.2.1.1 PARKFIELD 500 FIX, DISPLACEMENT

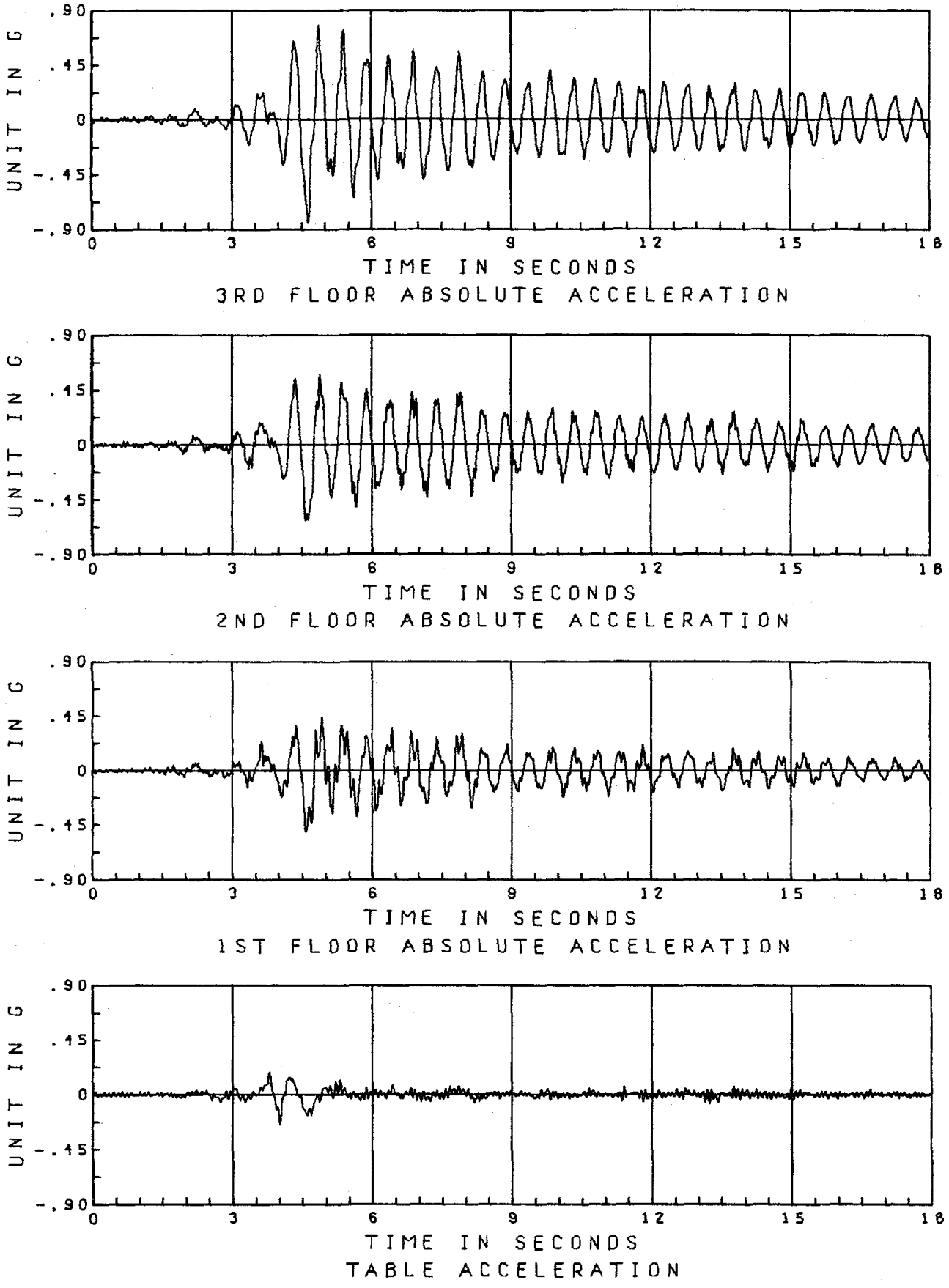

FIGURE 5.2.1.2 PARKFIELD 500 FIX, ACCELERATION

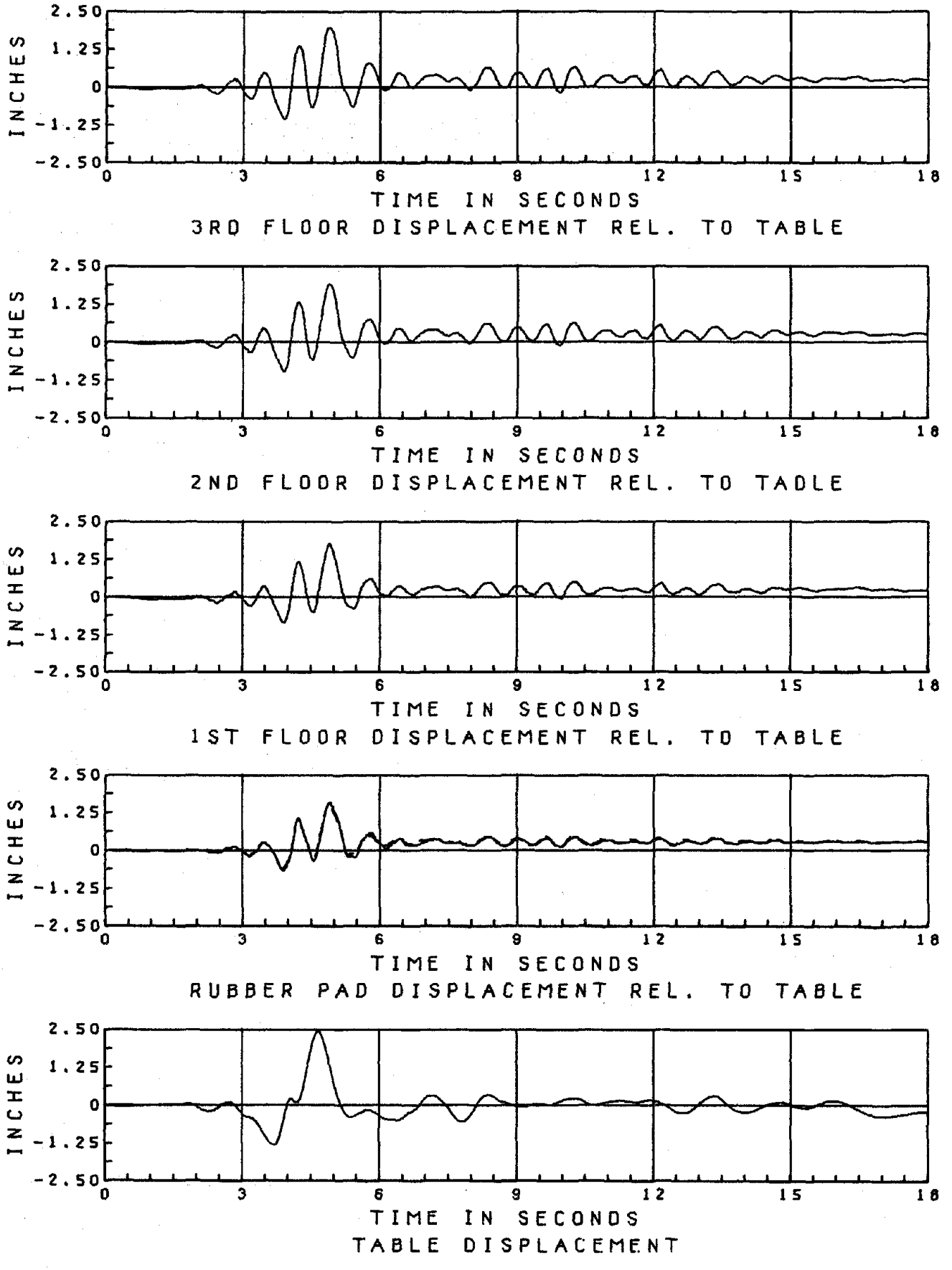

FIGURE 5.2.2.1 PARKFIELD 500 EA1, DISPLACEMENT

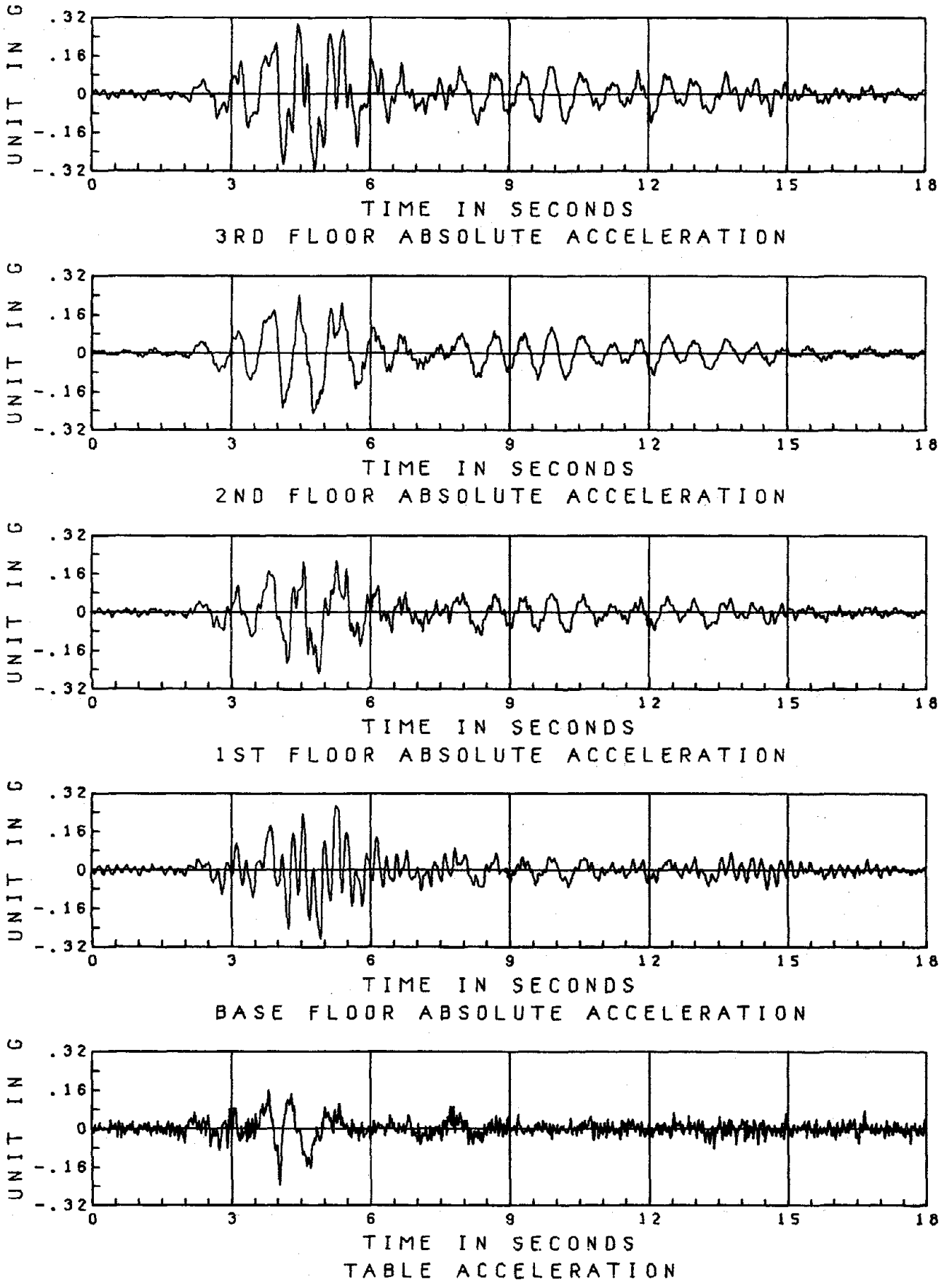

FIGURE 5.2.2.2 PARKFIELD 500 EA1, ACCELERATION

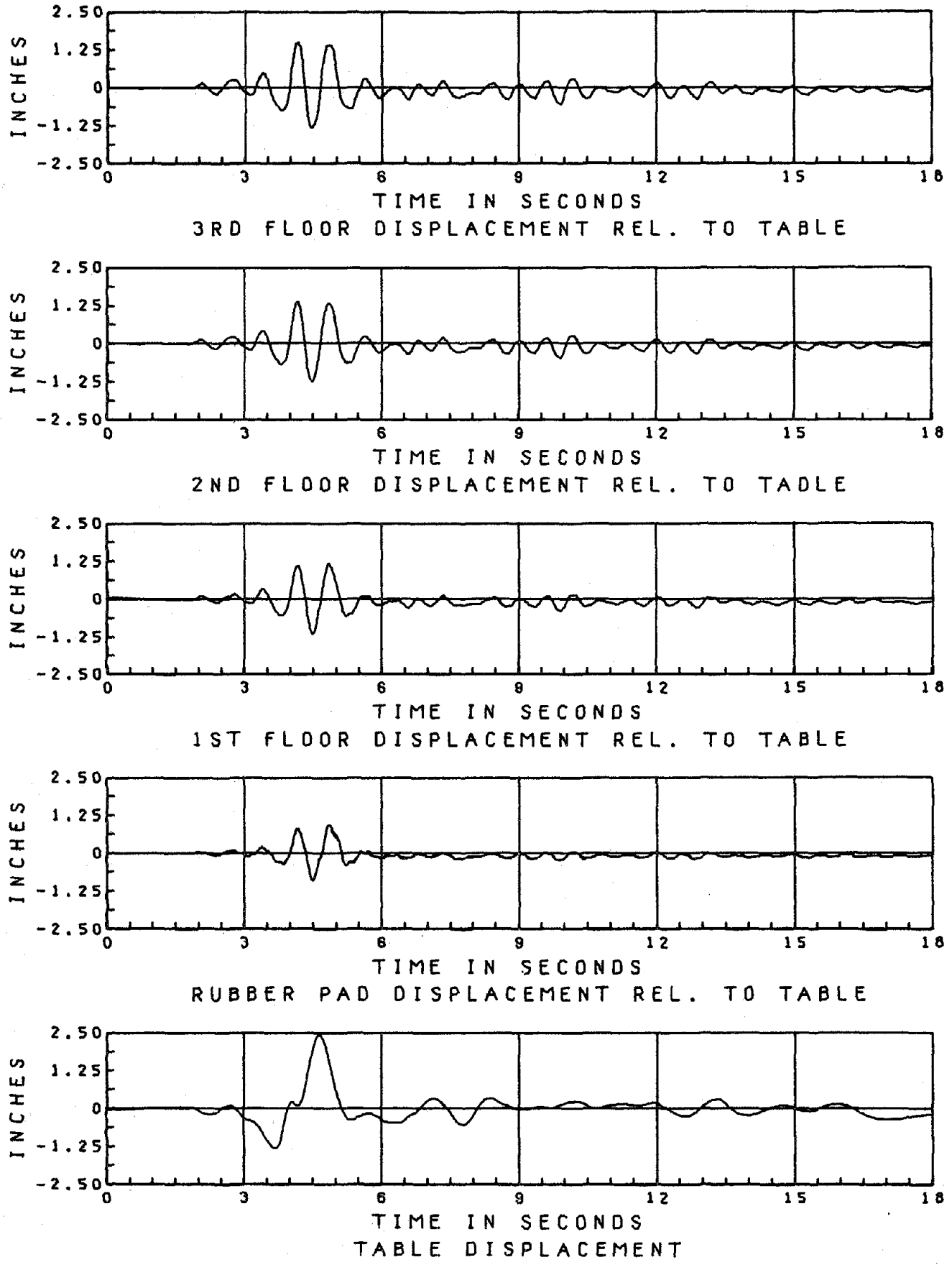

FIGURE 5.2.3.1 PARKFIELD 500 EA2, DISPLACEMENT

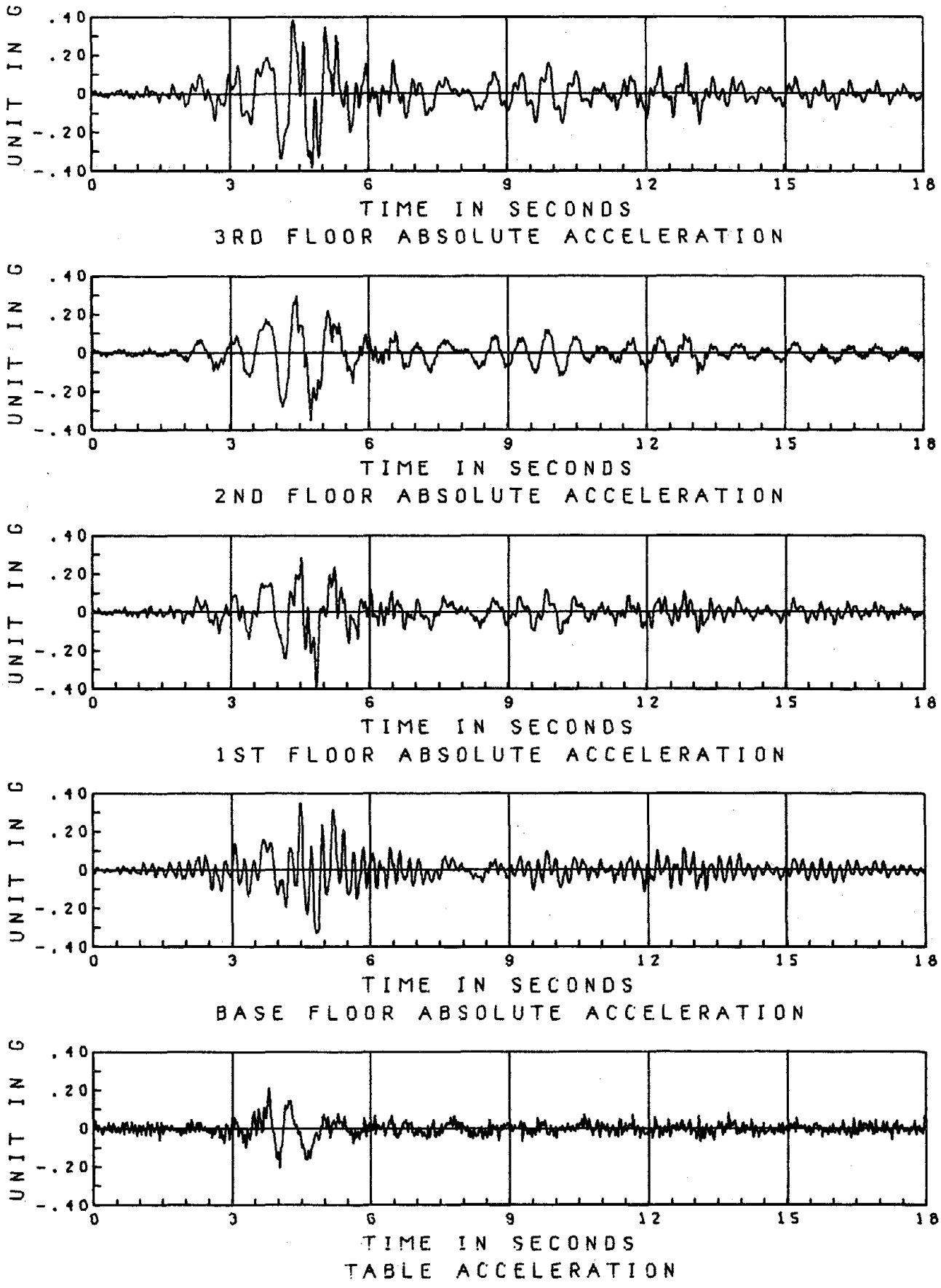

FIGURE 5.2.3.2 PARKFIELD EA2, ACCELERATION

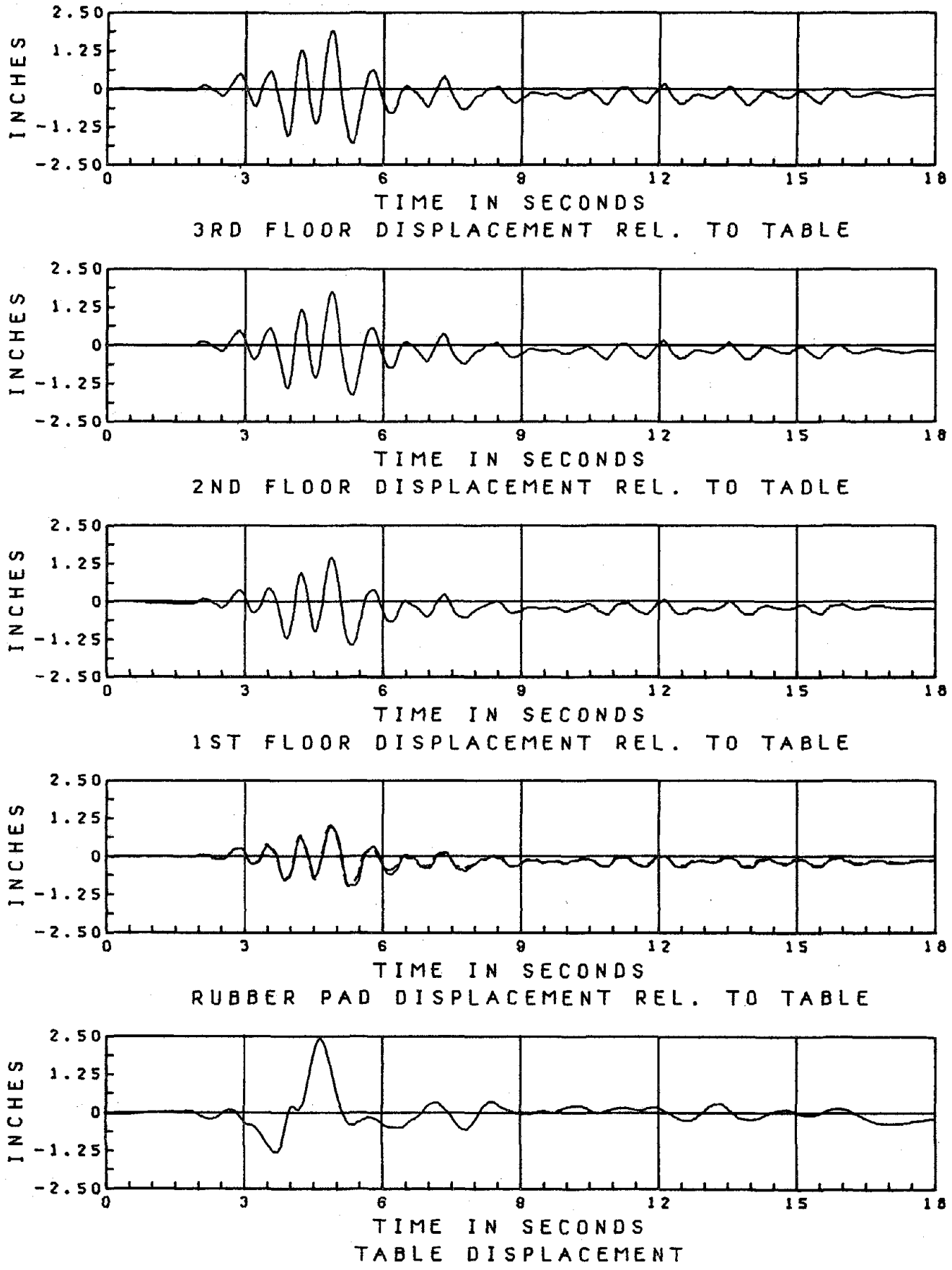

FIGURE 5.2.4.1 PARKFIELD 500 EA3, DISPLACEMENT

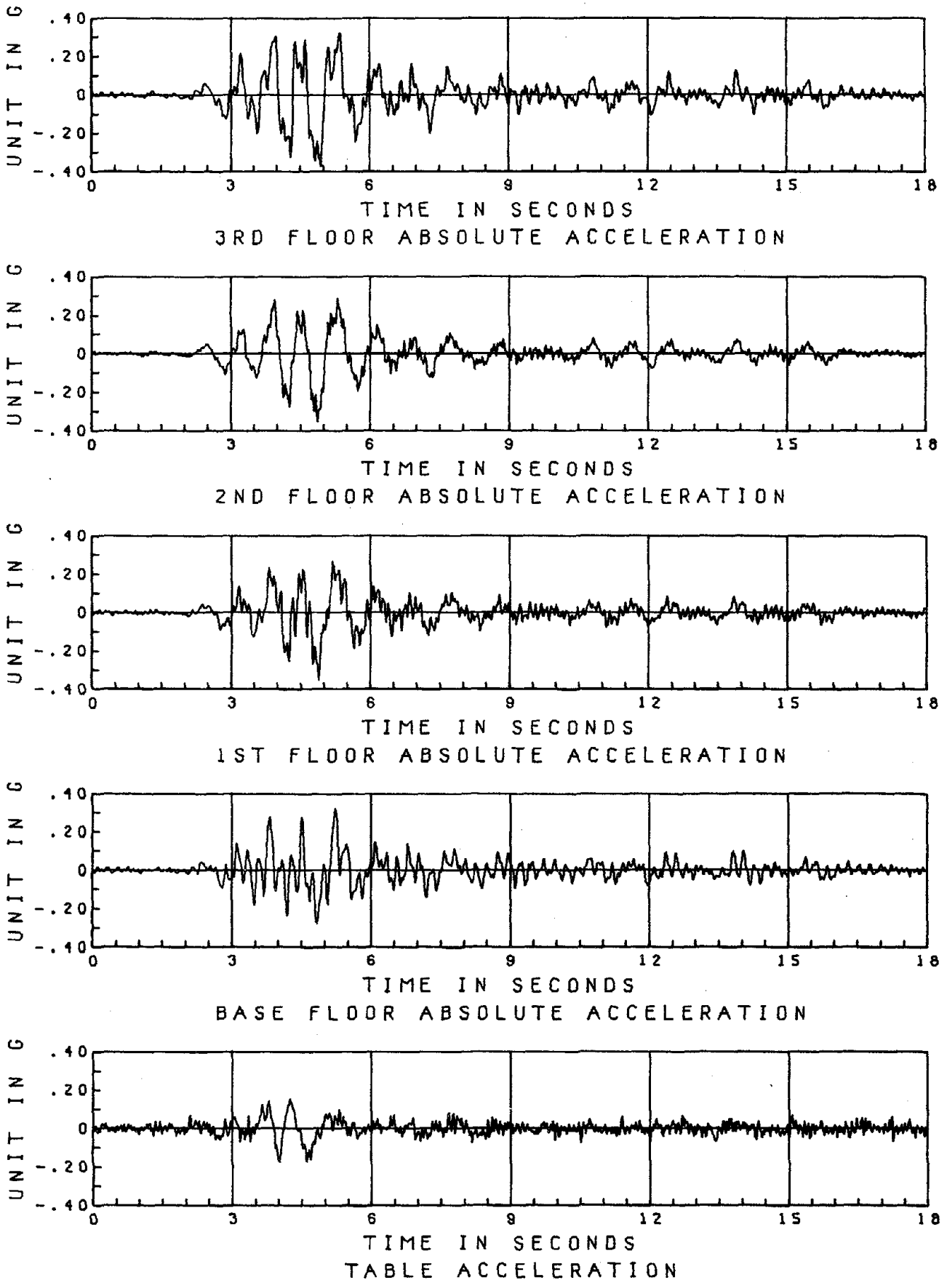

FIGURE 5.2.4.2 PARKFIELD 500 EA3, ACCELERATION

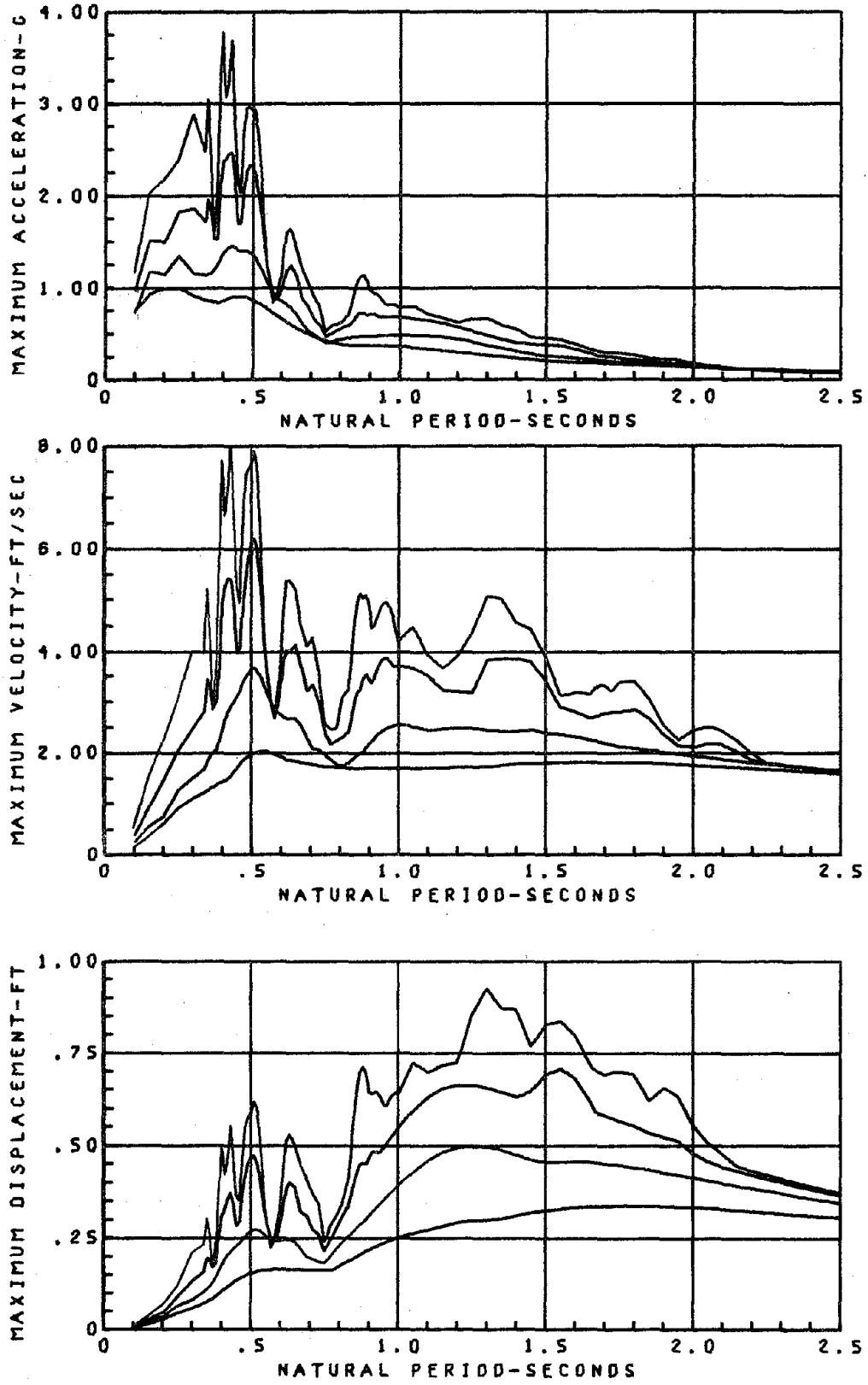

FIGURE 5.3 PACOIMA DAM 500 RESPONSE SPECTRA
ξ = 1, 3, 10, 25%

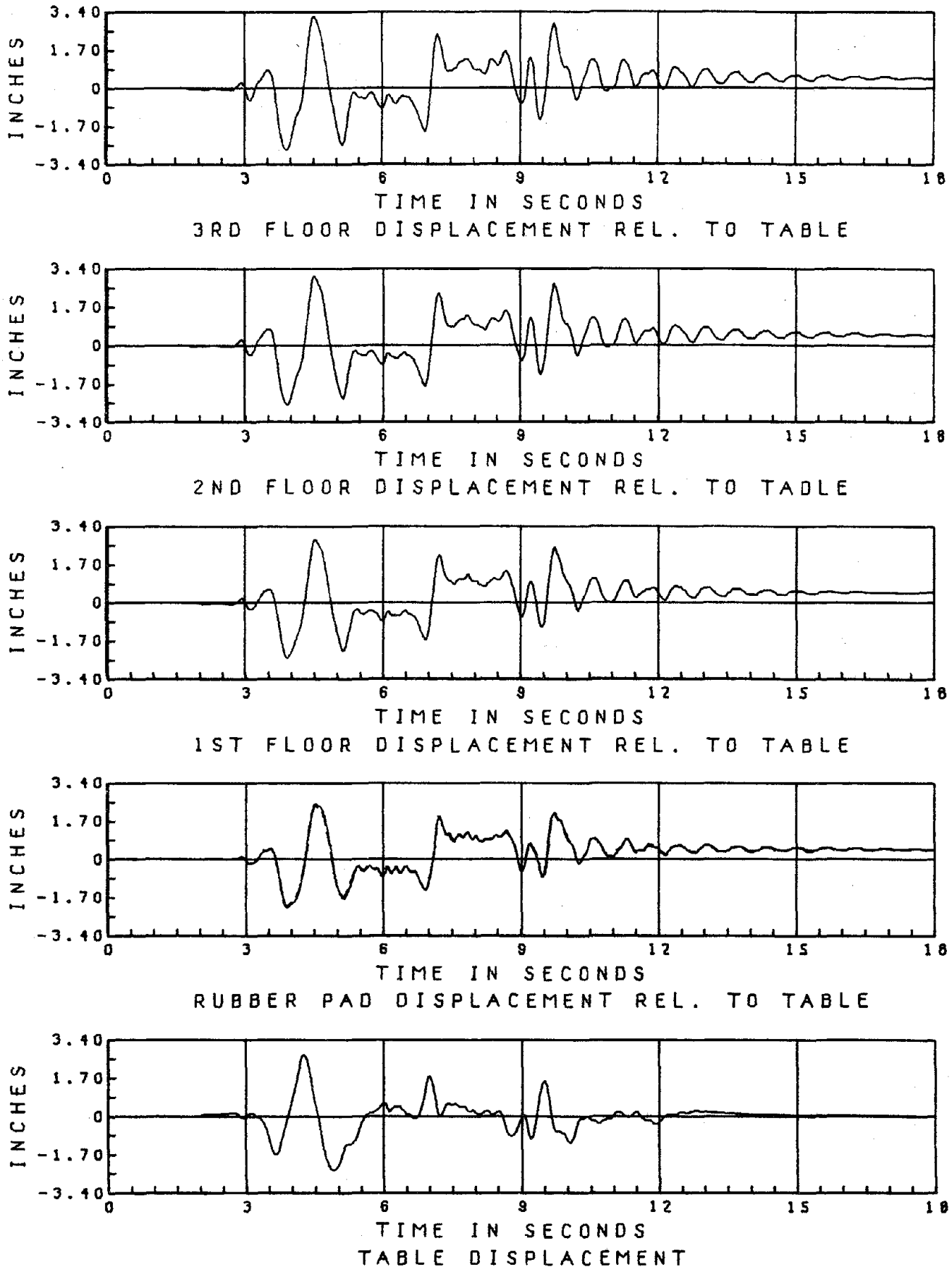

FIGURE 5.3.1.1 PACOIMA DAM 500 EA1, DISPLACEMENT

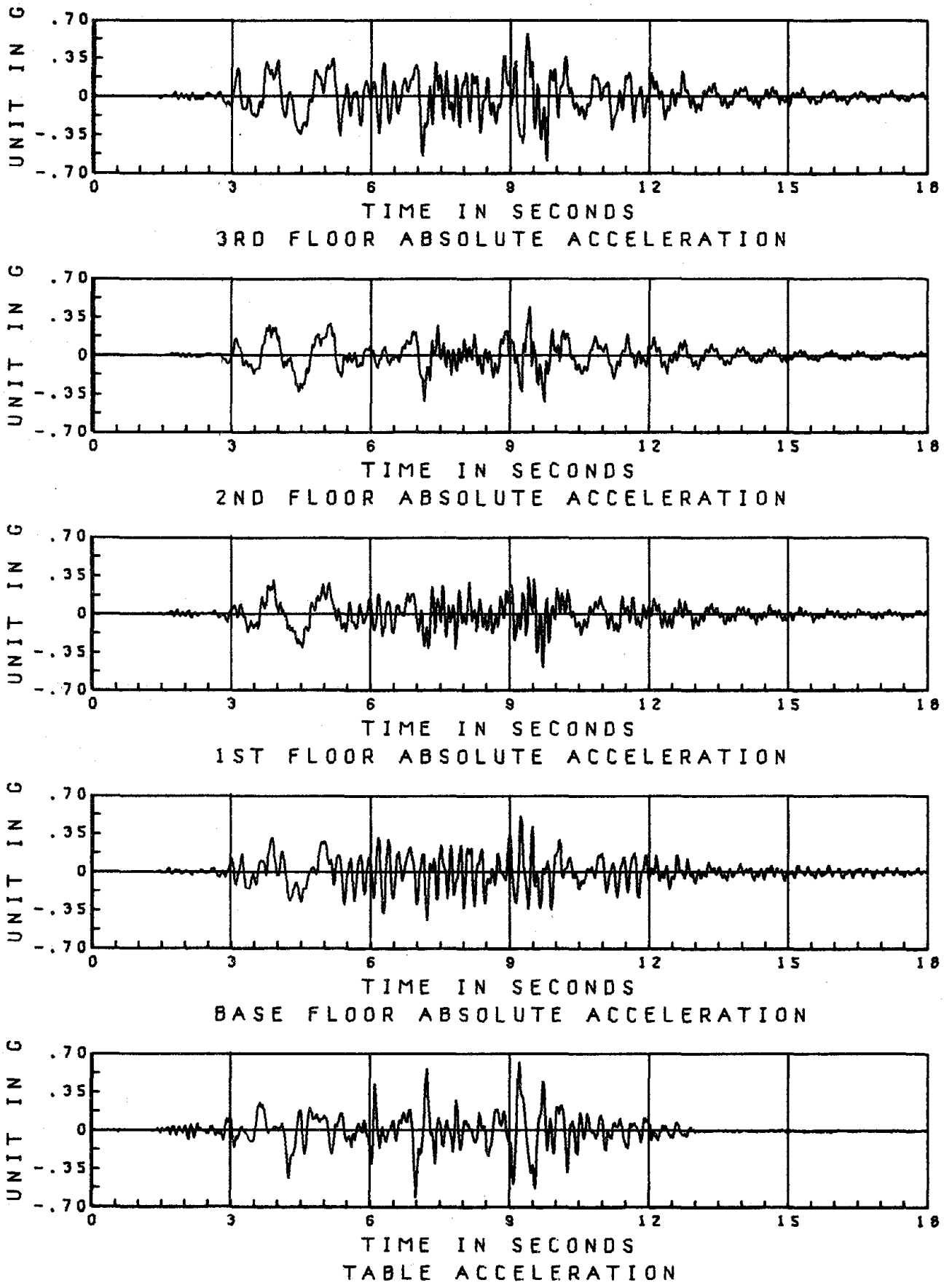

FIGURE 5.3.1.2 PACOIMA DAM 500 EA1, ACCELERATION

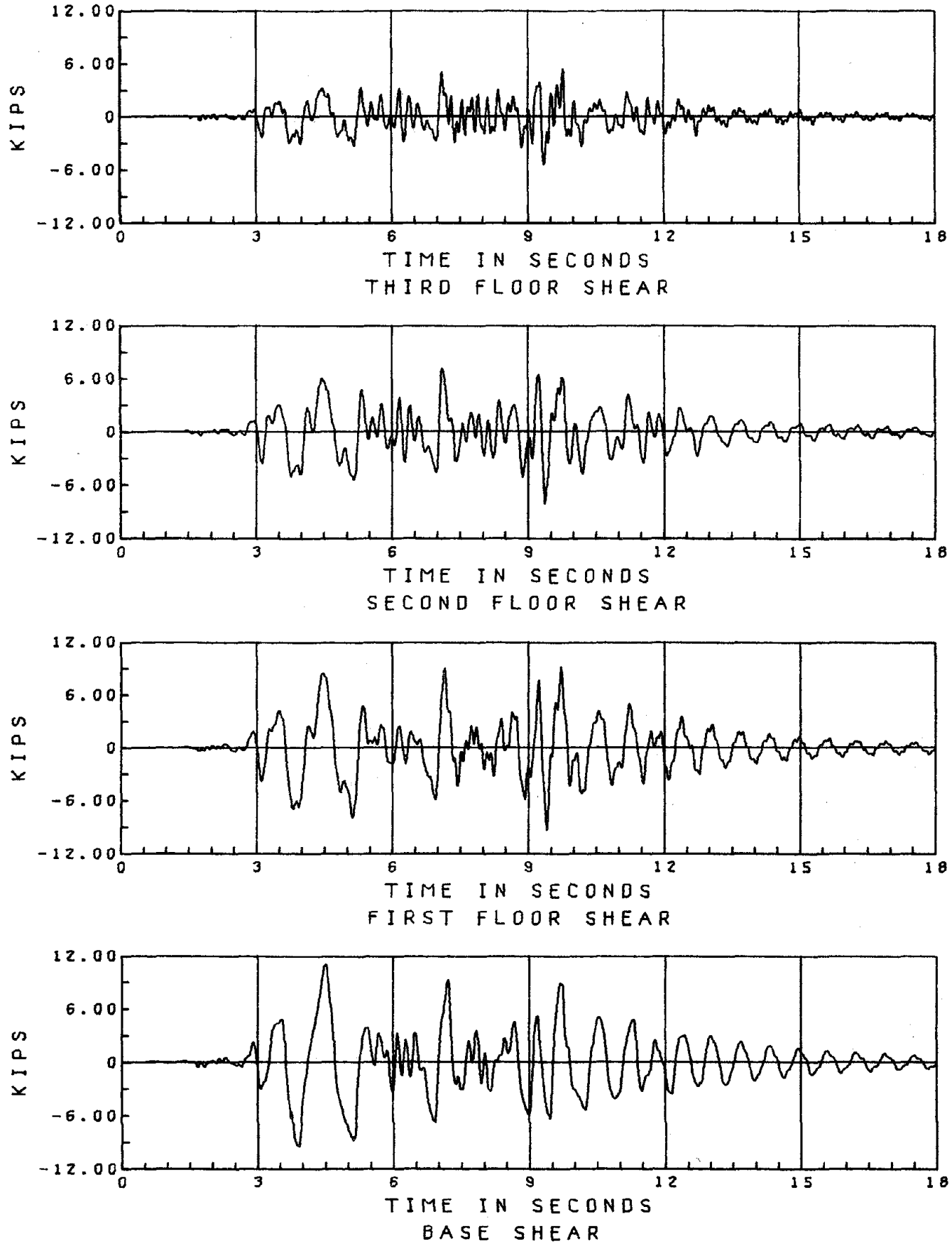

FIGURE 5.3.1.3 PACOIMA DAM 500 EA1, SHEARS

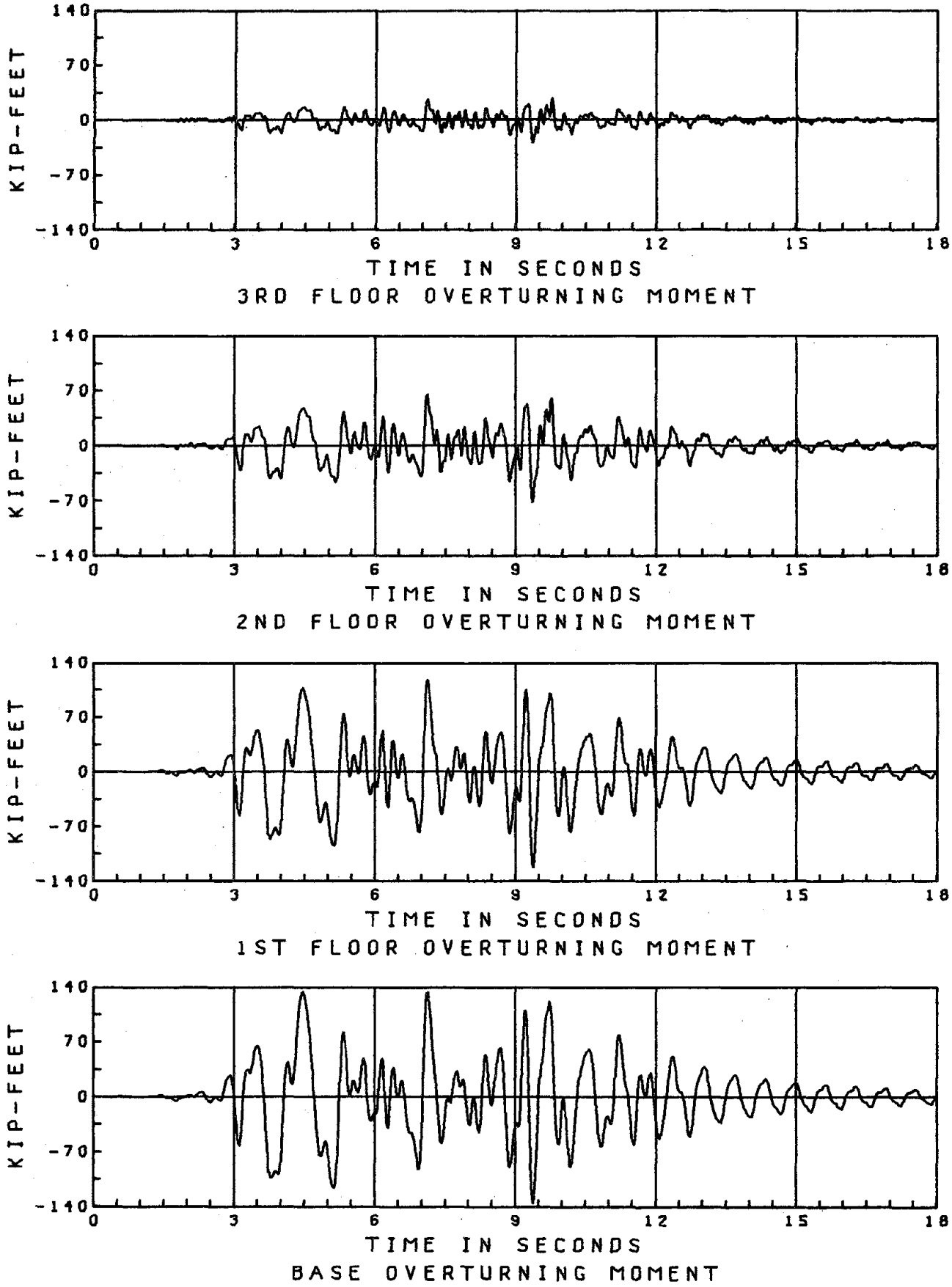

FIGURE 5.3.1.4 PACOIMA DAM 500 EA1, OVERTURNING MOMENTS

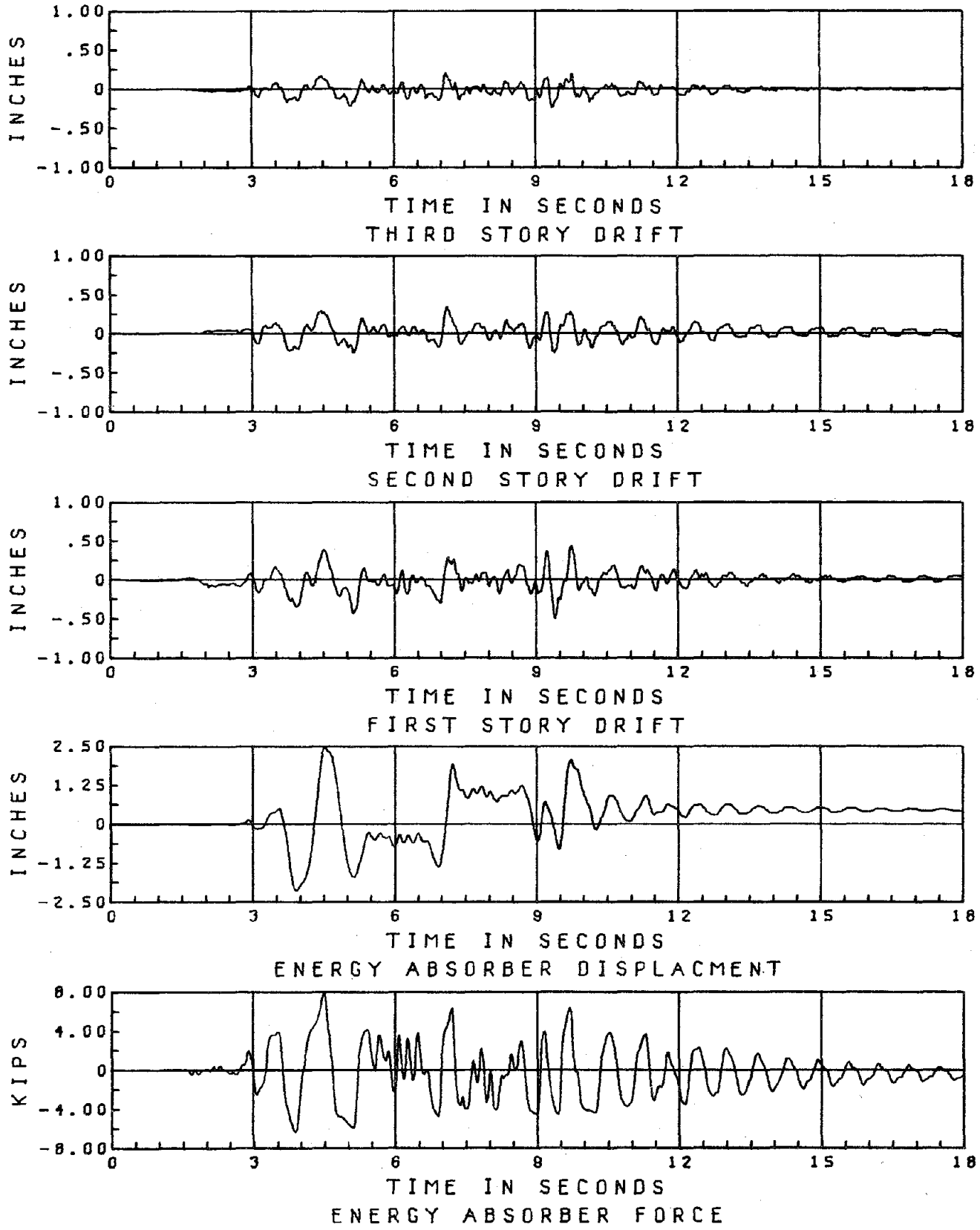

FIGURE 5.3.1.5 PACOIMA DAM 500 EA1, DRIFTS, DEVICE RESPONSE

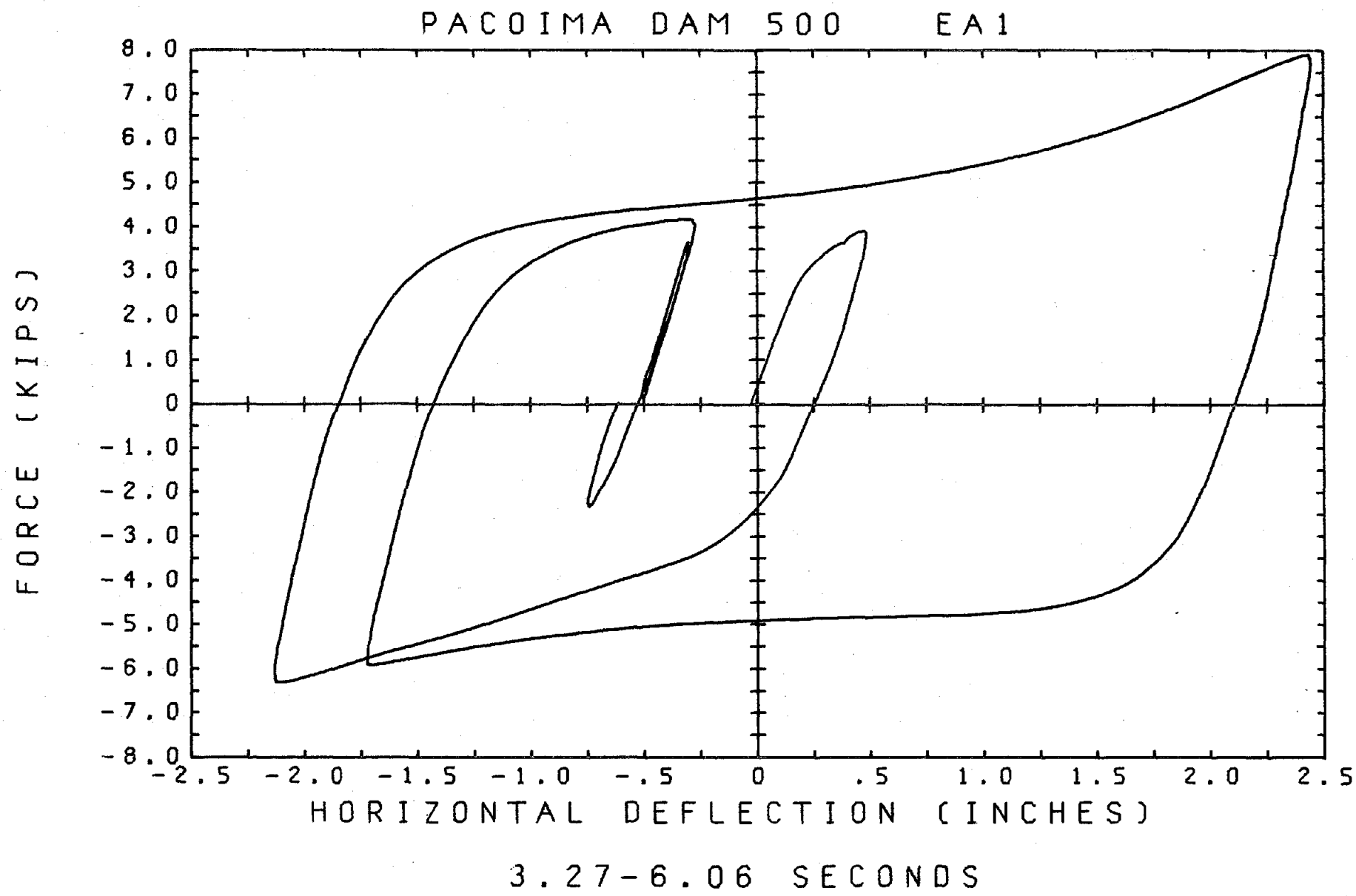

FIGURE 5.3.1.6 PACOIMA DAM 500 EA1, ENERGY-ABSORBER EA1 LOOPS

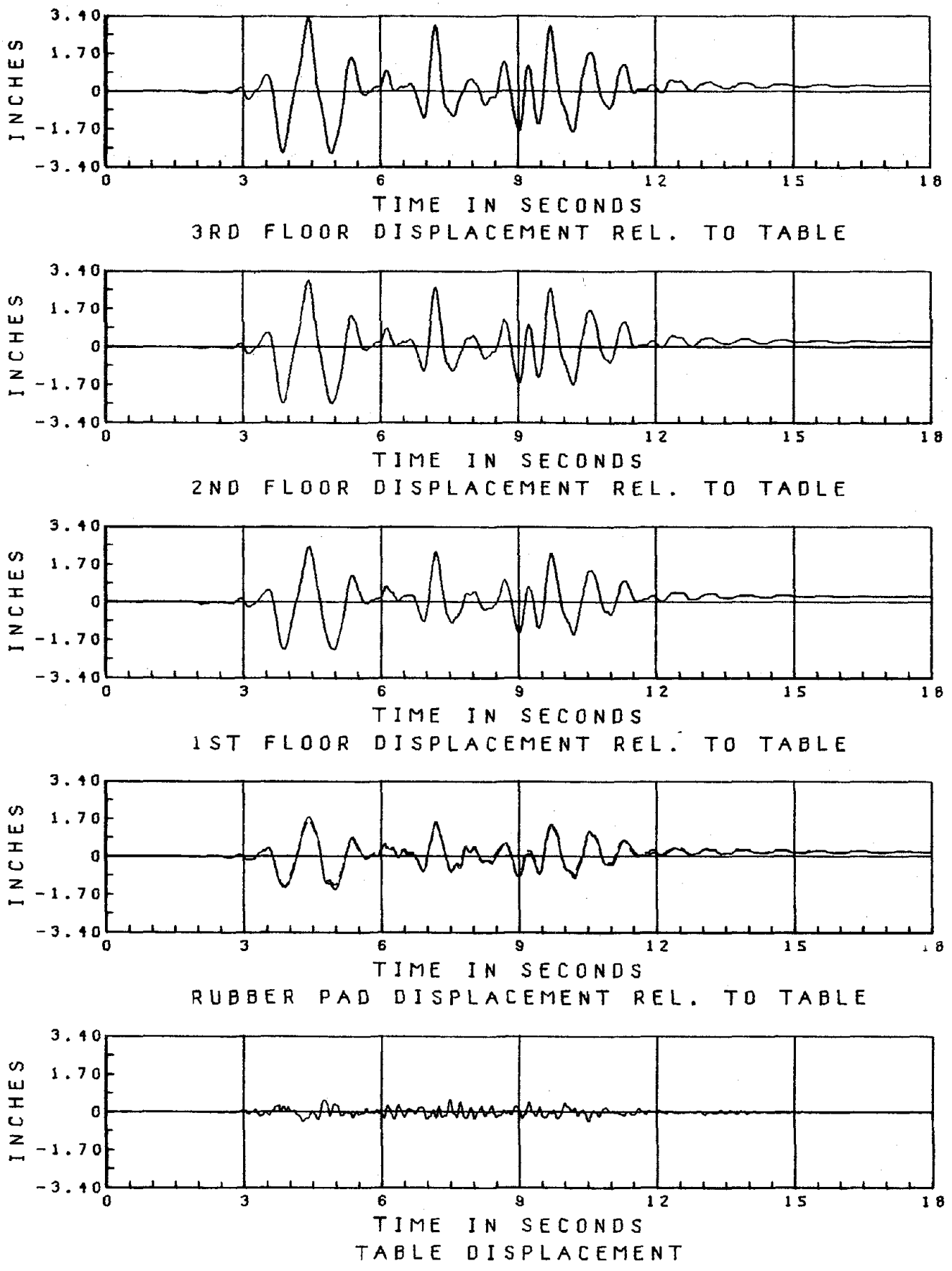

FIGURE 5.3.2.1 PACOIMA DAM 500 EA3, DISPLACEMENT

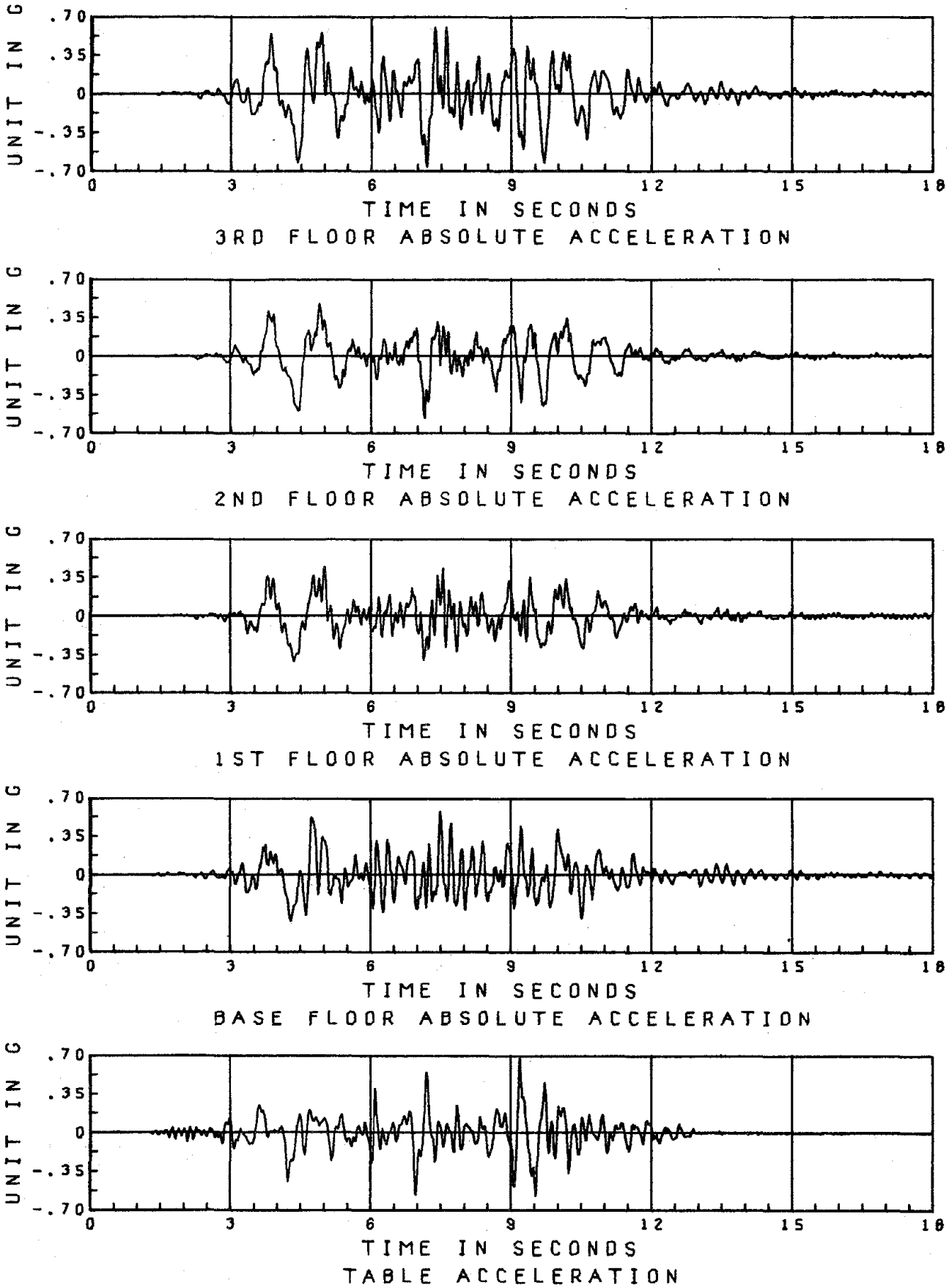

FIGURE 5.3.2.2 PACOIMA DAM 500 EA3, ACCELERATION

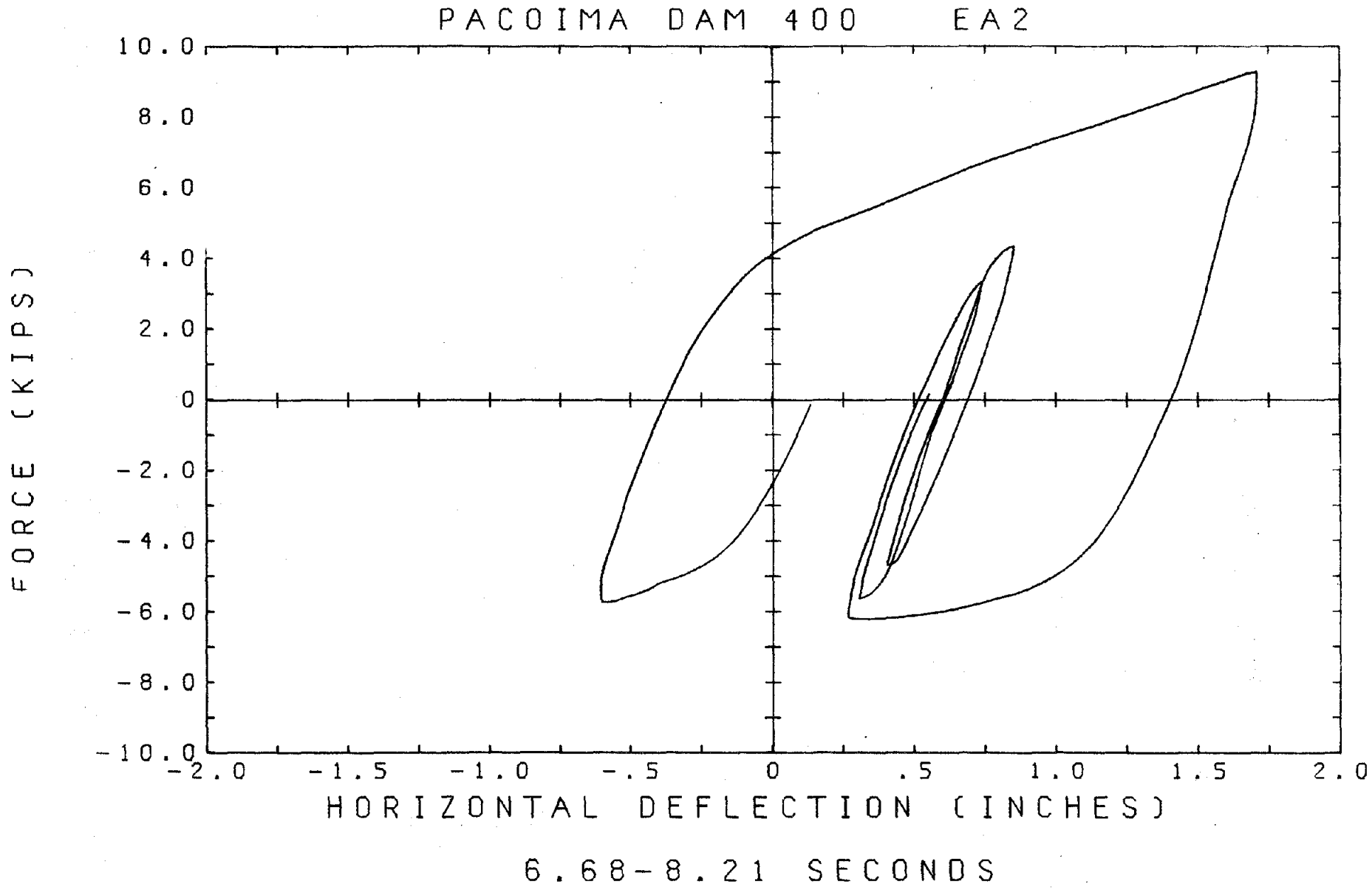

FIGURE 5.3.3 PACOIMA DAM 400, ENERGY-ABSORBER EA2 LOOPS

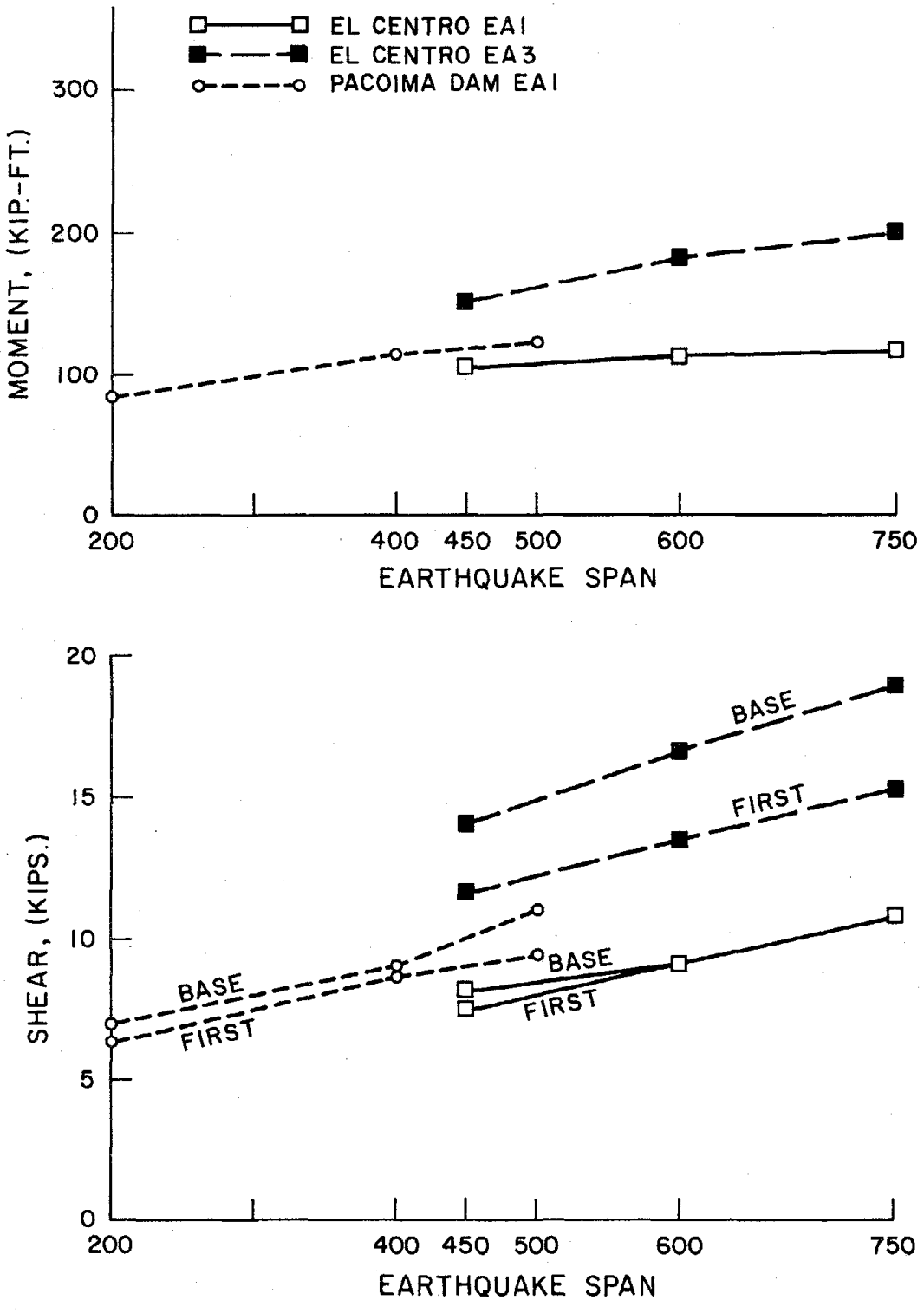

FIGURE 6.1a-b COMPARISON OF MAXIMUM BASE AND FIRST FLOOR SHEARS AND BASE OVERTURNING MOMENTS DUE TO INCREASING INTENSITY EARTHQUAKES

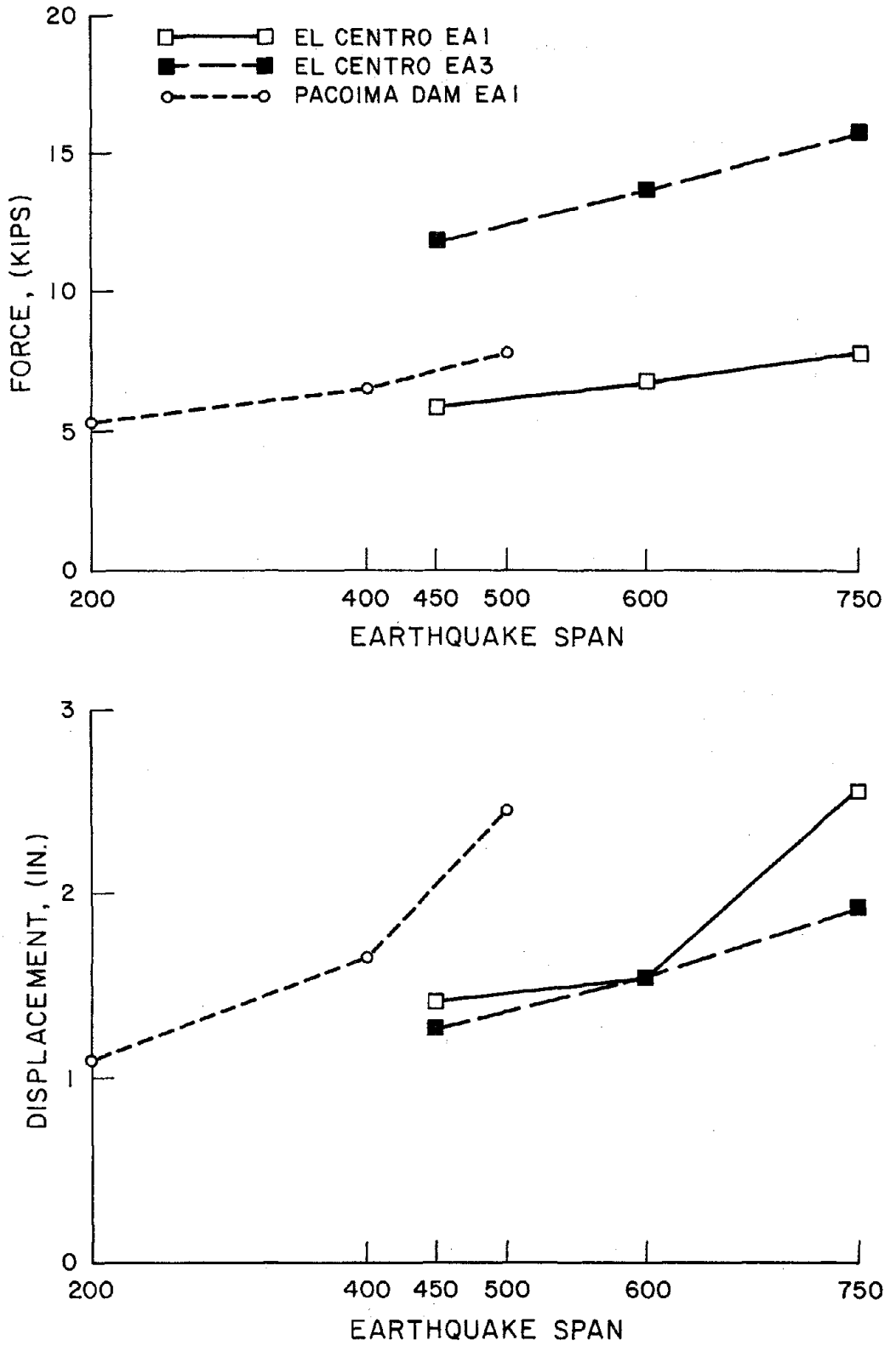

FIGURE 6.1c-d COMPARISON OF ENERGY-ABSORBER MAXIMUM DISPLACEMENTS AND FORCES DUE TO INCREASING INTENSITY EARTHQUAKES

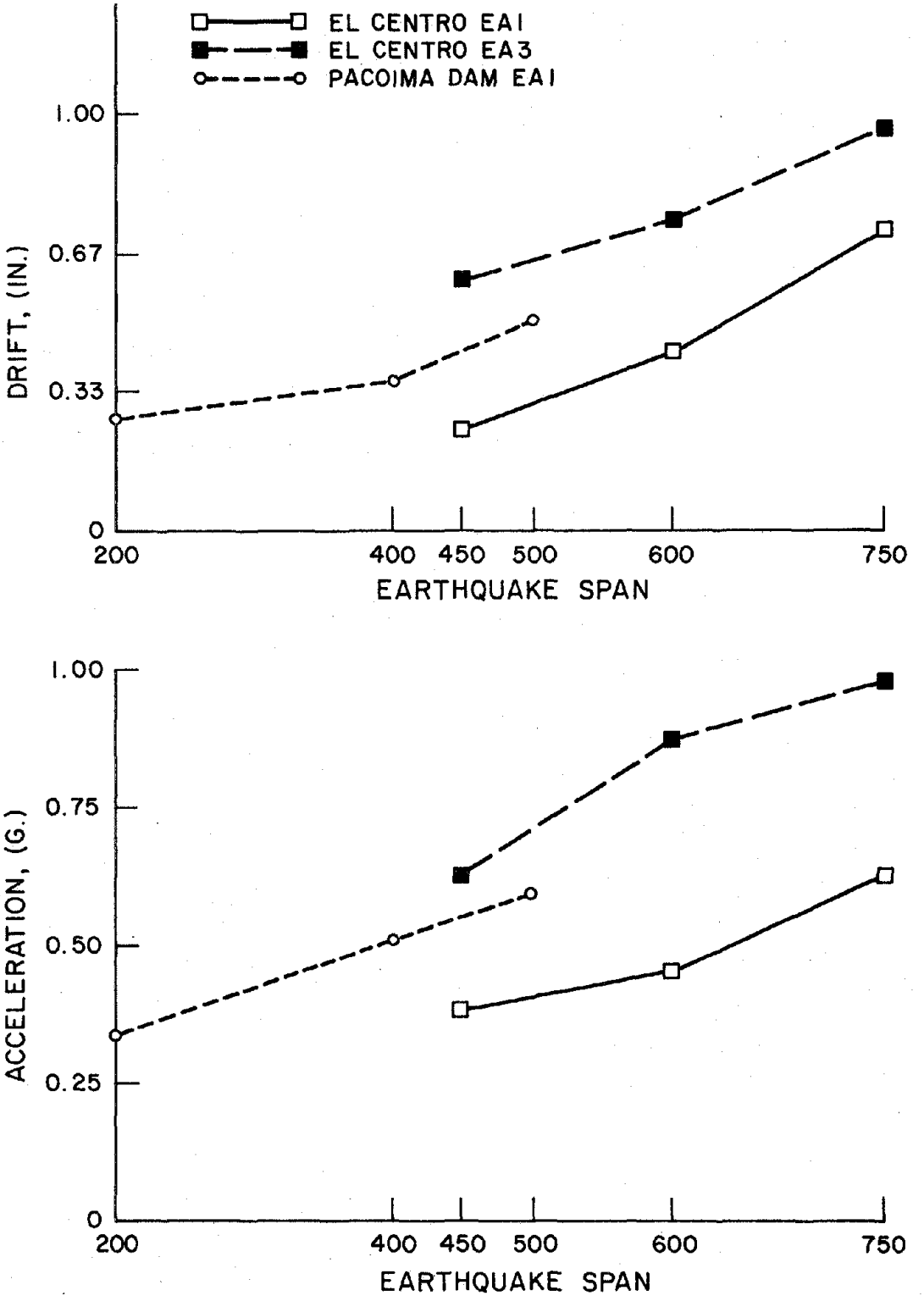

FIGURE 6.1e-f COMPARISON OF MAXIMUM THIRD FLOOR ACCELERATIONS AND FIRST FLOOR DRIFT DUE TO INCREASING INTENSITY EARTHQUAKES

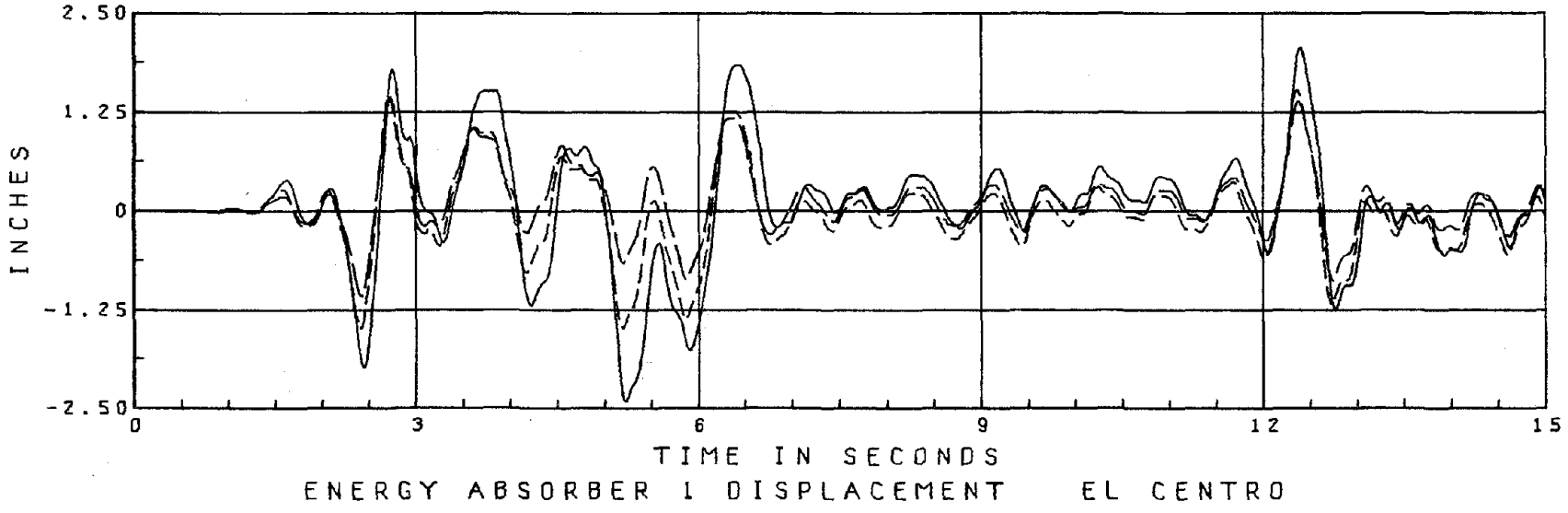

FIGURE 6.1.1.1 EA1 DISPLACEMENT RESPONSE TO INCREASING EL CENTRO MOTION

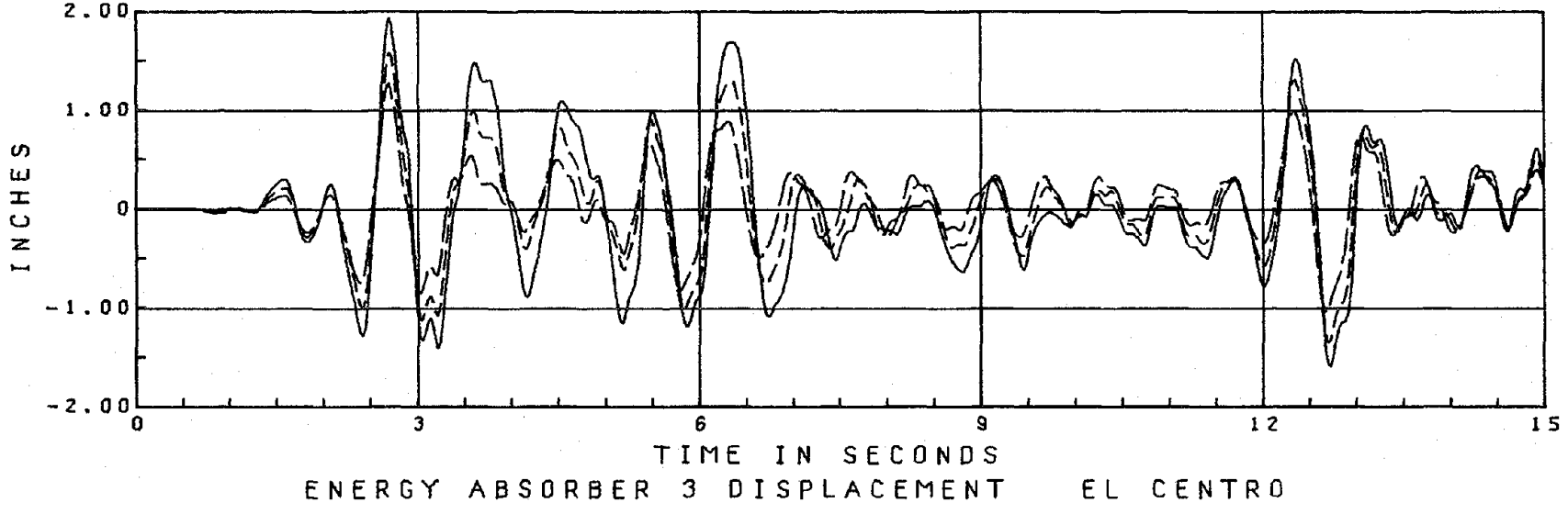

FIGURE 6.1.2.1 EA3 DISPLACEMENT RESPONSE TO INCREASING EL CENTRO MOTION

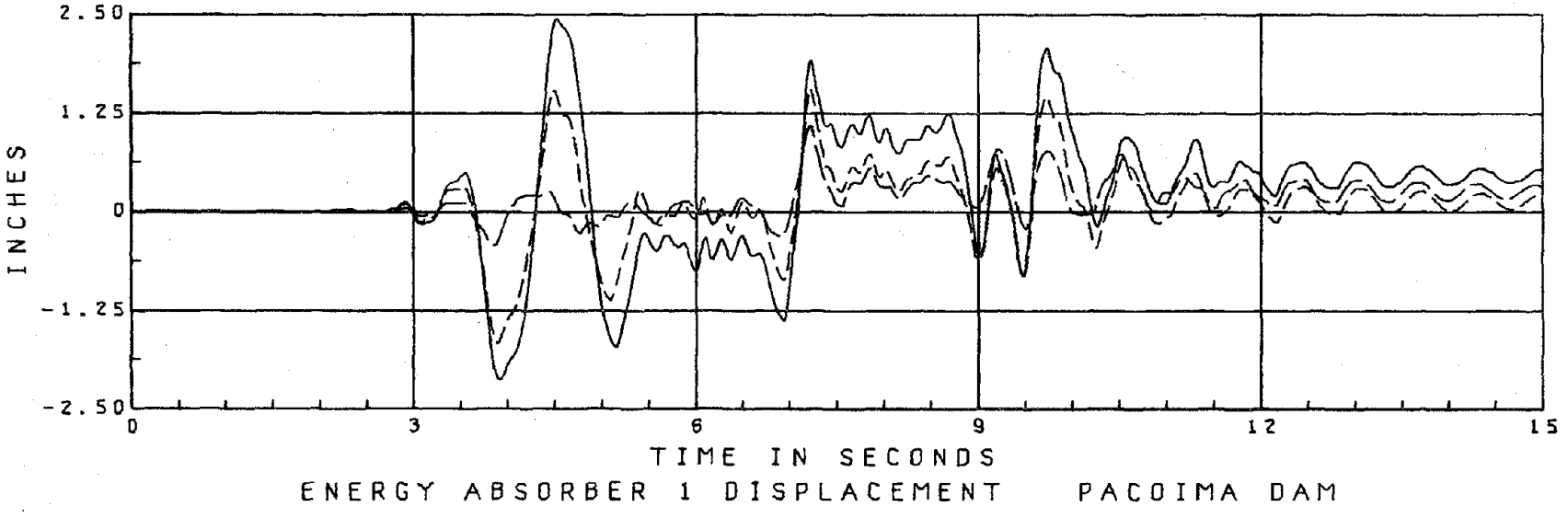

FIGURE 6.1.3.1 EA1 DISPLACEMENT RESPONSE TO INCREASING EL CENTRO MOTION

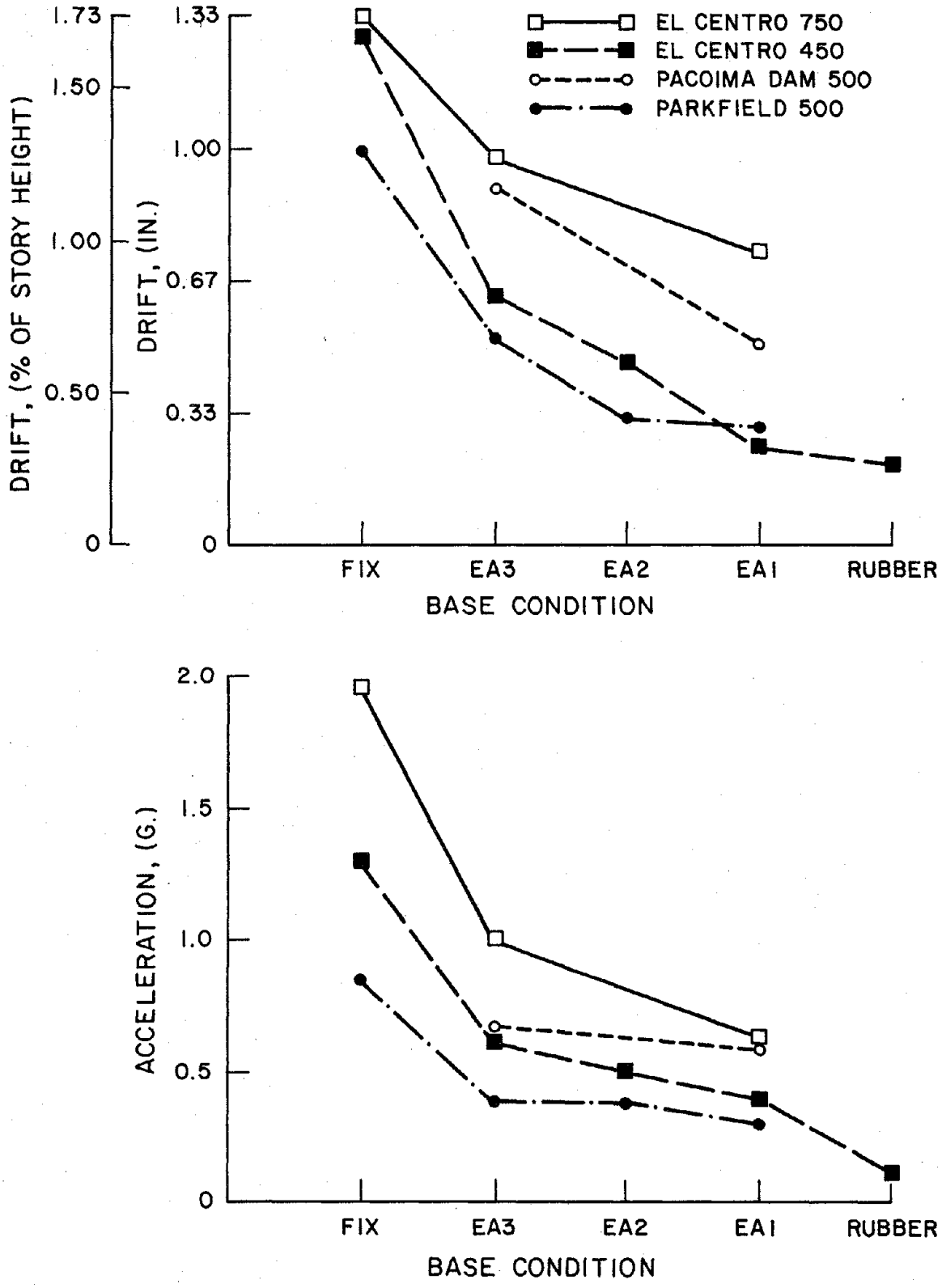

FIGURE 6.2a-b COMPARISON OF MAXIMUM THIRD FLOOR ACCELERATIONS AND FIRST FLOOR DRIFTS DUE TO DIFFERENT BASE CONDITIONS

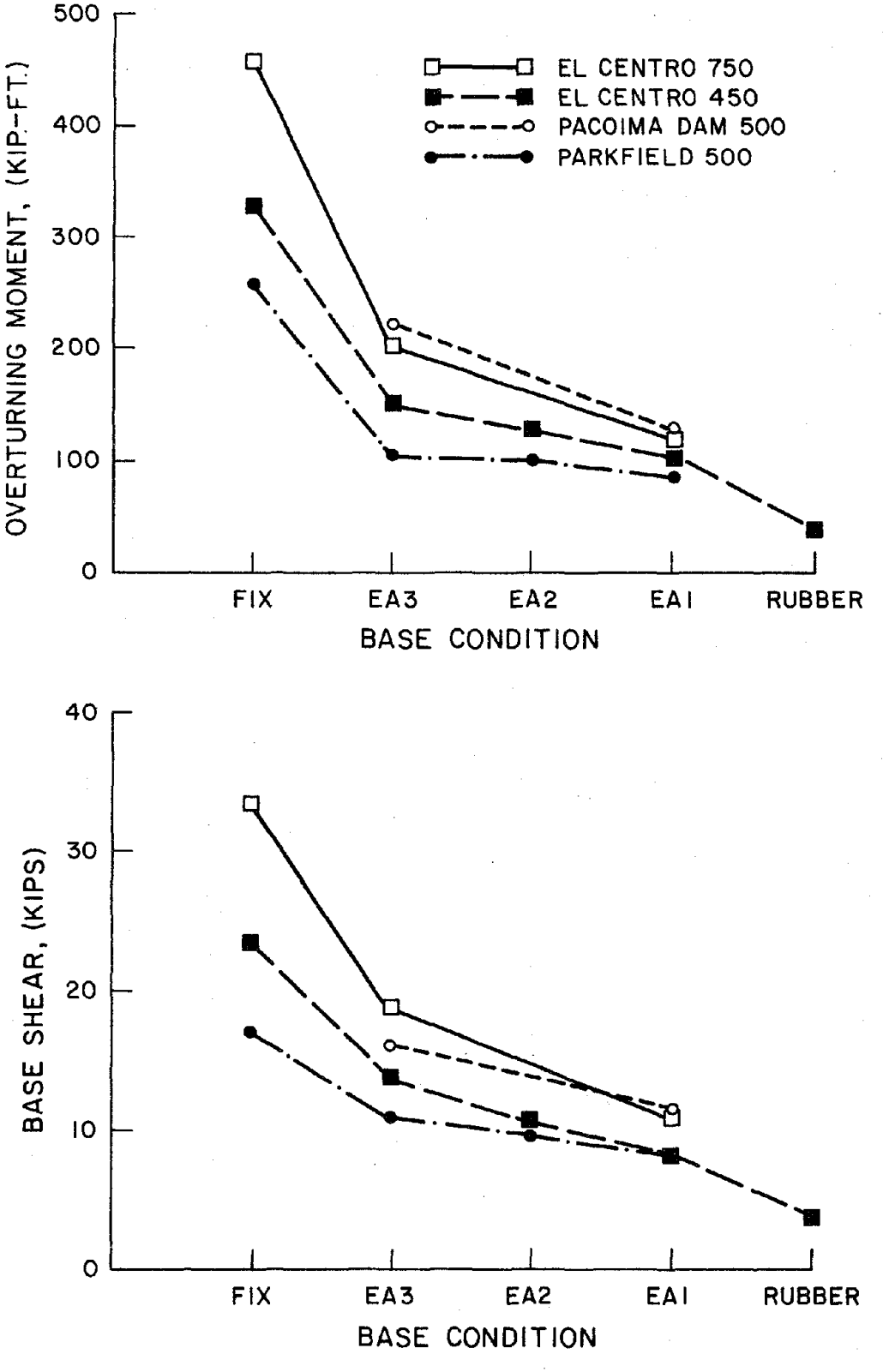

FIGURE 6.2c-d COMPARISON OF MAXIMUM BASE SHEARS AND OVERTURNING MOMENTS DUE TO DIFFERENT BASE CONDITIONS

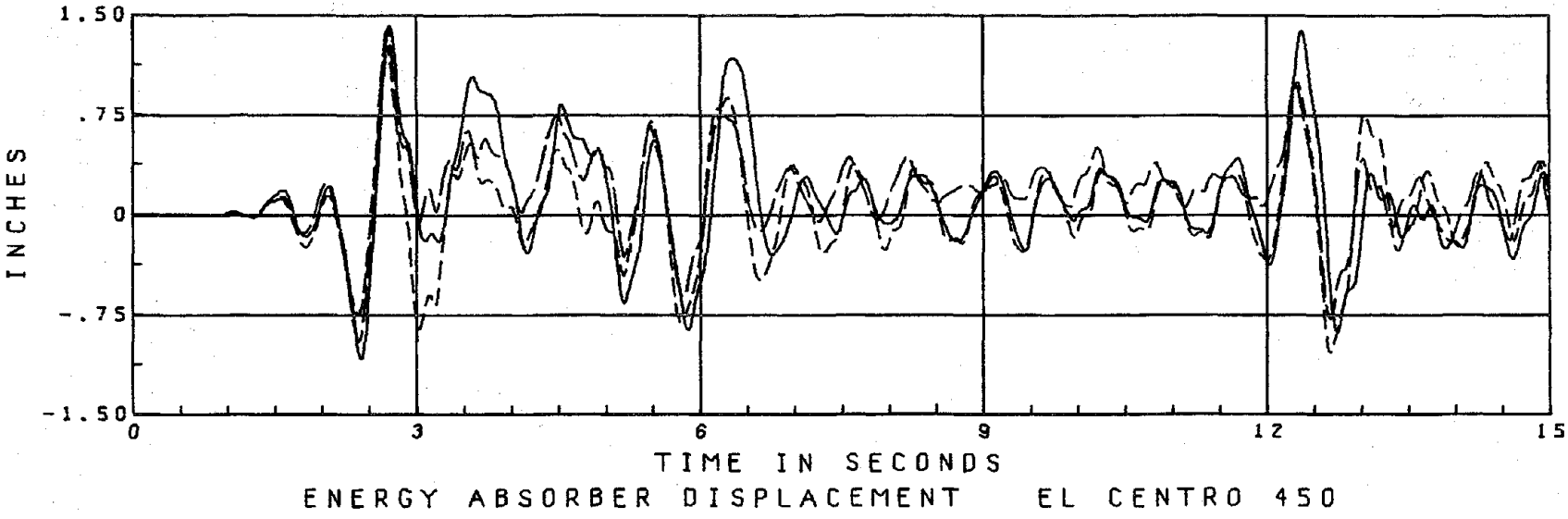

FIGURE 6.2.3.1 EA1, EA2, and EA3 DISPLACEMENT RESPONSE TO EL CENTRO 450 MOTION

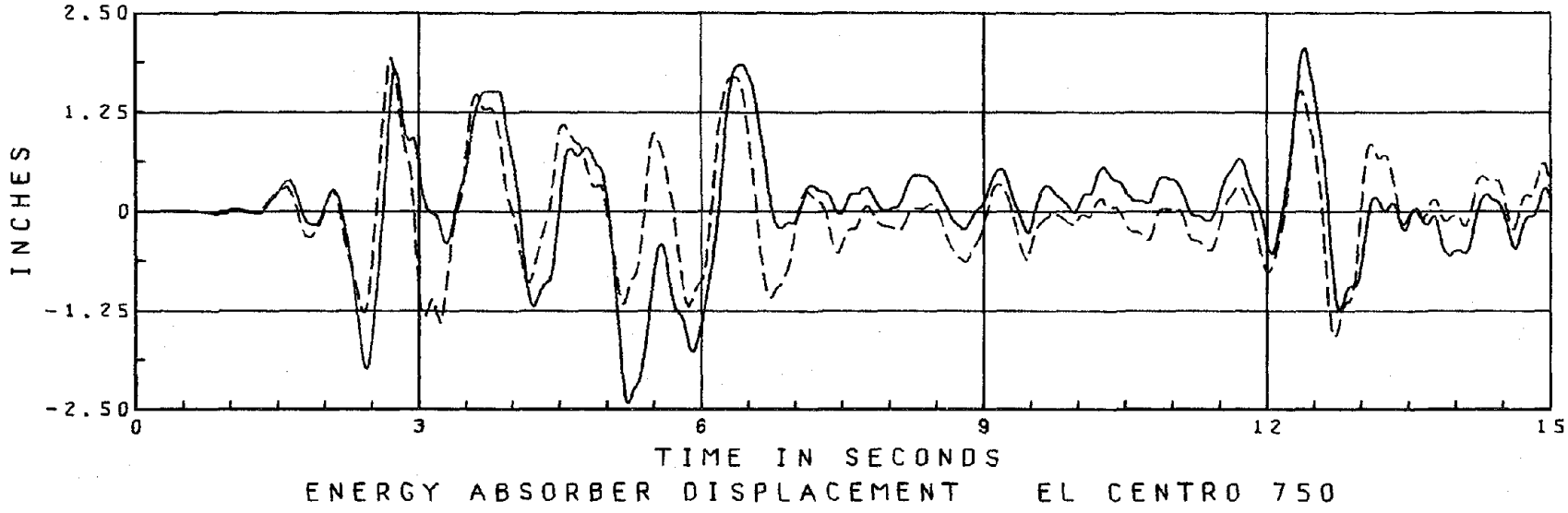

FIGURE 6.2.3.2 EA1, EA3 DISPLACEMENT RESPONSES TO EL CENTRO 750 MOTION

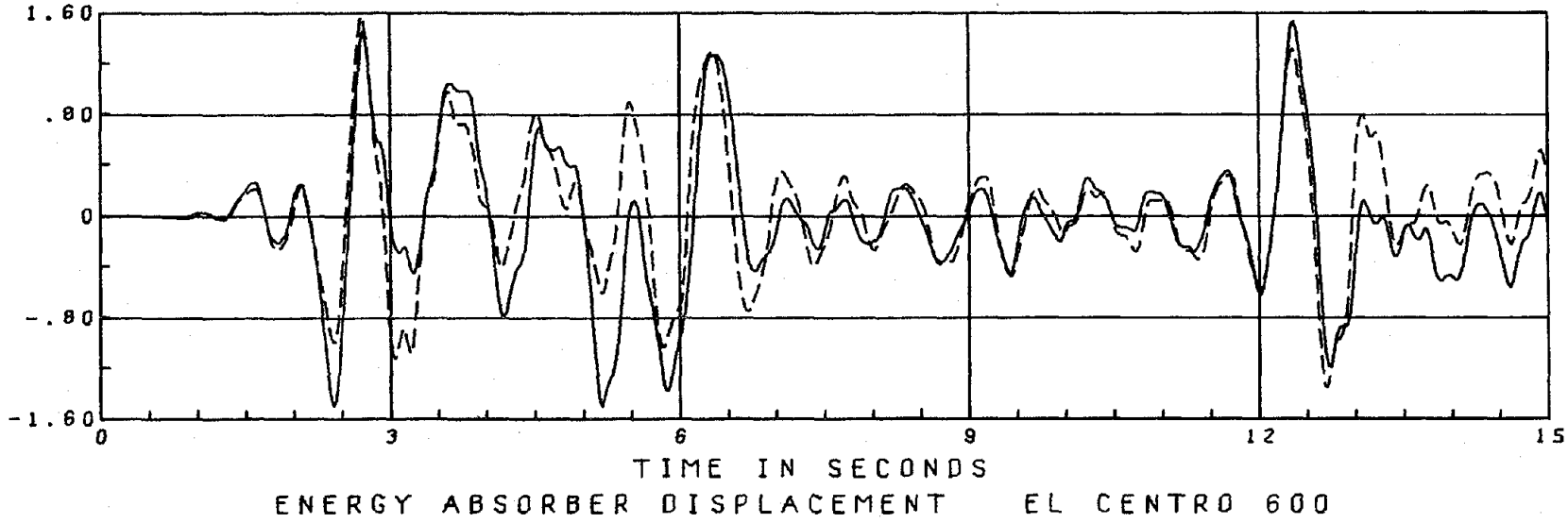

FIGURE 6.2.3.3 EA1, EA3 DISPLACEMENT RESPONSES TO PACOIMA DAM 500 MOTION

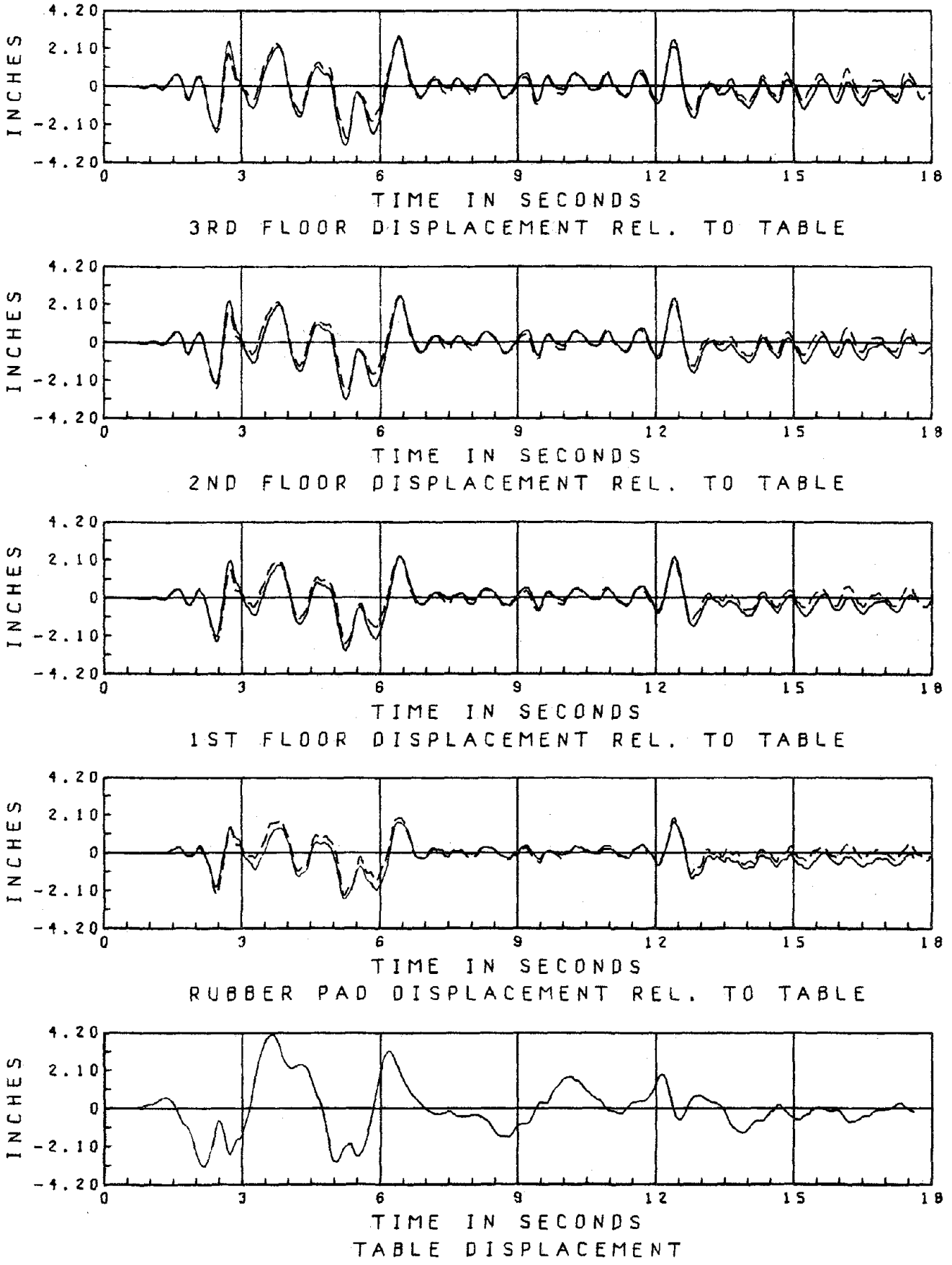

FIGURE 7.1 EL CENTRO 750 EA1, ANALYTICAL VERSUS EXPERIMENTAL

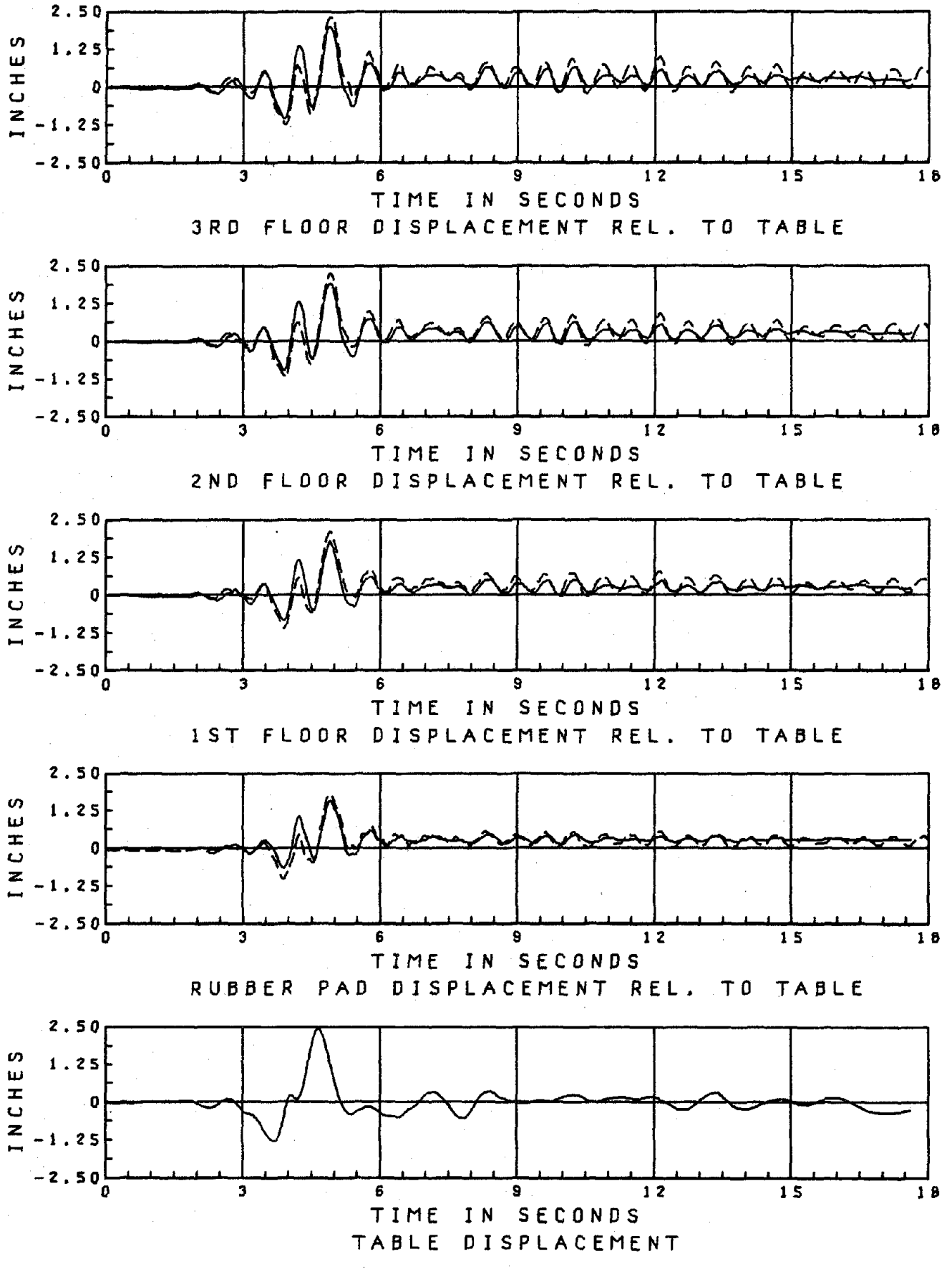

FIGURE 7.2 PARKFIELD 500 EA1, ANALYTICAL VERSUS EXPERIMENTAL

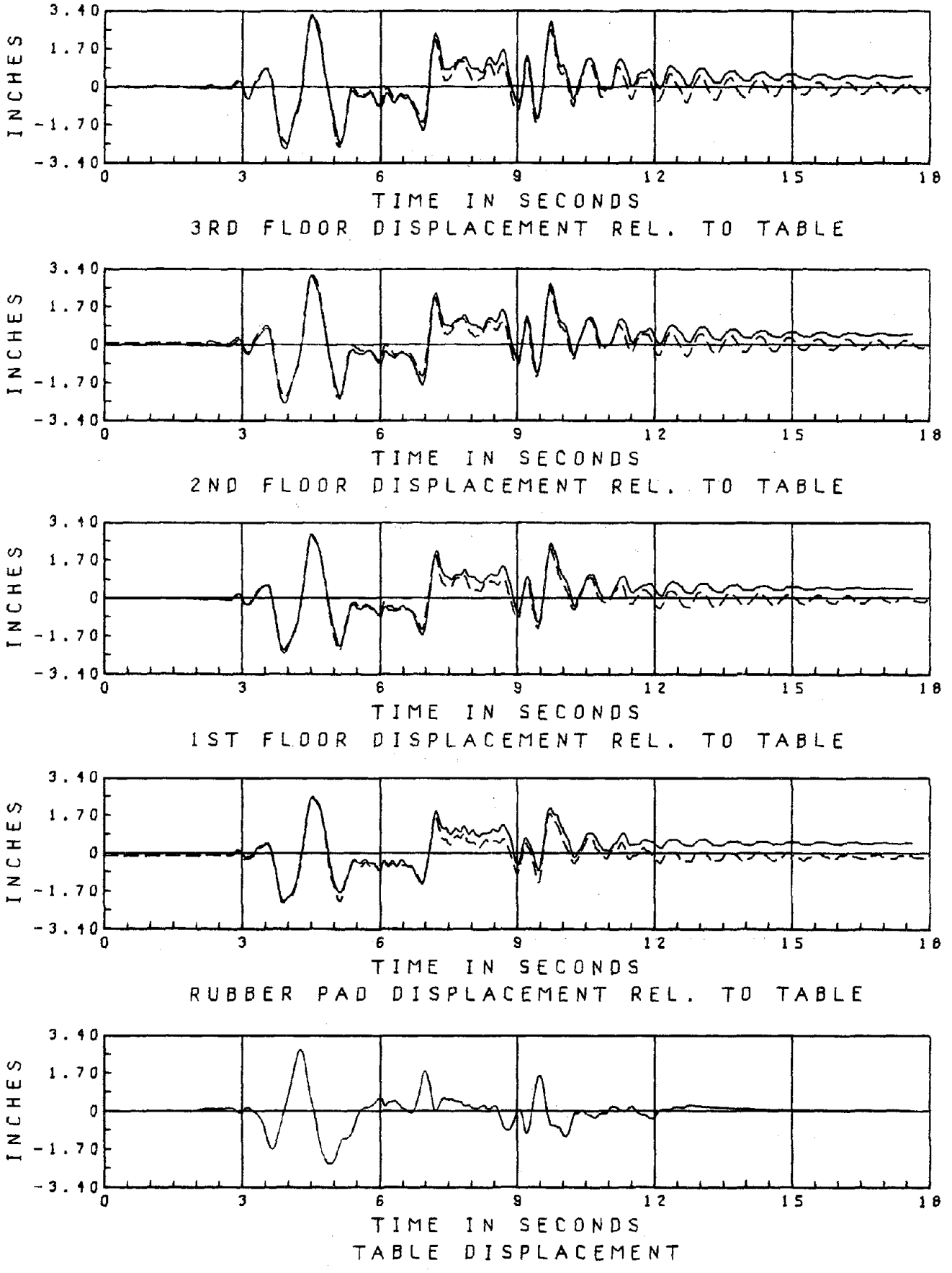

FIGURE 7.3 PACOIMA DAM 500 EA1, ANALYTICAL VERSUS EXPERIMENTAL

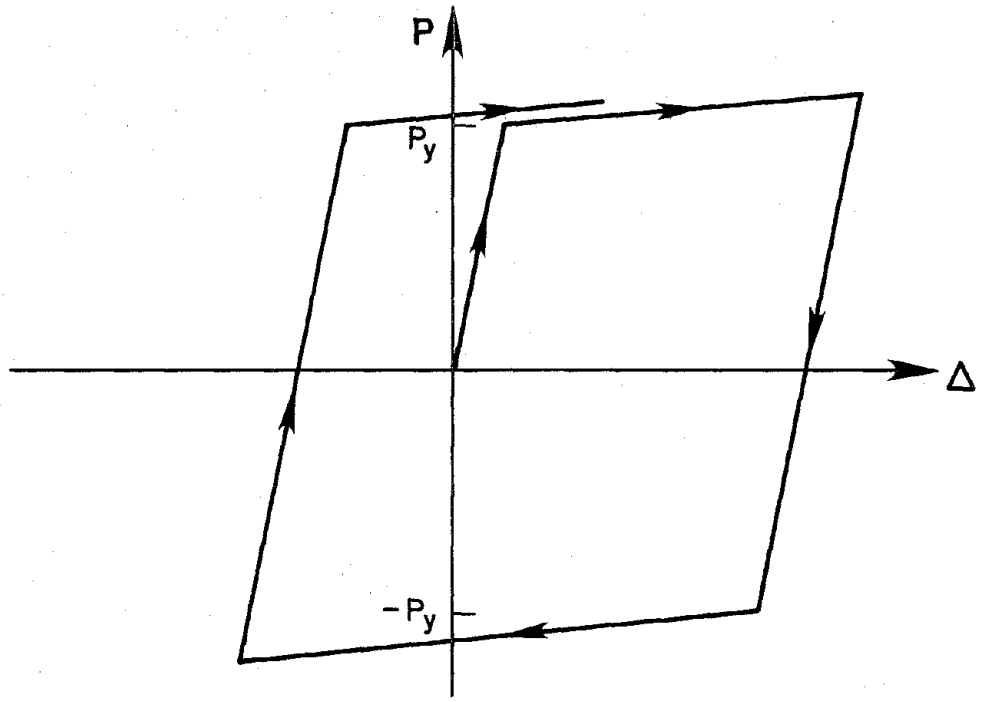

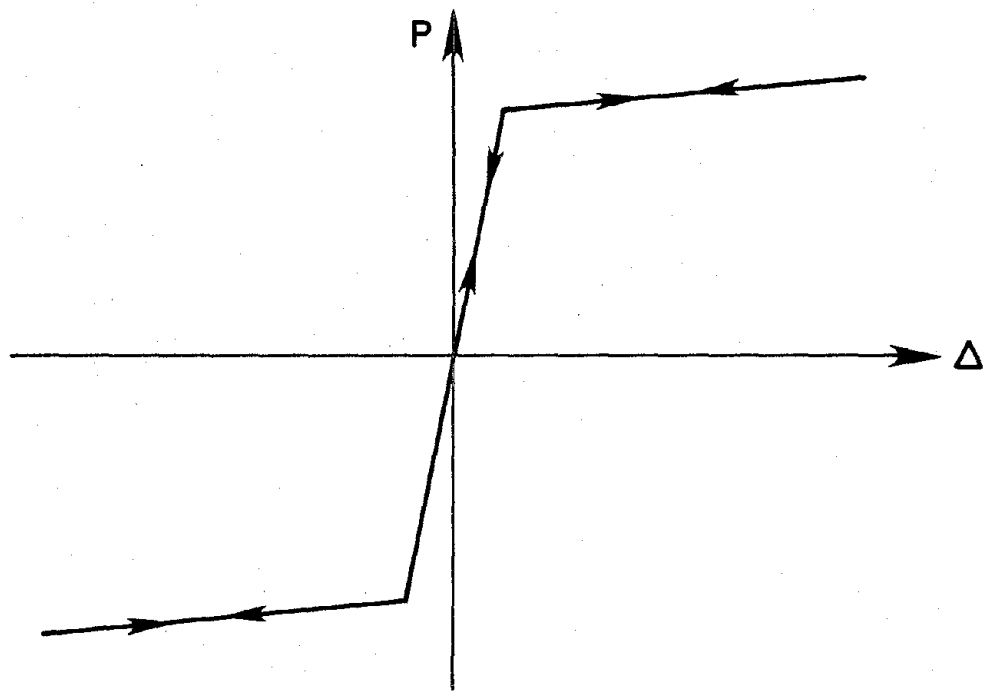

FIGURE 7.4a-b NONLINEAR ELASTIC AND HYSTERETIC ELEMENTS

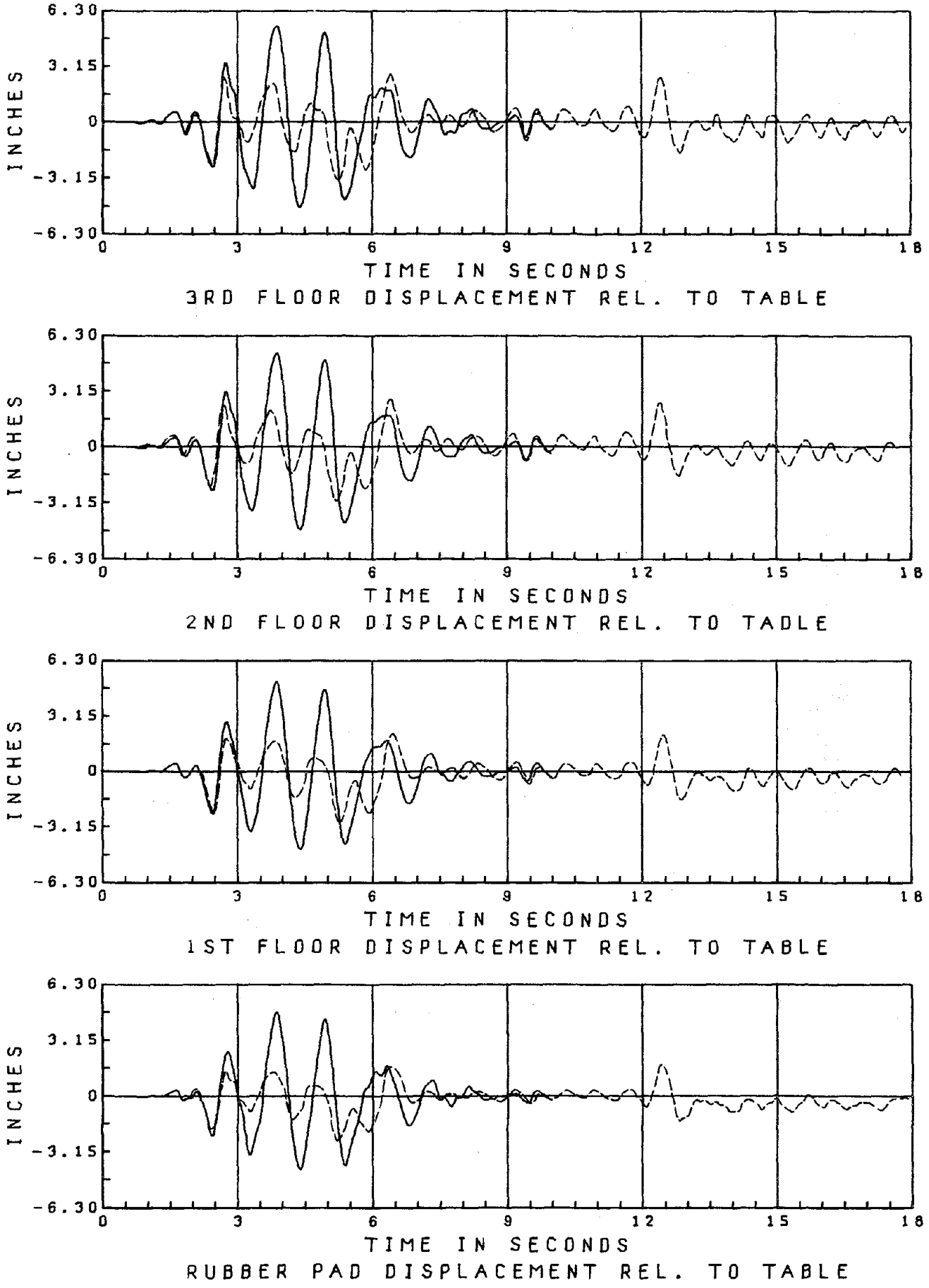

FIGURE 7.5 EL CENTRO 750 EA1, ELASTIC VERSUS HYSTERETIC

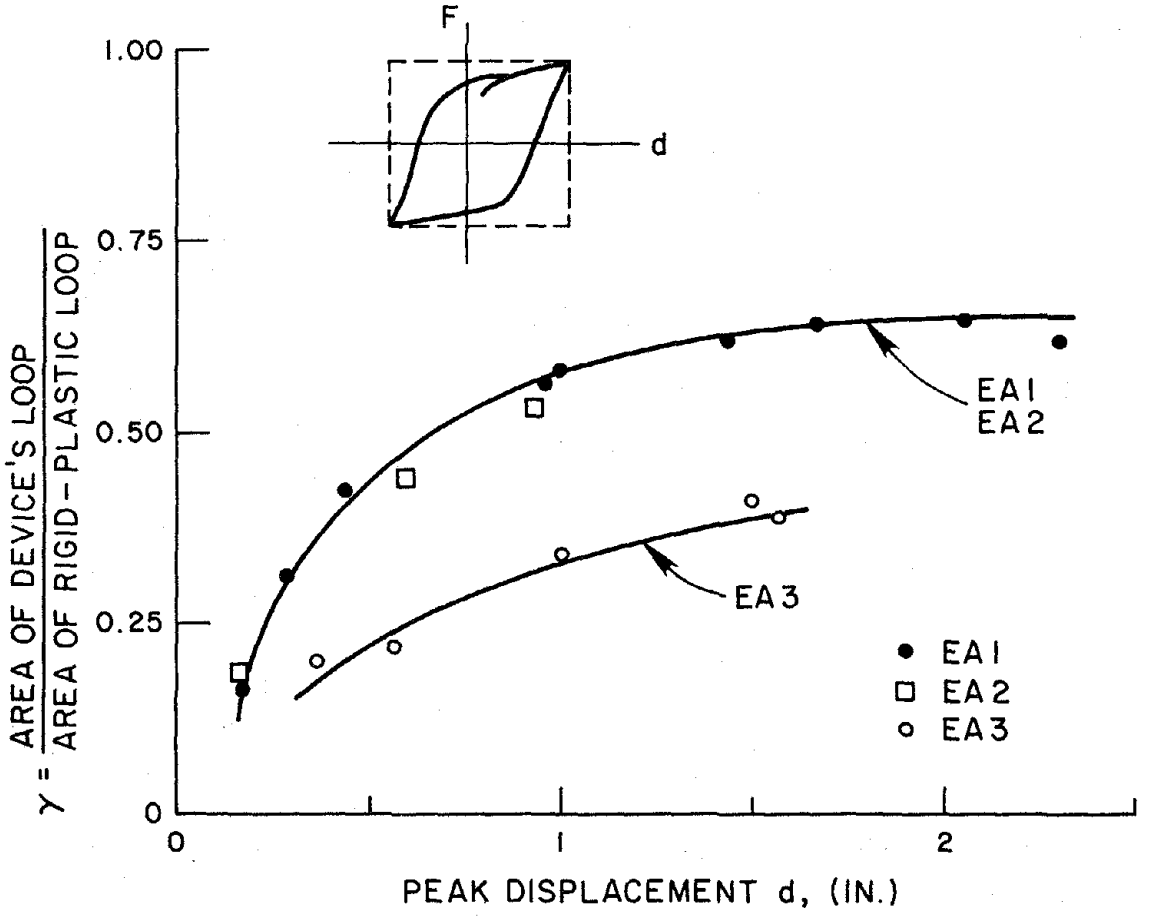

FIGURE 8.2.1 γ VERSUS PEAK DISPLACEMENT OF ENERGY-ABSORBING DEVICES

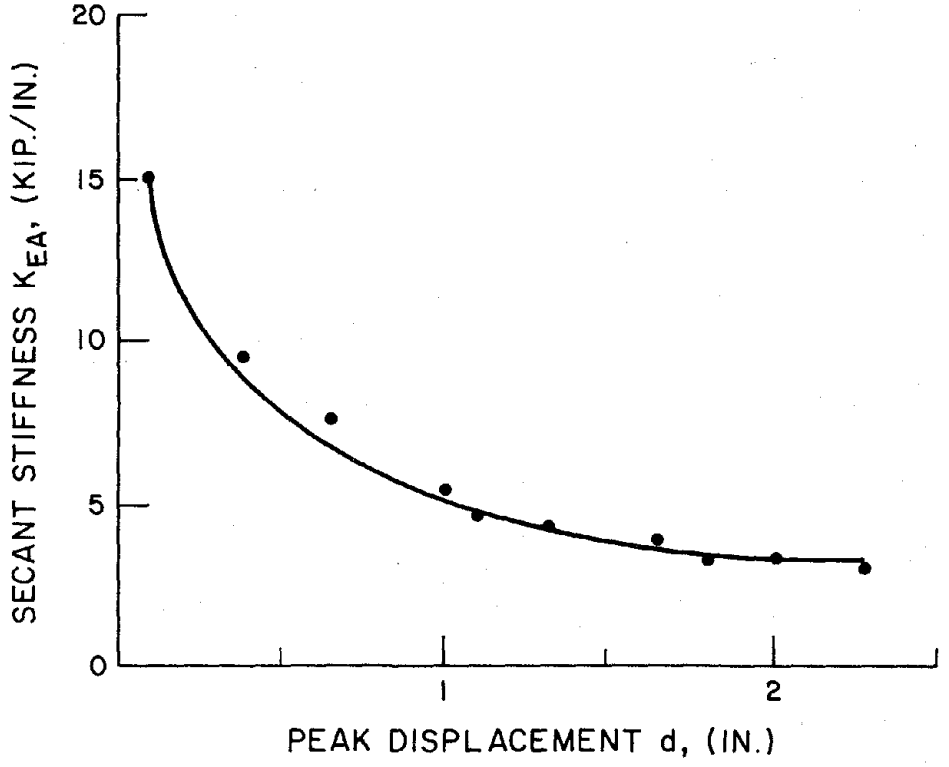

FIGURE 8.2.2 SECANT STIFFNESS OF EA1 ENERGY-ABSORBING DEVICES

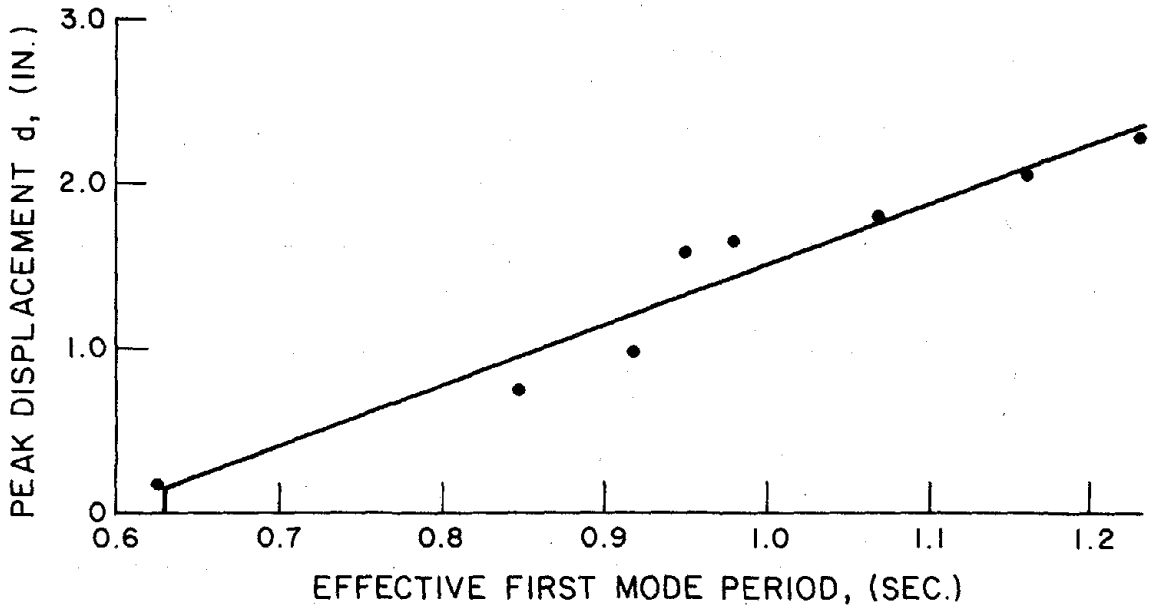

FIGURE 8.2.3 T_{ieff} VERSUS PEAK DISPLACEMENT OF EA1 DEVICE

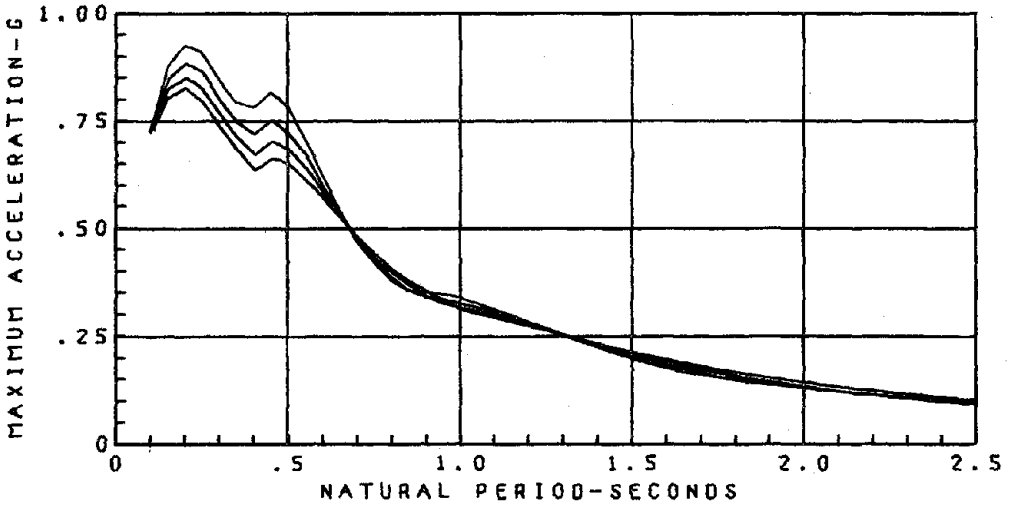

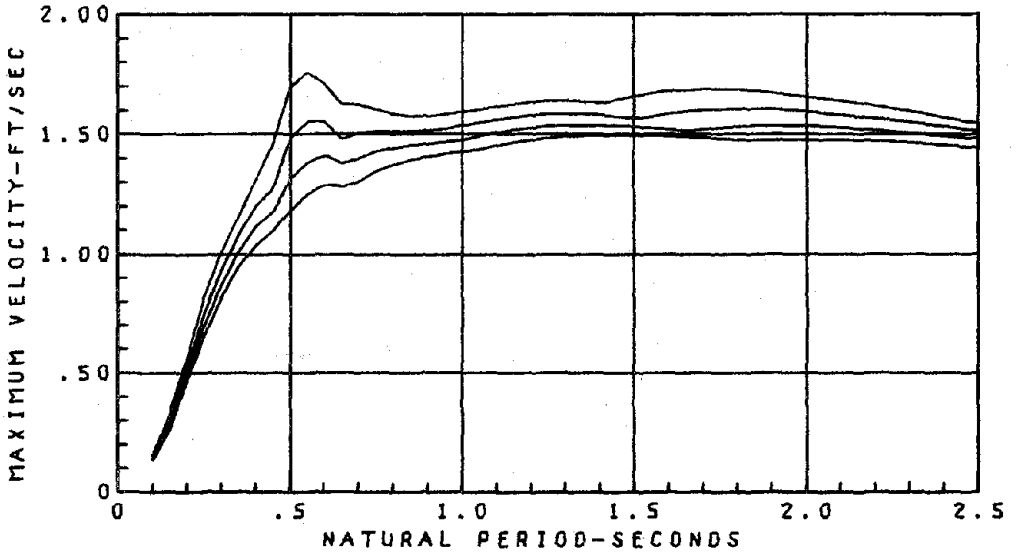

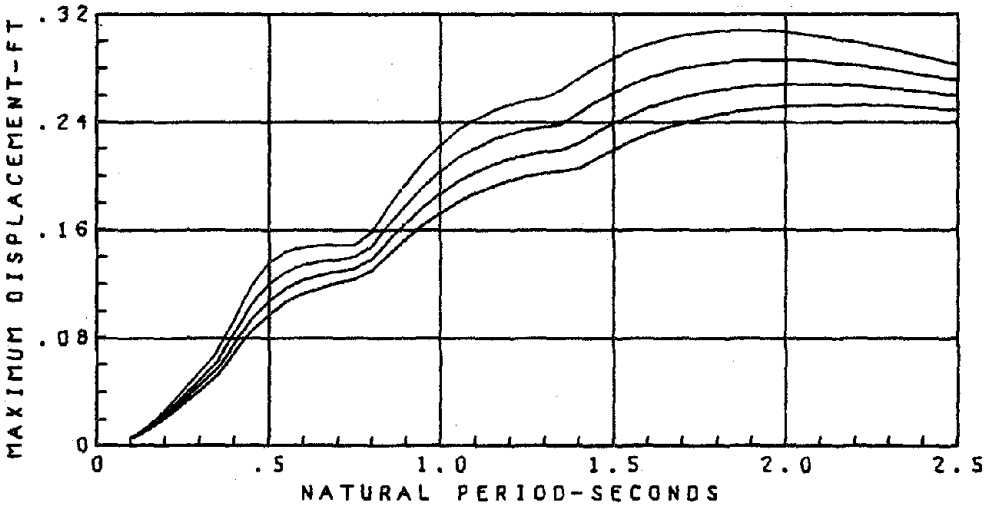

FIGURE 8.3.1 PACOIMA DAM 500 RESPONSE SPECTRA
ξ = 30, 35, 40, and 45%

EARTHQUAKE ENGINEERING RESEARCH CENTER REPORTS

EARTHQUAKE ENGINEERING RESEARCH CENTER REPORTS

NOTE: Numbers in parentheses are Accession Numbers assigned by the National Technical Information Service; these are followed by a price code. Copies of the reports may be ordered from the National Technical Information Service, 5285 Port Royal Road, Springfield, Virginia, 22161. Accession Numbers should be quoted on orders for reports (PB--- ---) and remittance must accompany each order. Reports without this information were not available at time of printing. Upon request, EERC will mail inquirers this information when it becomes available.

EERC 67-1 "Feasibility Study of Large-Scale Earthquake Simulator Facility," by J. Penzien, J. G. Bouwkamp, R. W. Clough, and D. Rea - 1967 (PB 187 905)A07

EERC 68-1 Unassigned

EERC 68-2 "Inelastic Behavior of Beam-to-Column Subassemblages under Repeated Loading," by V. V. Bertero - 1968 (PB 184 888)A05

EERC 68-3 "A Graphical Method for Solving the Wave Reflection-Refraction Problem," by H. D. McNiven and Y. Mengi - 1968 (PB 187 943)A03

EERC 68-4 "Dynamic Properties of McKinley School Buildings," by D. Rea, J. G. Bouwkamp, and R. W. Clough - 1968 (PB 187 902)A07

EERC 68-5 "Characteristics of Rock Motions during Earthquakes," by H. B. Seed, I. M. Idriss, and F. W. Kiefer - 1968 (PB 188 338)A03

EERC 69-1 "Earthquake Engineering Research at Berkeley," - 1969 (PB 187 906)A11

EERC 69-2 "Nonlinear Seismic Response of Earth Structures," by M. Dibaj and J. Penzien - 1969 (PB 187 904)A08

EERC 69-3 "Probabilistic Study of the Behavior of Structures during Earthquakes," by R. Ruiz and J. Penzien - 1969 (PB 187 886)A06

EERC 69-4 "Numerical Solution of Boundary Value Problems in Structural Mechanics by Reduction to an Initial Value Formulation," by N. Distefano and J. Schujman - 1969 (PB 187 942)A02

EERC 69-5 "Dynamic Programming and the Solution of the Biharmonic Equation," by N. Distefano - 1969 (PB 187 941)A03

EERC 69-6 "Stochastic Analysis of Offshore Tower Structures," by A. K. Malhotra and J. Penzien - 1969 (PB 187 903)A09

EERC 69-7 "Rock Motion Accelerograms for High Magnitude Earthquakes," by H. B. Seed and I. M. Idriss - 1969 (PB 187 940)A02

EERC 69-8 "Structural Dynamics Testing Facilities at the University of California, Berkeley," by R. M. Stephen, J. G. Bouwkamp, R. W. Clough and J. Penzien - 1969 (PB 189 111)A04

EERC 69-9 "Seismic Response of Soil Deposits Underlain by Sloping Rock Boundaries," by H. Dezfulian and H. B. Seed - 1969 (PB 189 114)A03

EERC 69-10 "Dynamic Stress Analysis of Axisymmetric Structures under Arbitrary Loading," by S. Ghosh and E. L. Wilson - 1969 (PB 189 026)A10

EERC 69-11 "Seismic Behavior of Multistory Frames Designed by Different Philosophies," by J. C. Anderson and V. V. Bertero - 1969 (PB 190 662)A10

EERC 69-12 "Stiffness Degradation of Reinforcing Concrete Members Subjected to Cyclic Flexural Moments," by V. V. Bertero, B. Bresler, and H. Ming Liao - 1969 (PB 202 942)A07

EERC 69-13 "Response of Non-Uniform Soil Deposits to Travelling Seismic Waves," by H. Dezfulian and H. B. Seed - 1969 (PB 191 023)A03

EERC 69-14 "Damping Capacity of a Model Steel Structure," by D. Rea, R. W. Clough, and J. G. Bouwkamp - 1969 (PB 190 663)A06

EERC 69-15 "Influence of Local Soil Conditions on Building Damage Potential during Earthquakes," by H. B. Seed and I. M. Idriss - 1969 (PB 191 036)A03

EERC 69-16 "The Behavior of Sands under Seismic Loading Conditions," by M. L. Silver and H. B. Seed - 1969 (AD 714 982)A07

EERC 70-1 "Earthquake Response of Gravity Dams," by A. K. Chopra - 1970 (AD 709 640)A03

EERC 70-2 "Relationships between Soil Conditions and Building Damage in the Caracas Earthquake of July 29, 1967," by H. B. Seed, I. M. Idriss, and H. Dezfulian - 1970 (PB 195 762)A05

EERC 70-3 "Cyclic Loading of Full Size Steel Connections," by E. P. Popov and R. M. Stephen - 1970 (PB 213 545)A04

EERC 70-4 "Seismic Analysis of the Charaima Building, Caraballeda, Venezuela," by Subcommittee of the SEAONC Research Committee: V. V. Bertero, P. F. Fratessa, S. A. Mahin, J. H. Sexton, A. C. Scordelis, E. L. Wilson, L. A. Wyllie, H. B. Seed, and J. Penzien, Chairman - 1970 (PB 201 455)A06

EERC 70-5 "A Computer Program for Earthquake Analysis of Dams," by A. K. Chopra and P. Chakrabarti - 1970 (AD 723 994)A05

EERC 70-6 "The Propagation of Love Waves Across Non-Horizontally Layered Structures," by J. Lysmer and L. A. Drake - 1970 (PB 197 896)A03

EERC 70-7 "Influence of Base Rock Characteristics on Ground Response," by J. Lysmer, H. B. Seed, and P. B. Schnabel - 1970 (PB 197 897)A03

EERC 70-8 "Applicability of Laboratory Test Procedures for Measuring Soil Liquefaction Characteristics under Cyclic Loading," by H. B. Seed and W. H. Peacock - 1970 (PB 198 016)A03

EERC 70-9 "A Simplified Procedure for Evaluating Soil Liquefaction Potential," by H. B. Seed and I. M. Idriss - 1970 (PB 198 009)A03

EERC 70-10 "Soil Moduli and Damping Factors for Dynamic Response Analysis," by H. B. Seed and I. M. Idriss - 1970 (PB 197 869)A03

EERC 71-1 "Koyna Earthquake of December 11, 1967 and the Performance of Koyna Dam," by A. K. Chopra and P. Chakrabarti - 1971 (AD 731 496)A06

EERC 71-2 "Preliminary In-Situ Measurements of Anelastic Absorption in Soils using a Prototype Earthquake Simulator," by R. D. Borcherdt and P. W. Rodgers - 1971 (PB 201 454)A03

EERC 71-3 "Static and Dynamic Analysis of Inelastic Frame Structures," by F. L. Porter and G. H. Powell - 1971 (PB 210 135)A06

EERC 71-4 "Research Needs in Limit Design of Reinforced Concrete Structures," by V. V. Bertero - 1971 (PB 202 943)A04

EERC 71-5 "Dynamic Behavior of a High-Rise Diagonally Braced Steel Building," by D. Rea, A. A. Shah, and J. G. Bouwkamp - 1971 (PB 203 584)A06

EERC 71-6 "Dynamic Stress Analysis of Porous Elastic Solids Saturated with Compressible Fluids," by J. Ghaboussi and E. L. Wilson - 1971 (PB 211 396)A06

EERC 71-7 "Inelastic Behavior of Steel Beam-to-Column Subassemblages," by H. Krawinkler, V. V. Bertero, and E. P. Popov - 1971 (PB 211 355)A14

EERC 71-8 "Modification of Seismograph Records for Effects of Local Soil Conditions," by P. Schnabel, H. B. Seed, and J. Lysmer - 1971 (PB 214 450)A03

EERC 72-1 "Static and Earthquake Analysis of Three Dimensional Frame and Shear Wall Buildings," by E. L. Wilson and H. H. Dovey - 1972 (PB 212 904)A05

EERC 72-2 "Accelerations in Rock for Earthquakes in the Western United States," by P. B. Schnabel and H. B. Seed - 1972 (PB 213 100)A03

EERC 72-3 "Elastic-Plastic Earthquake Response of Soil-Building Systems," by T. Minami - 1972 (PB 214 868)A08

EERC 72-4 " Stochastic Inelastic Response of Offshore Towers to Strong Motion Earthquakes," by M. K. Kaul - 1972 (PB 215 713)A05

EERC 72-5 "Cyclic Behavior of Three Reinforced Concrete Flexural Members with High Shear," by E. P. Popov, V. V. Bertero, and H. Krawinkler - 1972 (PB 214 555)A05

EERC 72-6 "Earthquake Response of Gravity Dams Including Reservoir Interaction Effects," by P. Chakrabarti and A. K. Chopra - 1972 (AD 762 330)A08

EERC 72-7 "Dynamic Properties of Pine Flat Dam," by D. Rea, C. Y. Liaw, and A. K. Chopra - 1972 (AD 763 928)A05

EERC 72-8 "Three Dimensional Analysis of Building Systems," by E. L. Wilson and H. H. Dovey - 1972 (PB 222 438)A06

EERC 72-9 "Rate of Loading Effects on Uncracked and Repaired Reinforced Concrete Members," by S. Mahin, V. V. Bertero, D. Rea and M. Atalay - 1972 (PB 224 520)A08

EERC 72-10 "Computer Program for Static and Dynamic Analysis of Linear Structural Systems," by E. L. Wilson, K.-J. Bathe, J. E. Peterson and H. H. Dovey - 1972 (PB 220 437)A04

EERC 72-11 "Literature Survey - Seismic Effects on Highway Bridges," by T. Iwasaki, J. Penzien, and R. W. Clough - 1972 (PB 215 613)A19

EERC 72-12 "SHAKE - A Computer Program for Earthquake Response Analysis of Horizontally Layered Sites," by P. B. Schnabel and J. Lysmer - 1972 (PB 220 207)A06

EERC 73-1 "Optimal Seismic Design of Multistory Frames," by V. V. Bertero and H. Kamil - 1973

EERC 73-2 "Analysis of the Slides in the San Fernando Dams during the Earthquake of February 9, 1971," by H. B. Seed, K. L. Lee, I. M. Idriss, and F. Makdisi - 1973 (PB 223 402)A14

EERC 73-3 "Computer Aided Ultimate Load Design of Unbraced Multistory Steel Frames," by M. B. El-Hafez and G. H. Powell - 1973 (PB 248 315)A09

EERC 73-4 "Experimental Investigation into the Seismic Behavior of Critical Regions of Reinforced Concrete Components as Influenced by Moment and Shear," by M. Celebi and J. Penzien - 1973 (PB 215 884)A09

EERC 73-5 "Hysteretic Behavior of Epoxy-Repaired Reinforced Concrete Beams," by M. Celebi and J. Penzien - 1973 (PB 239 568)A03

EERC 73-6 "General Purpose Computer Program for Inelastic Dynamic Response of Plane Structures," by A. Kanaan and G. H. Powell - 1973 (PB 221 260)A08

EERC 73-7 "A Computer Program for Earthquake Analysis of Gravity Dams Including Reservoir Interaction," by P. Chakrabarti and A. K. Chopra - 1973 (AD 766 271)A04

EERC 73-8 "Behavior of Reinforced Concrete Deep Beam-Column Subassemblages under Cyclic Loads," by O. Küstü and J. G. Bouwkamp - 1973 (PB 246 117)A12

EERC 73-9 "Earthquake Analysis of Structure-Founation Systems," by A. K. Vaish and A. K. Chopra - 1973 (AD 766 272)A07

EERC 73-10 "Deconvolution of Seismic Response for Linear Systems," by R. B. Reimer - 1973 (PB 227 179)A08

EERC 73-11 "SAP IV: A Structural Analysis Program for Static and Dynamic Response of Linear Systems," by K.-J. Bathe, E. L. Wilson, and F. E. Peterson - 1973 (PB 221 967)A09

EERC 73-12 "Analytical Investigations of the Seismic Response of Long, Multiple Span Highway Bridges," by W. S. Tseng and J. Penzien - 1973 (PB 227 816)A10

EERC 73-13 "Earthquake Analysis of Multi-Story Buildings Including Foundation Interaction," by A. K. Chopra and J. A. Gutierrez - 1973 (PB 222 970)A03

EERC 73-14 "ADAP: A Computer Program for Static and Dynamic Analysis of Arch Dams," by R. W. Clough, J. M. Raphael, and S. Mojtahedi - 1973 (PB 223 763)A09

EERC 73-15 "Cyclic Plastic Analysis of Structural Steel Joints," by R. B. Pinkney and R. W. Clough - 1973 (PB 226 843)A08

EERC 73-16 "QUAD-4: A Computer Program for Evaluating the Seismic Response of Soil Structures by Variable Damping Finite Element Procedures," by I. M. Idriss, J. Lysmer, R. Hwang, and H. B. Seed - 1973 (PB 229 424)A05

EERC 73-17 "Dynamic Behavior of a Multi-Story Pyramid Shaped Building," by R. M. Stephen, J. P. Hollings, and J. G. Bouwkamp - 1973 (PB 240 718)A06

EERC 73-18 "Effect of Different Types of Reinforcing on Seismic Behavior of Short Concrete Columns," by V. V. Bertero, J. Hollings, O. Küstü, R. M. Stephen, and J. G. Bouwkamp - 1973

EERC 73-19 "Olive View Medical Center Materials Studies, Phase I," by B. Bresler and V. V. Bertero - 1973 (PB 235 986)A06

EERC 73-20 "Linear and Nonlinear Sesismic Analysis Computer Programs for Long Multiple-Span Highway Bridges," by W. S. Tseng and J. Penzien - 1973

EERC 73-21 "Constitutive Models for Cyclic Plastic Deformation of Engineering Materials," by J. M. Kelly and P. P. Gillis - 1973 (PB 226 024)A03

EERC 73-22 "DRAIN-2D User's Guide," by G. H. Powell - 1973 (PB 227 016)A05

EERC 73-23 "Earthquake Engineering at Berkeley - 1973 " 1973 (PB 226 033)A11

EERC 73-24 Unassigned

EERC 73-25 "Earthquake Response of Axisymmetric Tower Structures Surrounded by Water," by C. Y. Liaw and A. K. Chopra - 1973 (AD 773 052)A09

EERC 73-26 "Investigation of the Failures of the Olive View Stairtowers during the San Fernando Earthquake and Their Implications on Seismic Design," by V. V. Bertero and R. G. Collins - 1973 (PB 235 106)A13

EERC 73-27 "Further Studies on Seismis Behavior of Steel Beam-Column Subassemblages," by V. V. Bertero, H. Krawinkler, and E. P. Popov - 1973 (PB 234 172)A06

EERC 74-1 "Seismic Risk Analysis," by C. S. Oliveira - 1974 (PB 235 920)A06

EERC 74-2 "Settlement and Liquefaction of Sands under Multi-Directional Shaking," by R. Pyke, C. K. Chan, and H. B. Seed - 1974

EERC 74-3 "Optimum Design of Earthquake Resistant Shear Buildings," by D. Ray, K. S. Pister, and A. K. Chopra - 1974 (PB 231 172)A06

EERC 74-4 "LUSH - A Computer Program for Complex Response Analysis of Soil-Structure Systems," by J. Lysmer, T. Udaka, H. B. Seed, and R. Hwang - 1974 (PB 236 796)A05

EERC 74-5 "Sensitivity Analysis for Hysteretic Dynamic Systems: Applications to Earthquake Engineering," by D. Ray - 1974 (PB 233 213)A06

EERC 74-6 "Soil Structure Interaction Analyses for Evaluating Seismic Response," by H. B. Seed, J. Lysmer, and R. Hwang - 1974 (PB 236 519)A04

EERC 74-7 Unassigned

EERC 74-8 "Shaking Table Tests of a Steel Frame - A Progress Report," by R. W. Clough and D. Tang - 1974 (PB 240 869)A03

EERC 74-9 "Hysteretic Behavior of Reinforced Concrete Flexural Members with Special Web Reinforcement," by V. V. Bertero, E. P. Popov, and T. Y. Wang - 1974 (PB 236 797)A07

EERC 74-10 "Applications of Realiability-Based, Global Cost Optimization to Design of Earthquake Resistant Structures," by E. Vitiello and K. S. Pister - 1974 (PB 237 231)A06

EERC 74-11 "Liquefaction of Gravelly Soils under Cyclic Loading Conditions," by R. T. Wong, H. B. Seed, and C. K. Chan - 1974 (PB 242 042)A03

EERC 74-12 "Site-Dependent Spectra for Earthquake-Resistant Design," by H. B. Seed, C. Ugas, and J. Lysmer - 1974 (PB 240 953)A03

EERC 74-13 "Earthquake Simulator Study of a Reinforced Concrete Frame," by P. Hidalgo and R. W. Clough - 1974 (PB 241 944)A13

EERC 74-14 "Nonlinear Earthquake Response of Concrete Gravity Dams," by N. Pal - 1974 (AD/A 006 583)A06

EERC 74-15 "Modeling and Identification in Nonlinear Structural Dynamics - I. One Degree of Freedom Models," by N. Distefano and A. Rath - 1974 (PB 241 548)A06

EERC 75-1 "Determination of Seismic Design Criteria for the Dumbarton Bridge Replacement Structure, Vol. I: Description, Theory and Analytical Modeling of Bridge and Parameters," by F. Baron and S.-H. Pang - 1975 (PB 259 407)A15

EERC 75-2 "Determination of Seismic Design Criteria for the Dumbarton Bridge Replacement Structure, Vol. II: Numerical Studies and Establishment of Seismic Design Criteria," by F. Baron and S.-H. Pang - 1975 (PB 259 408)A11 [For set of EERC 75-1 and 75-2 (PB 241 454)A09]

EERC 75-3 "Seismic Risk Analysis for a Site and a Metropolitan Area," by C. S. Oliveira - 1975 (PB 248 134)A09

EERC 75-4 "Analytical Investigations of Seismic Response of Short, Single or Multiple-Span Highway Bridges," by M.-C. Chen and J. Penzien - 1975 (PB 241 454)A09

EERC 75-5 "An Evaluation of Some Methods for Predicting Seismic Behavior of Reinforced Concrete Buildings," by S. A. Mahin and V. V. Bertero - 1975 (PB 246 306)A16

EERC 75-6 "Earthquake Simulator Story of a Steel Frame Structure, Vol. I: Experimental Results," by R. W. Clough and D. T. Tang - 1975 (PB 243 981)A13

EERC 75-7 "Dynamic Properties of San Bernardino Intake Tower," by D. Rea, C.-Y Liaw and A. K. Chopra - 1975 (AD/A 008 406)A05

EERC 75-8 "Seismic Studies of the Articulation for the Dumbarton Bridge Replacement Structure, Vol. 1: Description, Theory and Analytical Modeling of Bridge Components," by F. Baron and R. E. Hamati - 1975 (PB 251 539)A07

EERC 75-9 "Seismic Studies of the Articulation for the Dumbarton Bridge Replacement Structure, Vol. 2: Numerical Studies of Steel and Concrete Girder Alternates," by F. Baron and R. E. Hamati - 1975 (PB 251 540)A10

EERC 75-10 "Static and Dynamic Analysis of Nonlinear Structures," by D. P. Mondkar and G. H. Powell - 1975 (PB 242 434)A08

EERC 75-11 "Hysteretic Behavior of Steel Columns," by E. P. Popov, V. V. Bertero, and S. Chandramouli - 1975 (PB 252 365)A11

EERC 75-12 "Earthquake Engineering Research Center Library Printed Catalog " - 1975 (PB 243 711)A26

EERC 75-13 "Three Dimensional Analysis of Building Systems (Extended Version)," by E. L. Wilson, J. P. Hollings, and H. H. Dovey - 1975 (PB 243 989)A07

EERC 75-14 "Determination of Soil Liquefaction Characteristics by Large-Scale Laboratory Tests," by P. De Alba, C. K. Chan, and H. B. Seed - 1975 (NUREG 0027)A08

EERC 75-15 "A Literature Survey - Compressive, Tensile, Bond and Shear Strength of Masonry," by R. L. Mayes and R. W. Clough - 1975 (PB 246 292)A10

EERC 75-16 "Hysteretic Behavior of Ductile Moment-Resisting Reinforced Concrete Frame Components," by V. V. Bertero and E. P. Popov - 1975 (PB 246 388)A05

EERC 75-17 "Relationships Between Maximum Acceleration, Maximum Velocity, Distance from Source, Local Site Conditions for Moderately Strong Earthquakes," by H. B. Seed, R. Murarka, J. Lysmer, and I. M. Idriss - 1975 (PB 248 172)A03

EERC 75-18 "The Effects of Method of Sample Preparation on the Cyclic Stress-Strain Behavior of Sands," by J. Mulilis, C. K. Chan, and H. B. Seed - 1975 (Summarized in EERC 75-28)

EERC 75-19 "The Seismic Behavior of Critical Regions of Reinforced Concrete Components as Influenced by Moment, Shear and Axial Force," by M. B. Atalay and J. Penzien - 1975 (PB 258 842)A11

EERC 75-20 "Dynamic Properties of an Eleven Story Masonry Building," by R. M. Stephen, J. P. Hollings, J. G. Bouwkamp, and D. Jurukovski - 1975 (PB 246 945)A04

EERC 75-21 "State-of-the-Art in Seismic Strength of Masonry - An Evaluation and Review," by R. L. Mayes and R. W. Clough - 1975 (PB 249 040)A07

EERC 75-22 "Frequency Dependent Stiffness Matrices for Viscoelastic Half-Plane Foundations," by A. K. Chopra, P. Chakrabarti, and G. Dasgupta - 1975 (PB 248 121)A07

EERC 75-23 "Hysteretic Behavior of Reinforced Concrete Framed Walls," by T. Y. Wang, V. V. Bertero, and E. P. Popov - 1975

EERC 75-24 "Testing Facility for Subassemblages of Frame-Wall Structural Systems," by V. V. Bertero, E. P. Popov, and T. Endo - 1975

EERC 75-25 "Influence of Seismic History on the Liquefaction Characteristics of Sands," by H. B. Seed, K. Mori, and C. K. Chan - 1975 (Summarized in EERC 75-28)

EERC 75-26 "The Generation and Dissipation of Pore Water Pressures during Soil Liquefaction," by H. B. Seed, P. P. Martin, and J. Lysmer - 1975 (PB 252 648)A03

EERC 75-27 "Identification of Research Needs for Improving Aseismic Design of Building Structures," by V. V. Bertero - 1975 (PB 248 136)A05

EERC 75-28 "Evaluation of Soil Liquefaction Potential during Earthquakes," by H. B. Seed, I. Arango, and C. K. Chan - 1975 (NUREG 0026)A13

EERC 75-29 "Representation of Irregular Stress Time Histories by Equivalent Uniform Stress Series in Liquefaction Analyses," by H. B. Seed, I. M. Idriss, F. Makdisi, and N. Banerjee - 1975 (PB 252 635)A03

EERC 75-30 "FLUSH - A Computer Program for Approximate 3-D Analysis of Soil-Structure Interaction Problems," by J. Lysmer, T. Udaka, C.-F. Tsai, and H. B. Seed - 1975 (PB 259 332)A07

EERC 75-31 "ALUSH - A Computer Program for Seismic Response Analysis of Axisymmetric Soil-Structure Systems," by E. Berger, J. Lysmer, and H. B. Seed - 1975

EERC 75-32 "TRIP and TRAVEL - Computer Programs for Soil-Structure Interaction Analysis with Horizontally Travelling Waves," by T. Udaka, J. Lysmer, and H. B. Seed - 1975

EERC 75-33 "Predicting the Performance of Structures in Regions of High Seismicity," by J. Penzien - 1975 (PB 248 130)A03

EERC 75-34 "Efficient Finite Element Analysis of Seismic Structure-Soil-Direction," by J. Lysmer, H. B. Seed, T. Udaka, R. N. Hwang, and C.-F. Tsai - 1975 (PB 253 570)A03

EERC 75-35 "The Dynamic Behavior of a First Story Girder of a Three-Story Steel Frame Subjected to Earthquake Loading," by R. W. Clough and L.-Y. Li - 1975 (PB 248 841)A05

EERC 75-36 "Earthquake Simulator Story of a Steel Frame Structure, Volume II - Analytical Results," by D. T. Tang - 1975 (PB 252 926)A10

EERC 75-37 "ANSR-I General Purpose Computer Program for Analysis of Non-Linear Structural Response," by D. P. Mondkar and G. H. Powell - 1975 (PB 252 386)A08

EERC 75-38 "Nonlinear Response Spectra for Probabilistic Seismic Design and Damage Assessment of Reinforced Concrete Structures," by M. Murakami and J. Penzien - 1975 (PB 259 530)A05

EERC 75-39 "Study of a Method of Feasible Directions for Optimal Elastic Design of Frame Structures Subjected to Earthquake Loading," by N. D. Walker and K. S. Pister - 1975 (PB 247 781)A06

EERC 75-40 "An Alternative Representation of the Elastic-Viscoelastic Analogy," by G. Dasgupta and J. L. Sackman - 1975 (PB 252 173)A03

EERC 75-41 "Effect of Multi-Directional Shaking on Liquefaction of Sands," by H. B. Seed, R. Pyke, and G. R. Martin - 1975 (PB 258 781)A03

EERC 76-1 "Strength and Ductility Evaluation of Existing Low-Rise Reinforced Concrete Buildings - Screening Method," by T. Okada and B. Bresler - 1976 (PB 257 906)A11

EERC 76-2 "Experimental and Analytical Studies on the Hysteretic Behavior of Reinforced Concrete Rectangular and T-Beams," by S.-Y. M. Ma, E. P. Popov, and V. V. Bertero - 1976 (PB 260 843)A12

EERC 76-3 "Dynamic Behavior of a Multistory Triangular-Shaped Building," by J. Petrovski, R. M. Stephen, E. Gartenbaum, and J. G. Bouwkamp - 1976

EERC 76-4 "Earthquake Induced Deformations of Earth Dams," by N. Serff and H. B. Seed - 1976

EERC 76-5 "Analysis and Design of Tube-Type Tall Building Structures," by H. de Clercq and G. H. Powell - 1976 (PB 252 220)A10

EERC 76-6 "Time and Frequency Domain Analysis of Three-Dimensional Ground Motions,San Fernando Earthquake," by T. Kubo and J. Penzien - 1976 (PB 260 556)A11

EERC 76-7 "Expected Performance of Uniform Building Code Design Masonry Structures," by R. L. Mayes, Y. Omote, S. W. Chen, and R. W. Clough - 1976

EERC 76-8 "Cyclic Shear Tests on Concrete Masonry Piers, Part I - Test Results," by R. L. Mayes, Y. Omote, and R. W. Clough - 1976 (PB 264 424)A06

EERC 76-9 "A Substructure Method for Earthquake Analysis of Structure-Soil Interaction," by J. A. Gutierrez and A. K. Chopra - 1976 (PB 247 783)A08

EERC 76-10 "Stabilization of Potentially Liquefiable San Deposits using Gravel Drain Systems," by H. B. Seed and J. R. Booker - 1976 (PB 248 820)A04

EERC 76-11 "Influence of Design and Analysis Assumptions on Computed Inelastic Response of Moderately Tall Frames," by G. H. Powell and D. G. Row - 1976

EERC 76-12 "Sensitivity Analysis for Hysteretic Dynamic Systems: Theory and Applications," by D. Ray, K. S. Pister, and E. Polak - 1976 (PB 262 859)A04

EERC 76-13 "Coupled Lateral Torsional Response of Buildings to Ground Shaking," by C. L. Kan and A. K. Chopra - 1976 (PB 257 907)A09

EERC 76-14 "Seismic Analyses of the Banco de America," by V. V. Bertero, S. A. Mahin, and J. A. Hollings - 1976

EERC 76-15 "Reinforced Concrete Frame 2: Seismic Testing and Analytical Correlation," by R. W. Clough and J. Gidwani - 1976 (PB 261 323)A08

EERC 76-16 "Cyclic Shear Tests on Masonry Piers, Part II - Analysis of Test Results," by R. L. Mayes, Y. Omote, and R. W. Clough - 1976

EERC 76-17 "Structural Steel Bracing Systems: Behavior under Cyclic Loading," by E. P. Popov, K. Takanashi, and C. W. Roeder - 1976 (PB 260 715)A05

EERC 76-18 "Experimental Model Studies on Seismic Response of High Curved Overcrossings," by D. Williams and W. G. Godden - 1976

EERC 76-19 "Effects of Non-Uniform Seismic Disturbances on the Dumbarton Bridge Replacement Structure," by F. Baron and R. E. Hamati - 1976

EERC 76-20 "Investigation of the Inelastic Characteristics of a Single Story Steel Structure using System Identification and Shaking Table Experiments," by V. C. Matzen and H. D. McNiven - 1976 (PB 258 453)A07

EERC 76-21 "Capacity of Columns with Splice Imperfections," by E. P. Popov, R. M. Stephen and R. Philbrick - 1976 (PB 260 378)A04

EERC 76-22 "Response of the Olive View Hospital Main Building during the San Fernando Earthquake," by S. A. Mahin, V. V. Bertero, A. K. Chopra, and R. Collins," - 1976

EERC 76-23 "A Study on the Major Factors Influencing the Strength of Masonry Prisms," by N. M. Mostaghel, R. L. Mayes, R. W. Clough, and S. W. Chen - 1976

EERC 76-24 "GADFLEA - A Computer Program for the Analysis of Pore Pressure Generation and Dissipation during Cyclic or Earthquake Loading," by J. R. Booker, M. S. Rahman, and H. B. Seed - 1976 (PB 263 947)A04

EERC 76-25 "Rehabilitation of an Existing Building: A Case Study," by B. Bresler and J. Axley - 1976

EERC 76-26 "Correlative Investigations on Theoretical and Experimental Dynamic Behavior of a Model Bridge Structure," by K. Kawashima and J. Penzien - 1976 (PB 263 388)A11

EERC 76-27 "Earthquake Response of Coupled Shear Wall Buildings," by T. Srichatrapimuk - 1976 (PB 265 157)A07

EERC 76-28 "Tensile Capacity of Partial Penetration Welds," by E. P. Popov and R. M. Stephen - 1976 (PB 262 899)A03

EERC 76-29 "Analysis and Design of Numerical Integration Methods in Structural Dynamics," by H. M. Hilber - 1976 (PB 264 410)A06

EERC 76-30 "Contribution of a Floor System to the Dynamic Characteristics of Reinforced Concrete Buildings," by L. E. Malik and V. V. Bertero - 1976

EERC 76-31 "The Effects of Seismic Disturbances on the Golden Gate Bridge," by F. Baron, M. Arikan, R. E. Hamati - 1976

EERC 76-32 "Infilled Frames in Earthquake-Resistant Construction," by R. E. Klingner and V. V. Bertero - 1976 (PB 265 892)A13

UCB/EERC-77/01 "PLUSH - A Computer Program for Probabilistic Finite Element Analysis of Seismic Soil-Structure Interaction," by M. P. Romo Organista, J. Lysmer, and H. B. Seed - 1977

UCB/EERC-77/02 "Soil-Structure Interaction Effects at the Humboldt Bay Power Plant in the Ferndale Earthquake of June 7, 1975," by J. E. Valera, H. B. Seed, C.-F. Tsai, and J. Lysmer - 1977 (B 265 795)A04

UCB/EERC-77/03 "Influence of Sample Disturbance on Sand Response to Cyclic Loading," by K. Mori, H. B. Seed, and C. K. Chan - 1977 (PB 267 352)A04

UCB/EERC-77/04 "Seismological Studies of Strong Motion Records," by J. Shoja-Taheri - 1977 (PB 269 655)A10

UCB/EERC-77/05 "Testing Facility for Coupled Shear Walls," by L.-H. Lee, V. V. Bertero, and E. P. Popov - 1977

UCB/EERC-77/06 "Developing Methodologies for Evaluating the Earthquake Safety of Existing Buildings," No. 1 - B. Bresler; No. 2 - B. Bresler, T. Okada, and D. Zisling; No. 3 - T. Okada and B. Bresler; No. 4 - V. V. Bertero and B. Bresler - 1977 (PB 267 354)A08

UCB/EERC-77/07 "A Literature Survey - Transverse Strength of Masonry Walls," by Y. Omote, R. L. Mayes, S. W. Chen, and R. W. Clough - 1977

UCB/EERC-77/08 "DRAIN-TABS: A Computer Program for Inelastic Earthquake Response of Three Dimensional Buildings," by R. Guendelman-Israel and G. H. Powell - 1977

UCB/EERC-77/09 "SUBWALL: A Special Purpose Finite Element Computer Program for Practical Elastic Analysis and Design of Structural Walls with Substructure Option," by D. Q. Le, H. Petersson, and E. P. Popov - 1977

UCB/EERC-77/10 "Experimental Evaluation of Seismic Design Methods for Broad Cylindrical Tanks," by D. P. Clough - 1977

UCB/EERC-77/11 "Earthquake Engineering Research at Berkeley - 1976," - 1977

UCB/EERC-77/12 "Automated Design of Earthquake Resistant Multistory Steel Building Frames," by N. D. Walker, Jr. - 1977

UCB/EERC-77/13 "Concrete Confined by Rectangular Hoops and Subjected to Axial Loads," by J. Vallenas, V. V. Bertero, and E. P. Popov - 1977

UCB/EERC-77/14 "Seismic Strain Induced in the Ground during Earthquakes," by Y. Sugimura - 1977

UCB/EERC-77/15 "Bond Deterioration under Generalized Loading," by V. V. Bertero, E. P. Popov, and S. Viwathanatepa - 1977

UCB/EERC-77/16 "Computer-Aided Optimum Design of Ductile Reinforced Concrete Moment-Resisting Frames," by S. W. Zagajeski and V. V. Bertero - 1977

UCB/EERC-77/17 "Earthquake Simulation Testing of a Stepping Frame with Energy-Absorbing Devices," by J. M. Kelly and D. F. Tsztoo - 1977

UCB/EERC-77/18 "Inelastic Behavior of Eccentrically Braced Steel Frames under Cyclic Loadings," by C. W. Roeder and E. P. Popov - 1977

UCB/EERC-77/19 "A Simplified Procedure for Estimating Earthquake-Induced Deformation in Dams and Embankments," by F. I. Makdisi and H. B. Seed - 1977

UCB/EERC-77/20 "The Performance of Earth Dams during Earthquakes," by H. B. Seed, F. I. Makdisi, and P. de Alba - 1977

UCB/EERC-77/21 "Dynamic Plastic Analysis Using Stress Resultant Finite Element Formulation," by P. Lukkunapvasit and J.M. Kelly 1977

UCB/EERC-77/22 "Preliminary Experimental Study of Seismic Uplift of a Steel Frame," by R.W. Clough and A.A. Huckelbridge - 1977

UCB/EERC-77/23 "Earthquake Simulator Tests of a Nine-Story Steel Frame with Columns Allowed to Uplift," by A.A. Huckelbridge - 1977

UCB/EERC-77/24 "Nonlinear Soil-Structure Interaction of Skew Highway Bridges," by M.-C. Chen and Joseph Penzien - 1977

UCB/EERC-77/25 "Seismic Analysis of an Offshore Structure Supported on Pile Foundations," by D.D.-N. Liou - 1977

UCB/EERC-77/26 "Dynamic Stiffness Matrices for Homogeneous Viscoelastic Half-Planes," by G. Dasgupta and A.K. Chopra - 1977

UCB/EERC-77/27 "A Practical Soft Story Earthquake Isolation System," by J.M. Kelly and J.M. Eidinger - 1977